A thesis of the Degree of Doctor of Philosophy

A study on the role of Mef2d transcription factor in the modulation of B:T synapse formation and humoral immunity

Mef2d 전사인자의 B:T 시냅스 형성 및 체액성 면역을 조절하는 기전에 관한 연구

August 2023

Department of Biomedical Science

Seoul National University Graduate School

Ye-Ji Kim

의학박사 학위논문

Mef2d 전사인자의 B:T 시냅스 형성 및 체액성 면역을 조절하는 기전에 관한 연구

A study on the role of Mef2d transcription factor in the modulation of B:T synapse formation and humoral immunity

2023년 8월

서울대학교 대학원

의과학과 의과학전공

김 예 지

Mef2d 전사인자의 B:T 시냅스 형성 및 체액성 면역을 조절하는 역할에 관한 연구

지도교수 최 윤 수

이 논문을 의학박사 학위논문으로 제출함

2023년 04월

서울대학교 대학원

의과학과 의과학전공

김 예 지

김예지의 의학박사 학위논문을 인준함

2023년 7월

위 원 장

부위원장

위 원

위 원

위 원

A study on the role of Mef2d transcription factor in the modulation of B:T synapse formation and humoral immunity

Advisor: Youn Soo Choi

Submitting a Ph.D. Dissertation of Medicine

April 2023

Graduate School of Biomedical Sciences
Seoul National University
Biomedical Sciences Major

Ye-Ji Kim

Confirming the Ph.D. Dissertation written by
Ye-Ji Kim
July 2023

Prof.

Prof.

Prof.

Prof.

Prof.

ABSTRACT

A study on the role of Mef2d transcription factor in the modulation of B:T synapse formation and humoral immunity

Ye-Ji Kim

Department of Biomedical Sciences

The Graduate School

Seoul National University

Effective communication between CD4 T cells and cognate B cells is essential for the proper maturation of CD4 T cells into germinal center follicular helper T (GC-Tfh) cells, as well as for B cells to initiate a CD4 T-dependent (TD) humoral immune response. Although this communication is facilitated through the

formation of B:T immune synapse, the transcriptional regulation of this process by CD4 T cells is not completely understood. In this study, I propose a new mechanism in which the Mef2d transcription factor, an isoform of the myocyte enhancer factor 2 (Mef2) transcription factor family, regulates B:T synapse formation to control the development of GC-Tfh cells and further TD humoral immune response.

Mef2d expression in CD4 T cells negatively regulated the expression of *Sh2d1a,* which encodes SLAM-associated protein (SAP) that plays a crucial role in the regulation of B:T synapses. The direct repression of *Sh2d1a* expression by Mef2d led to the inhibition of SAP-dependent B:T synapse formation and the disruption of antigen-specific CD4 T cells differentiation into GC-Tfh cells. Additionally, Mef2d suppressed IL-21 production, an important B cell help signaling molecule, by directly repressing the *Il21* gene in CD4 T cells. This repression, combined with the inhibition of SAP-dependent B:T synapse formation, ultimately impeded B cell humoral immune responses.

In contrast, in the context of CD4 T cell-specific deletion of *Mef2d* resulted in a substantial increase in GC-Tfh differentiation, accompanied by a significant elevation in SAP expression and IL-21 production. Notably, the expression of *MEF2D* mRNA in CD4 T cells of systemic lupus erythematosus (SLE) patients showed inverse correlations with autoimmune parameters in SLE patients, such as circulating Tfh-like cell frequencies, autoantibody levels, and SLEDAI scores. These findings indicate that Mef2d functions as a vital regulator in CD4 T cells to maintain a delicate balance in GC formation and antibody production by B cells.

Keywords: Follicular helper T cells, Germinal centers, Humoral immunity, Mef2d transcription factor, B:T immune synapse, SLAM-associated protein, IL-21 cytokine, Autoimmune disease

Student Number: 2014-22010

Major parts of this thesis were previously published in Sci. Immunol., 2023 Mar 31;8(81):eadf2248.

TABLE OF CONTENTS

LISTS OF TABLES

LISTS OF FIGURES

LIST OF ABBREVIATIONS

Tfh: Follicular helper T

GC: Germinal center

APCs: Antigen-presenting cells

DCs: Dendritic cells

SAP: SLAM-associated protein

IL: Interleukin

Mef2: Myocyte enhancer factor 2

CXCR5: C-X-C chemokine receptor 5

PD-1: Programmed cell death protein 1

PSGL-1: P-selectin glycoprotein ligand 1

ICOS: Inducible T cell co-stimulator

Bcl6: B-cell lymphoma 6

Blimp-1: B lymphocyte-induced maturation protein 1

OVA: Ovalbumin

popLNs: popliteal lymph nodes

SLE: Systemic lupus erythematosus

PBMCs: Peripheral blood mononuclear cells

cTfh: Circulating follicular helper T

INTRODUCTION

1. Differentiation and function of follicular helper T (Tfh) cells

The production of high-affinity antibodies by B cells is crucial for effective defense against pathogens and long-term immune protection against infection, as well as for the development of successful vaccines. After infection or vaccination, B cells undergo affinity maturation within germinal centers (GCs), which are specialized structures that develop in secondary lymphoid tissues. This process allows B cells to improve the quality of their antibodies and enhance their ability to neutralize and eliminate invading pathogens. However, the generation of high-affinity antibodies against self-antigens can lead to the destruction of our body's own tissues and cells through antibody-mediated complement activation or antibody-dependent cell cytotoxicity, ultimately triggering the onset of autoimmune diseases. Pathological antibodies are frequently affinity-matured and isotype-switched, indicating that auto-reactive B cells form GCs to produce autoantibodies. This highlights the importance of precise regulation of the GC reaction in antibody production. As Tfh cells play essential roles in providing specialized assistance to B cells for GC development and affinity maturation, understanding the mechanisms that control Tfh cell differentiation and functions is crucial to elicit protective immune responses against pathogens as well as to gain insights into the pathogenesis of auto-reactive B cells contributing to autoimmune diseases.

1.1 The differentiation of Tfh cells

The Tfh differentiation of CD4 T cells is a multi-stage and multifactorial process

(*1*). It is well-known to initiate when naïve CD4 T cells interact with antigen-presenting cells (APCs), such as dendritic cells (DCs), in the T cell zone of secondary lymphoid organs. During priming by DCs, naïve CD4 T cells receive signals via co-stimulatory and cytokine receptors such as inducible T cell co-stimulator (ICOS) and interleukin-6 (IL-6) receptor, and are instructed to induce Tfh differentiation program. One of critical functions of these signals is to upregulate B-cell lymphoma 6 (Bcl6), a major fate-determining transcription factor of Tfh differentiation. Bcl6 programs Tfh differentiation in CD4 T cells by activating pro-Tfh differentiation genes such as *Cxcr5*, *Pdcd1*, *Icos*, and *Il6r*, while suppressing anti-Tfh differentiation genes (*2*), including *Prdm1*, the gene encodes Blimp-1, a key transcription repressor of the *Bcl6* gene (*3*). In addition to Bcl6, several transcription factors, including T cell factor 1 (Tcf1), Lymphoid enhancer-binding factor 1 (Lef1), Maf, and Basic leucine zipper transcription factor ATF-like (Batf), have been shown to play important roles during early Tfh differentiation. These transcription factors function as positive regulators of *Bcl6* or cooperate with Bcl6 to instruct early Tfh differentiation of CD4 T cells (*4-6*).

A major immunological function of Tfh cells is to assist B cells in the formation of GCs within B cell follicles in secondary lymphoid tissues. Thus, unlike other effector CD4 T cells, Tfh cells need to migrate to the follicle for interaction with cognate B cells. This migration is facilitated by the transcriptional regulation of surface molecules that control the localization of CD4 T cells into T cell zone and B cell follicles. For instance, Bcl6 upregulates the expression of CXCR5, while downregulating the expression of CCR7, the chemokine receptors inducing B and CD4 T cells to migrate to CXCL13-rich B cell follicles and to T cell zone, where CCL19 and CCL21 are highly produced, respectively (*1*). Tfh cells that develop during DC priming in the T cell zone are able to move to the B cell follicle and localize at the B:T border, which is the region where the B cell follicles and the T cell zone are conjoined. At this point, Tfh cells can interact with B cells by

recognizing peptide antigens presented on B cell MHCII molecules through their T cell receptors (TCRs). Once a cognate interaction is established between Tfh cells and B cells, Tfh cells provide "help signals" to B cells, including co-stimulatory molecules such as CD28 and CD40L, as well as adhesion molecules like signaling lymphocyte activation molecule (SLAM) family receptors, leading to the proliferation of B cells and the formation of GCs (*3*).

Interaction with cognate B cells at the B:T border is also crucial for the full maturation of Tfh cells into germinal center Tfh (GC-Tfh) cells. To ensure the migration of Tfh cells into GC areas, full maturation involves further increases in the surface expression of CXCR5, ICOS, and programmed cell death protein 1 (PD-1), and declines in the expression of the chemoattractant receptor Epstein-Barr virus-induced molecule 2 (Ebi2) (*7*) and P-selectin glycoprotein ligand 1 (PSGL-1), respectively. In this process, ICOS and PD-1 are shown to promote CXCR5 upregulation and the downregulation of CCR7 and PSGL-1 expression (*1*), and to inhibit CXCR3 upregulation on Tfh cells, preventing their escape from the follicles and promoting their concentration within the GC area (*8*). The full maturation process also involves the upregulation of SLAM family members and SLAM-associated protein (SAP) expression, which provides positive signals for sufficient B:T communication, a key immunological phenomenon to GC formation (*9*).

1.2 Functions of Tfh cells in GC reaction

GCs are specialized microenvironments within secondary lymphoid tissues where B cells undergo dynamic immunological reactions, leading to clonal expansion and the evolution of BCR affinity to antigens (Ags). Anatomically, GCs are organized into the dark zone (DZ) and light zone (LZ). In the DZ, B cells undergo rapid proliferation and intense somatic hypermutation (SHM) mediated by activation-

induced cytidine deaminase (AID), resulting in the introduction of random mutations into the variable regions of the B cell receptor (BCR) genes. This diversification engenders a B cell of the same germline BCR to generate daughter B cells with varying affinities for the targeted antigens. Subsequently, the daughter GC B cells with diverse BCR affinities to bind to the Ags migrate to the LZ, where they compete for binding to the Ags presented on the surface of follicular dendritic cells (FDCs). B cells expressing BCRs with high-affinity for the Ags have a competitive advantage in capturing and processing the Ags for presentation on MHCII molecules. Therefore, the daughter GC B cells with affinity-matured BCRs can interact with GC-Tfh cells in the LZ and receive signals from them, promoting the migration to the DZ for successive rounds of the evolution of affinity maturation. This collective process contributes to the establishment of a highly effective and long-lasting humoral immune response (*10*).

Tfh cells play a crucial role in supporting the selection of cognate, affinity-matured GC B cells by providing essential signals during the advancement of GC reactions. As B cells progress through the GCs, those expressing BCRs with stronger affinity for the Ags are positively selected. This process needs to be tightly controlled by the immune system to prevent the development of auto-reactive B cells undergoing affinity maturation against self-antigens. It is accomplished by allowing only GC B cells that present cognate peptide antigens on MHCII molecules to form immune synapses with GC-Tfh cells (Checkpoint 1). Through these immune synapses, Tfh cells provide activation signals to GC B cells via co-stimulatory molecules and ligands (i.e., ICOS/ICOS-L and CD40L/CD40), as well as cytokines and cytokine receptors (Checkpoint 2). The interaction between ICOS receptors on GC-Tfh cells and ICOS-L of GC B cells enhances the surface expression of CD40L on GC-Tfh cells (*11*). This, in turn, leads to the pairing of CD40L with CD40 on GC B cells, triggering intracellular signals to promote B cell proliferation via NF-κB – c-Myc pathway (*12*). Additionally,

cytokines produced by GC-Tfh cells support GC B cells in undergoing GC reactions and isotype-switching of immunoglobulin heavy chains. Among these cytokines, IL-21 plays a crucial role in these processes by maintaining *Bcl6* expression and inducing *Aicda* expression in GC B cells, which is a key transcription factor for the GC response (*13, 14*) and functions in class-switch recombination (*15, 16*), respectively. The combined expression of IL-21, IL-2, and IL-4 by Tfh cells, along with CD40L signaling, further contributes to these processes, ultimately resulting in effective protection against pathogens (*17*).

Via GC-Tfh cell-dependent GC responses, Ag-specific B cells differentiate into antibody-secreting plasma cells (PCs) and memory B cells. Although the exact mechanisms by which daughter GC B cells are fate-determined to become PCs or memory B cells are not fully understood, GC-Tfh cell functions appear to play critical roles in this selection process. For instance, strong CD40L signaling from GC-Tfh cells leads to alteration in the expression of surface molecules such as SLAM (CD150), ICAM-1, and CD40 (*18*), thereby facilitating prolonged interaction between GC-Tfh cells and GC B cells. In this context, GC B cells are instructed to undergo PC differentiation through the upregulation of *Irf4* and the downregulation of *Bcl6.* Additionally, the IL-21 cytokine produced by GC-Tfh cells promotes PC differentiation of GC B cells via induction of Blimp-1 expression (*18, 19*). While the mechanisms by which GC-Tfh cells program memory B cell differentiation in GC B cells are not well elucidated, evidence suggests that this process seems to be less dependent on GC-Tfh cell function. Kurosaki and colleagues demonstrated that Ag-specific B cells, in the presence of moderate GC-Tfh help signals, maintain relatively high expression of Bach2, resulting in preferential differentiation into memory B cells (*20*). However, further investigations are needed to fully understand the mechanisms underlying how GC-Tfh cells program memory B cell differentiation pathway(s) (*21, 22*).

2. SLAM-associated protein (SAP) molecule in B:T synapse formation

In the previous chapter, I highlighted the significance of the interaction between CD4 T cells and APCs to properly elicit immune responses of effector CD4 T cells. To achieve this, CD4 T cells need to establish stable interactions with Ag-presenting APCs, facilitated by the formation of immune synapses composed of TCR/Ag complex, co-stimulatory molecules, and adhesion molecules (*23*). While CD4 T cells utilize various molecules in common to establish immune synapse with DCs and B cells, SAP protein is selectively required for the stable synapse formation of CD4 T cells with cognate B cells.

The protein SAP, encoded by the *Sh2d1a* gene, is a 15 kD adaptor protein expressed in T cells, NK cells, and some B cell populations. It plays a crucial role in regulating signaling pathways downstream of SLAM molecules. When the SLAM family molecules are crosslinked, tyrosine phosphorylation occurs on the immunotyrosine switch motif (ITSM) of their cytoplasmic domain, initiating intracellular signal transduction cascades (*24*). SAP, with its single Src homology 2 (SH2) domain, binds to the phosphorylated tyrosine residues on the SLAM molecules, which subsequently recruits downstream protein tyrosine kinases such as Fyn and Lck. The binding of these kinases prevents dephosphorylation of phospho-tyrosine residues and establishes a bridge between the SLAM co-receptor signal and the Ag-specific TCR signal at the immune synapse, ultimately generating activation signals in CD4 T cells (*25*). In the absence of SAP, SH2 domain-containing phosphatase 1 (SHP1) and 2 (SHP2) can be recruited to the phospho-tyrosine residues and transmit inhibitory signals to the immune synapse (*26*).

Although SAP is expressed in both CD4 T and B cells, its expression in CD4 T cells is crucial for stable B:T synapse formation. CD4 T cells lacking SAP exhibit

impaired interaction with B cells, leading to defective GCs and diminished generation of long-lived plasma cells (LLPCs) and memory B cells (*9, 27, 28*). Therefore, SAP deficiencies, observed in X-linked lymphoproliferative disease (XLP), result in compromised immune responses against viral infections, particularly Epstein-Barr virus (EBV) (*29*). This primary immunodeficiency is associated with hypogammaglobulinemia and severe defects in the generation of isotype-switched memory B cells (*30*). Despite its critical roles in B:T synapse formation and GC-dependent humoral immunity, there is currently limited information available on how *SH2D1A* (*Sh2d1a*) gene expression is regulated in CD4 T cells.

3. Similarity between the nervous and immune systems

The synaptic structures play a crucial role in transmitting signals and facilitating intercellular communications both in the central nervous system and in the immune system (*31*). While neuronal synapses are formed between pre- and post-synaptic neurons, immune synapses are established between CD4 T cells and APCs, as well as between CD8 T cells and target cells. Interestingly, these two systems share some features in common to regulate synapse formation. Synaptic structures are built by receptor-ligand interactions and adaptor protein functions, whereas communication signals transit across plasma membranes present between the communicating cells.

Despite autonomously developing specific molecules to regulate synapse formation and downstream signaling, the immune system appears to have adapted certain molecules involved in the nervous system to induce appropriate immune responses. For instance, immune cells utilize receptor-ligand complexes typically involved in neuronal axon guidance as adhesion molecules to facilitate stable interactions in the immune synapse. CD4 T cells express members of the

semaphorin family, such as Sema4A and Sema4C, which are known to interact with plexins to guide neuronal axon growth and modulate synaptic plasticity (*32, 33*). The expression of Sema4A in CD4 T cells is crucial for the priming of CD4 T cells by DCs and the differentiation of effector CD4 T cells, such as Th1 cells, during immune responses to protein Ags (*34*). Additionally, Sema4C plays a role in facilitating the proper recruitment of Tfh cells to germinal centers (GCs) through plexin B2-dependent interactions with GC B cells, thereby promoting the generation of humoral immune responses (*35*). Another example is Ephrin-B1, a transmembrane ligand that interacts with the Eph receptor and is involved in axon guidance and synaptic structure in neuronal cells (*36*). Recent research by Qi and colleagues demonstrated that Ephrin-B1 inhibits the retention of Tfh cells in GCs by interacting with the Eph-B6 receptor and transmitting signaling. This mechanism helps to ensure that the potentially dangerous GC reaction is kept under control (*37*).

In addition to molecules that play roles in cell-to-cell adhesion, the immune system employs cytoplasmic adaptors and signaling molecules from the nervous system to regulate immune synapse formation. Dlgh1, a member of the membrane-associated guanylate kinase (MAGUK) protein family, functions as a neuronal synaptic scaffolding molecule (*38*). Previous study has demonstrated that Dlgh1 plays an important role in organizing TCR-induced activation signal transduction in CD4 T cells by being recruited to the TCR-enriched synaptic sites (*39*). Furthermore, activated CD4 T cells have been found to produce acetylcholine and dopamine, which are well-known neurotransmitters (*40*), indicating potential immunological roles of these signaling molecules. Acetylcholine has been shown to promote the differentiation of B cells into splenic plasma cells (SPPC) after immunization, and CD4 T cell-derived acetylcholine could enhance SPPC generation (*41*). Moreover, Tfh cells in human tonsils have been revealed to produce dopamine, which functions to expand the synapse area via the

accumulation of ICOS-L on the B cell surface (*42, 43*). This expansion facilitates maximal B:T interaction, ultimately accelerating the GC reaction (*43*). Collectively, these findings suggest a co-evolved feature of the nervous and immune systems to fine-tune synapse formation, based on which I hypothesize that the two systems might share regulation circuits in this process.

4. The role of the myocyte enhancer factor 2 (Mef2) transcription factors in the immune and nervous system

4.1 Features of Mef2 transcription factors

Mef2 proteins are a family of transcription factors expressed in various tissues, including muscle, brain, and lymphocytes. In mammals, this family comprises four members: MEF2A (Mef2a), MEF2B (Mef2b), MEF2C (Mef2c), and MEF2D (Mef2d). These transcription factors play crucial roles in regulating transcriptional programs associated with cell differentiation, proliferation, survival, and apoptosis during cell development (*44*).

Mef2 transcription factors are composed of distinct domains, including the MADS-box, MEF2, and C-terminal transactivation domains (TAD). The MADS-box domain is highly conserved across the isoforms and facilitates their binding to the $CC[A/T]_6GG$ motif in DNA. The MEF2 domain, which is relatively conserved among the family members, governs DNA-binding affinity of the Mef2 transcription factors through interaction with co-factors and other Mef2 proteins. In contrast, the TAD undergoes tissue-specific alternative splicing processes, enabling the Mef2 transcription factors to interact with various co-activators and co-repressors and control multiple target genes (*45*). In addition, Mef2 transcription factors exhibit diverse transcriptional activities depending on the nature of extracellular stimuli, homotypic or heterotypic dimerization, and post-translational

modification signals (*46, 47*). Specifically, phosphorylation and dephosphorylation of tyrosine residues of Mef2 protein by various kinases, including PKA, CaMK, and Cdk5, have been shown to regulate DNA-binding affinity, interactions with transcriptional co-activators or co-repressors, acetylation and sumoylation modifications, nuclear and cytoplasmic trafficking, as well as caspase-mediated degradation of the Mef2 transcription factors (*44*).

4.2 Expression patterns of Mef2 transcription factors

Understanding the expression pattern of Mef2 during development is an important step in investigating its potential role in different cell types. In muscle cells, Mef2c expression is detected early in somitic muscle and remains abundant throughout skeletal muscle development, indicating its role in early muscle development and differentiation. On the other hand, Mef2a and Mef2d exhibit delayed expression, approximately a day later, with Mef2d showing a comparatively weaker expression pattern in somitic muscle. The high Mef2a expression in somites containing differentiated muscle fibers suggests its involvement in the later stages of muscle differentiation (*48, 49*).

In neuronal cells, Mef2 isoforms are variably expressed across different brain regions and during developmental stages. For instance, in the cerebellum, abundant expression of Mef2a, Mef2c, and Mef2d persist in granule cells from birth to adulthood, while Mef2b expression decreases during the early stage of development and is not detectable in mature granular cells. In the cortex, Mef2c is the first isoform detected, primarily in immature cortical excitatory neurons. In contrast, Mef2a exhibits robust expression in the developing thalamus. These distinct expression patterns suggest specific roles for Mef2 isoforms in the development and function of discrete neuronal populations (*45*).

Studies using whole or conditional gene knockout mice have discovered that the expression of Mef2 transcription factors is associated with their respective functions in the regulation of target gene expression during muscle and neuronal cells development (*50, 51*). Therefore, investigations of the expression of Mef2 transcription factors in the immune system would provide valuable information to speculate on their roles in regulating the development and functions of immune cells of interest. In a previous study, the abundant presence of *Mef2b* and *Mef2c* transcripts was observed in postnatal and adult spleens, particularly in the region where kappa light chain-expressing B cells are localized, suggesting their enrichment in lymphoid tissue containing B lymphocytes. Furthermore, all four Mef2 isoforms were detected in cell lines representing various stages of B cell differentiation (*52*). Recent studies have further supported these findings by observing the high expression of Mef2c and Mef2d during B cell differentiation (*53*). Additionally, MEF2B expression was found to be elevated in human GC B cells (*54*). Although limited research exists on the expression of Mef2 transcription factors in CD4 T cells, recent studies have reported increased expression of Mef2d in Treg cells compared to other effector cell types (*55, 56*). These findings shed light on the potential roles of Mef2 transcription factors in regulating the differentiation and functions of various immune cells. Further investigations into the expression patterns of Mef2 transcription factors in immune cells will deepen our understanding of their specific contributions to immune responses.

4.3 Mef2 functions in the immune and nervous system

Following the original discovery of Mef2 transcription factors as critical regulators in muscle cell development (*57*), investigations have been conducted to understand their roles in immune and neuronal cells. In the immune system, Mef2 transcription factors exhibit a wide range of functions, from determining the developmental fate

of lymphocytes to regulating differentiation and functions of effector cells. MEF2C upregulates the expression of genes associated with B cell development and B cell transcriptional regulators, such as *RAG*, *EBF1*, and *RUNX1*. Simultaneously, it antagonizes Notch signaling, a crucial regulator of T lineage development, thereby inhibiting T cell lineage differentiation in hematopoietic cells. Hence, MEF2C represents a regulator of B/T lineage fate determination (*58*). In addition, the expression of Mef2c and Mef2d plays a crucial role in early B cell development by forming regulatory complexes with several B cell transcription factors, facilitating coordinated progression through subsequent phases of B cell development (*53*). Moreover, elevated expression of MEF2B in GC B cells directly activates *BCL6*, an essential transcription factor for GC formation (*54*). In CD4 T cells, Mef2c and Mef2d have been found to play critical roles in Treg cells. Increased expression of Mef2d in Treg cells activates genes associated with effector Treg function, including *Il10*, *Ctla4*, and *Icos* (*55*). Although Mef2c is expressed at lower levels in Treg cells compared to Mef2d, recent research has revealed that Mef2c supports the acquisition of regulatory functions by Treg cells by suppressing *Hdac9*, a transcriptional co-repressor of Mef2d. Consequently, Mef2c enables Mef2d to function as a transcriptional activator in Treg cells (*56*).

In the nervous system, Mef2 transcription factors primarily serve as negative regulators of neuronal synapse formation. Mef2a, Mef2c, and Mef2d were found to restrict the number of synapses by modulating the expression of genes involved in synapse development. For example, Mef2a and Mef2d promote the transcription of *Arc* and *SynGAP* genes, which limit the number of excitatory synapses during development (*59*). Arc negatively regulates the surface expression of the AMPA-type glutamate receptors (AMPAR) by promoting their endocytosis, leading to decreased synaptic efficacy and the weakening of synapses (*60*). Similarly, Mef2c regulates *Arc* expression to prevent excessive increase in excitatory postsynaptic sites, resulting in decreased synapse number and function (*61*). Therefore, Mef2

transcription factors play a crucial role in fine-tuning synaptic plasticity in the nervous system.

PURPOSE OF THE STUDY

Effective communication between CD4 T cells and cognate B cells is crucial for the full maturation of CD4 T cells into GC-Tfh cells, as well as for B cells to initiate CD4 T cell-dependent (TD) humoral immune response. Although this interaction occurs in a B:T synapse-dependent manner, the transcriptional regulation of B:T synapse formation by CD4 T cells remains largely unknown. Given the similarities between the nervous system and the immune system in the use of synaptic structures for communication and the use of common molecules to elicit appropriate responses, I hypothesized that molecules that regulate neuronal synapses might play important roles in the regulation of the immune synapse including B:T immune synapses.

Mef2d transcription factor is known to negatively regulate neuronal synapse formation by increasing the expression of genes related to limiting synapse development. Interestingly, a recent study identified a rare genetic variant in the *MEF2D* gene, which has an inhibitory effect on the splicing of the alternative isoform and modifies the target genes, in a subgroup of Swedish SLE patients, and is strongly associated with autoantibodies. These findings suggest a potential role of MEF2D (Mef2d) in the regulation of B:T synapse formation, a critical immune check-point for Tfh cells to mount Ag-specific humoral immune responses from B cells.

Thus, the aim of the study is to investigate whether the MEF2D (Mef2d) transcription factor, known to have a negative effect on neuronal synapse formation, also plays a significant role in the formation of synapses between CD4 T cells and cognate B cells. Furthermore, the study aims to determine the impact of MEF2D (Mef2d) on Tfh and GC-Tfh differentiation of CD4 T cells and TD humoral (auto)immunity.

MATERIALS AND METHODS

Mice

C57BL/6J mice were purchased from DBL (Seongnam, Republic of Korea). μMT and *ROSA26*$^{CAG\text{-}Cas9\text{-}EGFP}$ mice were acquired from Jackson Laboratory. *Mef2d*$^{fl/fl}$ mice (RIKEN BRC) were kindly provided by Dr. Takahisa Furukawa at Osaka University (*62*). *Cd4*^{Cre}*Bcl6*$^{fl/fl}$, OTII, and SMARTA (TCRtg specific for LCMV glycoprotein amino acids 66-77 presented by I-A^{b}) mice were kindly provided by Dr. Shane Crotty. The breeding of all mice strains on a C57BL/6J background was carried out in accordance with the guidelines of the Institute for Experimental Animals at Seoul National University, under specific pathogen-free conditions. TCRtg mice (6-12 weeks of age) were utilized for adoptive transfer experiments with sex- and age-matched recipient mice. All animal experiments were conducted in accordance with the guidelines of the Seoul National University Institutional Animal Care and Use Committee (IACUC # SNU-220713-1).

Human Studies

Healthy donors were recruited from the Department of Otorhinolaryngology and the Department of Pathology at Seoul National University Hospital. Demographic information is provided in **Table 1**. All studies were reviewed and authorized by the SNUH Institutional Review Board (SNUH IRB # 1609-129-795 and 1504-059-664), and written informed consent was obtained from healthy donors prior to their enrollment.

Systemic lupus erythematosus (SLE) patients and healthy individuals were recruited with informed consent after receiving IRB approval from the Department of Rheumatology at Ajou University Hospital (demographic information in **Table**

4). All studies were reviewed and permitted by the Ajou Institutional Review Board (IRB # AJIRB-BMR-SMP-17-155).

Adoptive cell transfer and immunization

To evaluate donor cells, intravenous transfer of naïve, retrovirus-transduced, or RNP-transfected TCRtg CD4 T cells was performed via the retro-orbital sinus, with 0.1-2 × 10^6 cells/mouse transferred on days 3 and 7 (or 8) post-immunization (*63*). After the adoptive transfer, subcutaneous footpad injection of NP-OVA (Biosearch Technologies) or gp61-KLH (GenScript) emulsified in Addavax (InvivoGen) or CFA (Sigma Aldrich) was performed to immunize the mice.

Plasmids and retrovirus production

The coding sequences of murine Mef2a, Mef2b, Mef2d, or Bcl6 were cloned into a retroviral expression vector (pMIG). A site-directed mutagenesis kit (Agilent Technologies) was used to generate the R24L Mef2d-pMIG vector according to the manufacturer's instructions. The plasmid containing the murine Sh2d1a coding sequence was kindly provided by Dr. Hai Qi at Tsinghua University and was cloned into the pMIG-mAmetrine (pMIA) vector. The single-guide RNA (sgRNA) sequences, listed in **Table 5** (https://chopchop.cbu.uib.no), were cloned into the pLsg-mAmetrine (pLsgA) plasmid (provided by Dr. Shane Crotty) (*2*). To produce retrovirus, Plat-E cells were transfected with the plasmids of interest. Culture supernatants were collected at 24 and 48 hours after transfection, filtered through a 0.45 μm syringe filter, and stored at 4 °C until use.

Retroviral transduction

The TCRtg or polyclonal CD4 T cells were isolated from splenocytes using the EasySep kit (STEMCELL Technologies) by negative selection and resuspended in R10 medium [RPMI1640 containing 10 % fetal bovine serum, 2 mM GlutaMax (Gibco), and 100 U/mL penicillin and streptomycin (Biowest)] supplemented with 2 ng/mL recombinant mouse IL-7 (PeproTech), 50 μM β-mercaptoethanol (BME, Gibco), and 1× non-essential amino acids (NEAA, Gibco). The cells were seeded at a concentration of 1×10^6 per well in 24 well plates and stimulated with 8 μg/mL plate-bound anti-CD3 (17A2; BioXcell) and anti-CD28 (37.51; BioXcell). The cells were transduced 24 and 36 hours after stimulation by centrifugation for 90 minutes at 1,500 rpm at 37 °C with retroviral supernatant supplemented with 50 μM BME and 10 μg/mL polybrene (Santa Cruz Biotechnology). The following day after the second transduction, CD4 T cells were transferred into six-well plates in D10 medium [DMEM containing 10 % fetal bovine serum, 2 mM GlutaMax (Gibco), and 100 U/mL penicillin and streptomycin (Biowest)] containing 50 μM BME, 10 ng/mL recombinant mouse IL-2 (PeproTech), and 1× NEAA, and incubated for an additional 3 days. The transduced cells were sorted using FACSAria III (BD Bioscience) based on the expression of fluorescent reporter proteins before adoptive transfer.

Electroporation of ribonucleoprotein (RNP) complex

The CRISPR RNA (crRNA) sequences targeting to murine *Mef2a* or *Mef2d* gene were obtained from CHOPCHOP (listed in **Table 5**). The crRNAs, ATTO 550-conjugated trans-activating CRISPR RNA (tracrRNA), and Cas9 nuclease were purchased from Integrated DNA Technologies. To produce the RNP complexes, the crRNA and tracrRNA were mixed in a 1:1 ratio and duplexed by heating 95 °C for 5 minutes. The Cas9 nuclease was then added to duplexes in a 1:3 ratio. To prepare the cells for transfection, OTII CD4 T cells were isolated and cultured in R10

medium supplemented with 10 ng/mL recombinant mouse IL-7, 10 ng/mL recombinant mouse IL-2, 50 μM BME, and 1× NEAA for 24 hours. Up to 1×10^7 cells were transfected with the RNP complexes using P4 Primary Cell 4D-Nucleofector™ X Kit S (Lonza) on a 4D-Nucleofector X Unit (Lonza), according to the manufacturer's instructions. The transfected cells were then incubated in the medium for an additional 2 or 3 days before being sorted based on the expression of fluorescent reporter protein using FACSAria III (BD Bioscience).

Isolation of human tonsil cells

Tonsil tissues were obtained from healthy donors, fragmented into smaller pieces and homogenized using syringe plungers. Cells were then isolated through density gradient centrifugation for 30 minutes at 400 × g at room temperature using Histopaque (Merck). The isolated cells were resuspended in a freezing medium containing 90 % fetal bovine serum and 10 % sterile DMSO and stored at -80 °C until use. Additional information about donors can be found in **Table 1**.

In vitro polarization of IL-21-producing CD4 T cells

Polyclonal CD4 T cells were obtained and transduced with empty-retroviral (empty-RV) or Mef2d-retroviral (Mef2d-RV) as described in the Retroviral transduction section. During and after transduction, cells were cultured in IL-21 polarizing medium [D10 with 50 μM BME, 10 ng/mL recombinant mouse IL-21 (BioLegend), 10 μg/mL anti-IFNγ (XMG1.2; BioXcell), and 10 μg/mL anti-IL-4 (11B11; BioXcell)] for an additional 4 days.

Flow cytometry

Single-cell suspensions were obtained from draining lymph nodes (LNs) or spleens of mice or after *in vitro* stimulation. The cells were stained with fluorochrome-conjugated antibodies against CD4 (RM4-5), CD45.1 (A20), CD18 (M18/2), and CD19 (6D5) from BioLegend; CD4 (RM4-5), B220 (RA3-6B2), ICOS (7E.17G9), and CD44 (IM7) from eBioscience; PD-1 (J43) from Invitrogen; CD8 (53-6.7), B220 (RA3-6B2), TCR Vα2 (B20.1), CD45.1 (A20), CD45.2 (104), PSGL-1 (2PH1), PD-1 (J43), and Fas (Jo2) from BD Biosciences; PNA (FL-1071) from Vector Laboratories; NP-BSA-Biotin from Biosearch Technologies. The transferred cells were analyzed by FACS on day 3 after immunization using a two-step CXCR5 staining method with a biotinylated anti-CXCR5 (2G8) antibody. For days 7-8 post-immunization, a three-step CXCR5 staining method was used, which involved purified anti-CXCR5 (2G8) antibody from BD Bioscience (*4*). To perform intracellular cytokine staining, cells were stimulated for 3 hours with 40 ng/mL PMA (Merck) and 1.5 μg/mL ionomycin (Abcam) in the presence of 2 μg/mL brefeldin A (Merck). After staining the cell surface markers, cells were fixed, permeabilized using the Foxp3/Transcription Factor Staining Buffer Set (eBioscience), and stained with antibodies against IL-2 (JES6-5H4), IFNγ (XMG1.2), IL-17A (TC11-18H10.1) (from Biolegend), and recombinant mouse IL-21 receptor Fc (R&D Systems) followed by anti-human IgG (Jackson Immunoresearch).

Human mononuclear cells were stained with the following fluorochrome-conjugated antibodies: CD4 (RPA-T4), CD8 (HIT8a), CD45RO (UCHL1) (BioLegend), Fixable Viability Dye, CXCR5 (MU5UBEE) (eBioscience), CD19 (HIB19) (Invitrogen), CXCR5 (RF8B2), and PD-1 (EH12.1) (BD Biosciences). For intracellular SAP or Bcl6 staining, fluorochrome-conjugated antibodies [anti-SAP (1A9) and anti-Bcl6 (K112-91) from BD Biosciences] were used after fixation and permeabilization.

All stained cells were acquired using LSRII, LSRFortessa, or LSRFortessa X-20

(BD Biosciences) and analyzed using FlowJo software v.9.6 (FlowJo).

Quantitative RT-PCR

Enrichment of human CD4 T cells from tonsil samples was performed using biotin-conjugated anti-human CD4 Ab (OKT4, BioLegend) followed by streptavidin microbeads (Miltenyi Biotec). The cells, including GC-Tfh ($CD4^+CD45RO^+PD\text{-}1^{hi}CXCR5^+$), non-Tfh ($CD4^+CD45RO^+PD\text{-}1^-CXCR5^-$), and naïve ($CD4^+CD45RO^-$), were then sorted using a FACSAria III (BD Bioscience). Total RNA was extracted from the sorted human CD4 cells, as well as *in vitro* activated and transduced mouse CD4 T cells, using the RNeasy Mini Kit (Qiagen). The extracted RNA was reverse-transcribed with M-MLV reverse transcriptase (Invitrogen), following the manufacturer's instructions. The synthesized cDNA was then diluted in nuclease-free water and analyzed for target gene expression using SYBR Green Supermix (Bio-Rad) on a CFX Connect Real-Time PCR Detection System (Bio-Rad). The primer sequences used for quantitative analyses of gene expression are described in **Table 5**.

Immunoblot analysis

GC-Tfh, non-Tfh and naïve ($CD45RO^-$ or $CD45RA^+$) CD4 T cells were isolated from human tonsils to measure the amount of MEF2D protein. RV^+ CD4 T cells, $sgRNA^+Cas9^+$ CD4 T cells, or RNP^+ OTII CD4 T cells were examined for Mef2d overexpression or disruption of *Mef2d* or *Mef2a* gene. CD4 T cells and B220 B cells were MACS-isolated from both the *Mef2d* CKO and littermate control mice to confirm CD4 T cell-specific deficiency of Mef2d protein expression in the *Mef2d* CKO mice. Equal numbers of cells were lysed in RIPA buffer (Biosesang) containing a protease and phosphatase inhibitor cocktail (Thermo Fisher

Scientific). The proteins were separated on 8-10 % SDS-PAGE gels and transferred onto PVDF membranes (GE Healthcare). The membranes were incubated overnight at 4 °C with the primary antibodies against MEF2D (Invitrogen; Abcam), MEF2A (Abcam), β-actin (Santa Cruz Biotechnology), and GAPDH (Santa Cruz Biotechnology). After incubation with horseradish peroxidase (HRP)-conjugated secondary antibody for 1 hour at room temperature, the bands were visualized using an ECL detection kit (GE Healthcare) by exposing the membranes to X-ray film (AGFA).

Luciferase assay

A region of approximately 1 kb from the *Sh2d1a* or *Il21* gene, which included potential Mef2d binding sites, was PCR amplified from mouse genomic DNA and cloned into the pGL4.10 vector (*Sh2d1a* +6.9kb-Luc or *Il21* +3.2kb-Luc and *Il21* +6.6kb-Luc, respectively). A vector that included the 3X Mef2 binding sequence, amplified from the 3XMEF2-Luc plasmid (a gift from Dr. Ron Prywes at Columbia University; Addgene plasmid # 32967), was used as a positive control. HEK293T cells were transfected with luciferase plasmids and a β-galactosidase plasmid as an internal control in the presence of empty-pCMV, pCMV-Mef2d, or pCMV-R24L Mef2d plasmids. Three days post-transfection, cells were lysed using the Luciferase Cell Culture Lysis 5X Reagent buffer (Promega), and luminescent signals in the cell lysates were measured with the Luciferase Assay System (Promega) according to the manufacturer's instructions. The luciferase activity was normalized with β-galactosidase activity, which was quantified using o-nitrophenyl-β-D-galactopyranoside (ONPG) substrate.

ELISA

Serum was collected from NP-OVA-immunized *Cd4*^{Cre}*Bcl6*$^{fl/fl}$ mice and stored at -20 °C until analysis. The levels of high- and low-affinity NP-specific antibodies were measured as previously reported (*64*), with slight modifications to quantify low-affinity IgG. In brief, 96 well plates (Thermo Fisher Scientific) were coated with 1-2 μg/mL NP_8-BSA or NP_{49}-BSA in PBS overnight at 4 °C. After washing with PBST (0.1 % Tween 20 in PBS), the plates were blocked with PBST-B (0.5 % BSA and 0.05 % Tween 20 in PBS) for 90 minutes, followed by incubation with serially diluted serum samples in PBST-B for 90 minutes. Following the washing step, the plates were incubated with anti-mouse IgG-HRP (1:5,000 in PBST-B) (GeneTex) for 60 minutes. A colorimetric assay was performed using TMB chromogen solution (Invitrogen), and the reaction was stopped using ELISA Stop solution (Invitrogen). The absorbance was read at 450 and 570 nm (reference wavelength) using a Sunrise microplate reader (Tecan).

Immunofluorescence staining

Popliteal LNs (popLNs) were obtained from C57BL/6J mice that had been received empty-RV or Mef2d-RV CD45.1 OTII CD4 T cells and were immunized with NP-OVA. The LNs were then embedded in OCT medium (Sakura Finetek), frozen, and sectioned into 6 μm thick slice. The sections were fixed with an acetone/methanol solution for 10 minutes at -20 ℃ and blocked with Fc block (2.6G2; BioXcell) for 1 hour at room temperature. The sections were then stained with fluorochrome-conjugated antibodies against TCRβ (H57-597), CD45.1 (A20), IgD (11-26c.2a) (BioLegend), and Fas (Jo2, from BD Biosciences) to distinguish the T cell zone, OTII cells, B cell zone, and germinal centers, respectively. The stained tissues were mounted with mounting solution (Agilent Technologies), and images were scanned using an FV3000 confocal laser scanning microscope (OLYMPUS). The location of OTII cells in each area was analyzed using ImageJ

software (NIH).

In vitro conjugation assay

The B:T conjugation assay (*9, 65*) was conducted as follows: Empty-GFP (CD45.11) and Mef2d-GFP (CD45.12) OTII CD4 T cells were prepared, and splenic B cells were isolated from C57BL/6J mice and stimulated with LPS (1 μg/mL) for two days. The activated B cells were then labeled with 50 μM CMF2HC (Invitrogen) for 30 minutes at room temperature and briefly pulsed with $OVA_{323-339}$ peptide (0, 1, or 10 μg/mL) for 30 minutes at 37 °C. Co-culture of 1.25×10^5 empty-GFP and 1.25×10^5 Mef2d-GFP OTII CD4 T cells with 5.0×10^5 B cells was performed for 20 or 30 minutes at 37 °C.

The DC:T conjugation assay was done similarly to the B:T conjugation assay with the following modifications. Splenic DCs were isolated with CD11c microbeads (Miltenyi Biotec) and subsequently stained with CD11c antibody for 20 minutes at 4 °C. The DCs were then pulsed with $OVA_{323-339}$ peptide for 2 hours at 37 °C. Co-culture of 2.5×10^5 DCs with empty-GFP and Mef2d-mAmetrine OTII CD4 T cells was performed.

Conjugate formation of the respective OTII CD4 T cells with B cells or DCs was analyzed based on the expression of congenic molecule (CD45.11 vs. CD45.12) or the expression of GFP and mAmetrine among CD4 T cells in the conjugates.

ChIP-qPCR

ChIP was performed as described by Abcam (X-ChIP, Abcam) with the following modifications. HEK293T cells were transfected with pGL4.10-*Sh2d1a* +6.9kb in the presence of either empty pCMV or pCMV-Mef2d-HA plasmid. After two days

of transfection, the cells were cross-linked with 0.75 % formaldehyde and 125 mM glycine. Then, the cells were lysed with FA lysis buffer (50 mM HEPES-KOH pH 7.5, 1 mM EDTA pH 8.0, 1 % Triton X-100, 0.1 % sodium deoxycholate, 0.1 % SDS, 140 mM NaCl, and 1X protease inhibitors) and sonicated for 13 minutes to obtain DNA fragments of 200-500 bp (Sonics Materials). Sheared chromatin containing 25 μg of DNA was immunoprecipitated overnight at 4 °C with rotation using an anti-HA antibody (5 μg) (Abcam) conjugated with Dynabeads Protein G (Invitrogen). The Dynabeads-antibody-DNA complex was washed four times, three times with wash buffer (20 mM Tris-HCl pH 8.0, 2 mM EDTA pH 8.0, 1 % Triton X-100, 0.1 % SDS, and 150 mM NaCl) and once with final wash buffer (20 mM Tris-HCl pH 8.0, 2 mM EDTA pH 8.0, 1 % Triton X-100, 0.1 % SDS, and 500 mM NaCl). The complex was then resuspended in elution buffer (100 mM $NaHCO_3$ and 1 % SDS) to remove Dynabeads and antibody-DNA bonds, and the samples were placed on a magnet to collect the supernatants. To purify the precipitated DNA, the crosslinks between the antibody and the DNA were removed by incubating the elutes with proteinase K and RNase for 4 hours at 65 °C, and DNA was purified using the Wizard® DNA Purification Kit (Promega).

The enrichment of target DNA was determined by quantitative PCR using the isolated DNA and the primers described in **Table 5**. To calculate the Mef2d binding enrichment to *Sh2d1a*, the recovery of each ChIP sample transfected with pCMV-Mef2d-HA was normalized to the corresponding ChIP samples transfected with empty-pCMV.

RNA sequencing

$CD45.1^+$ empty-GFP OTII CD4 T cells or $CD45.1^+$ Mef2d-GFP OTII CD4 T cells were transferred into $CD45.2^+$ C57BL/6J mice, which were subsequently immunized with NP-OVA. Three days later, popLNs were collected from 8-12

mice in each group and pooled to separate empty-GFP Tfh from empty-GFP non-Tfh cells or Mef2d-GFP Tfh from Mef2d-GFP non-Tfh cells, which were considered one biological replicate each for RNA-seq analysis. CD45.1$^+$ OTII CD4 T cells were enriched by staining cells with PE-conjugated anti-mouse CD45.1 (eBioscience), followed by anti-PE microbeads (Miltenyi Biotec). Enriched CD45.1$^+$ GFP OTII CD4 T cells were then stained with antibodies against CD4, PD-1, PSGL-1, and CXCR5 to sort PSGL-1$^+$CXCR5$^-$ non-Tfh cells or PSGL-1^{lo}CXCR5$^+$ Tfh cells into Trizol LS reagent (Invitrogen) for RNA extraction.

As previously described, cells were prepared for RNA-seq analysis (*66, 67*). Briefly, total RNA was extracted from the sorted cells (5,000-250,000) using the miRNAeasy micro kit (Qiagen). Approximately 1 ng of isolated RNA was amplified using the Smart-seq2 protocol and the whole transcriptome cDNA was purified using Ampure XP magnetic bead solution (0.8:1 [vol: vol] ratio, Beckman Coulter). Quality control steps were included to determine (i) fragment size distribution quality by capillary DNA electrophoresis, (ii) quantity by fluorescent Picogreen assay (Invitrogen), (iii) the optimal number of PCR preamplification cycles for optimal cDNA amplification, and (iv) fragment size selection efficiency. Samples that failed to reach quality control standards were eliminated from further downstream steps. For each sample, 0.5 ng was used to prepare a volume-reduced Nextera XT reaction (Nextera XT DNA Sample Preparation Kit and Index Kit; Illumina). For optimized sequencing performance, barcoded Illumina sequencing libraries (Nextera; Illumina) were generated and underwent size selection (0.6 to 0.8 volume ratio, Beckman Coulter). Samples that passed all steps were then sequenced to generate more than 8 million 100-bp paired-end reads on a Novaseq6000 (Illumina).

Transcriptome analysis

The paired-end reads were filtered for reads aligned to tRNA, rRNA, adapter sequences, and spike-in controls. The reads were then aligned to the mm10 reference genome using STAR (v2.6.1) (*68*). PRINSEQ Lite (v 0.20.3) (*69*) was used to calculate DUST scores, and low-complexity reads with DUST scores higher than 4 were removed during the generation of the BAM files. The alignment results were parsed using SAM tools (*70*) to generate SAM files. Read counts for each genomic feature were obtained with featureCounts (v 1.6.5) (*71*) using the default option along with a minimum quality cut-off (Phred > 10). The raw read counts obtained after filtering out features with zero counts in all samples were used as input data for the DESeq2 (v 1.24.0) package in R (*72*) to identify differentially expressed genes (DEG) between (1) control Tfh and Mef2d Tfh, (2) control non-Tfh and Mef2d non-Tfh, (3) control Tfh and control non-Tfh, and (4) Mef2d Tfh and Mef2d non-Tfh cells. DEseq2 calculates the size factor of each column (sample) to generate a generalized fitting model for a suitable comparison. The calculated p-values were further adjusted using the Benjamini-Hochberg algorithm for multiple-test correction. Genes with adjusted p-values lower than 0.05 and a fold-change greater than log2 (0.585) were considered as DEGs.

Heat maps

Heatmaps were generated using pheatmap software from R packages with normalized RNA-seq data.

Gene Set Enrichment Analysis (GSEA)

The gene sets were generated by utilizing previously published studies that identified gene lists demonstrating enriched expression in Tfh cells compared to Th1 or Th17 cells (GEO accession code GSE11924) and non-Tfh cells (GEO

accession codes GSE21379 and GSE40068). The enrichment of upregulated genes in control Tfh cells compared with control non-Tfh cells was then ranked using GSEA software (Broad Institute).

Investigation of human peripheral blood mononuclear cells (PBMCs)

Sample preparation: PBMCs were isolated from both SLE patients and healthy donors as previously described (*73*). PBMC samples from the first cohort were subjected to FACS and quantitative RT-PCR (qPCR) analyses, while PBMCs from the second cohort were used to isolate naïve ($CD45RA^+$) CD4 T cells for qPCR analysis.

FACS analysis: PBMCs were stained with Fixable Viability Dye (Invitrogen) in PBS, followed by staining with fluorochrome-conjugated antibodies against CD4 (RPA-T4), CD45RA (HI100), CXCR5 (J252D4), CXCR3 (G025H7), CCR6 (11A9), PD-1 (EH12.2H7), and ICOS (C398.4A) (from BioLegend and BD Biosciences). The staining was performed in MACS buffer (0.5 % FBS, 1 % penicillin and streptomycin, and 2 mM EDTA in PBS) for 30 min at 4°C.

qPCR analysis: Total or naïve CD4 T cells were isolated from PBMCs using either the Human CD4 T cell Isolation Kit (Miltenyi Biotec) or by FACS-sorting. RNA was extracted using Tri Reagent (MRC) according to the manufacturer's instructions. For cDNA synthesis, Oligo(dT) primers (Promega) and the Improm-II Reverse Transcriptase kit (Promega) were used following the manufacturer's instructions. qPCR was performed on a Rotor-Gene Q (Qiagen) using SYBR Premix Ex Taq (Takara). The primer sequences for *MEF2D* and *GAPDH* are listed in **Table 5**.

Quantification of autoantibody production: Serum samples from SLE patients were assessed for the presence of anti-nuclear and anti-dsDNA antibodies. Anti-nuclear antibodies (ANA) were measured using ANA HEp-2 Plus (Generic Assays), and anti-dsDNA was measured using the Amerlex Anti-dsDNA Kit (Trinity Biotech) following the manufacturer's instructions.

MEF (Mef) transcription factor family expression analysis in CD4 T cells

The Human Cell Atlas database (immunecellatlas.net) was utilized to obtain data for analyzing the MEF2 isoforms in human naïve ($TCR\beta^{+}CD45RA^{+}CD62L^{+}$) and effector memory ($CD45RO^{+}$) CD4 T cells. The normalized expression of these isoforms in human CD4 T cells is shown in **Figure 3**.

To measure the expression of Mef2 isoforms in murine Tfh and non-Tfh cells (**Figure 1 and Figure 33**), microarray datasets (GSE24574, GSE21381, and an unpublished dataset from Dr. Shane Crotty's laboratory) were used in addition to my RNA-seq dataset. My RNA-seq dataset was excluded for quantifying the *Mef2d* expression in naïve, non-Tfh, and Tfh cells (**Figure 1**) due to the absence of naïve CD4 T cell samples.

Statistical analysis

The experiments were performed two or three times independently. Data sets were analyzed using Prism 7.0 software (GraphPad) with appropriate statistical tests, including the two-tailed Student's *t*-test, one-way ANOVA with Tukey's multiple comparisons test, two-way ANOVA with Bonferroni's multiple comparisons test, or Pearson's correlation. Statistical significance was set at $P < 0.05$.

Table 1. Information from tonsil donors.

	Number	Name	Gender	Age
Tonsil	Tonsil-1	K○Y	M	4
	Tonsil-2	C○G	M	6
	Tonsil-3	K○G	M	15
	Tonsil-4	P○J	M	4
	Tonsil-5	J○Y	F	15
	Tonsil-6	Y○B	M	16
	Tonsil-7	A○W	F	6
	Tonsil-8	K○H	F	8
	Tonsil-9	K○W	F	5
	Tonsil-10	L○E	F	11

Table 2. Genes regulated by Mef2d in Tfh and non-Tfh cells that developed in mice after NP-OVA immunization.

Upregulated in both Mef2d Tfh and Mef2d non-Tfh cells	Downregulated in both Mef2d Tfh and Mef2d non-Tfh cells
4930420K17RIK	DENND2D
CCL3	DPP4
CCL4	GM4902
CD83	GNG2
CLIC4	GPR183
CTSW	IKZF3
GUCY1A3	KBTBD11
GUCY1B3	NSG2
ITM2A	PYDC3
KLHDC2	S100A11
MAN1A	S100A6
MEF2D	SH2D1A
MYO1E	SIT1
NRGN	SMAD3
PLA1A	ST8SIA1
RGS16	TIGIT
SPP1	IL21
TMBIM1	
TNFSF4	
TWSG1	
ZFP771	

Table 3. Clinical information from SLE patients and healthy individuals.

a. Cohort #1: FACS analysis with PBMC samples and qPCR to measure *MEF2D* mRNA in total CD4 T cells.

	CD4 (% live singlet)	CD45RA-CXCR5- (% CD4)	CXCR3+CCR6- Th1 (% CD45RA-CXCR5-)	CXCR3-CCR6- Th2 (% CD45RA-CXCR5-)	CXCR3-CCR6+ Th17 (% CD45RA-CXCR5-)	CD45RA-CXCR5+ (% CD4)	PD1+ICOS+ cTfh (% CD45RA-CXCR5+)	MEF2D qPCR-Normalized by GAPDH (PBMC CD45RA+ CD4)	SLEDAI	ANA	dsDNA Ig	age	sex
NC 1	48	23.7	30.5	11.2	12.3	17.3						35	F
NC 2	32.7	38	33.4	10.6	8.11	14.6						34	F
NC 3	35.4	36.6	48.7	12.8	6.72	13.9						38	F
NC 4	33.2	16.1	33.9	17.5	14.8	8.51						42	F
NC 5	36	26.6	36.1	30.9	14.2	17.5						43	F
NC 6	49.2	18.6	37	23.6	10.5	9.98						33	F
NC 7	43.4	33.1	28.4	19.4	24.6	16.7		1.95884				44	F
NC 8	52.2	23.4	38.3	22.5	16.1	12.1		2.44528				31	F
NC 9	45.9	21.5	28	23.6	21.7	9.11		2.80889				35	F
NC 10	37.5	35.9	28.1	24	24.8	15.9		0.00832				25	F
NC 11	59.8	28.3	18.2	50.1	13.3	8.62						22	F
NC 12	30.1	27.7	23.5	41.4	16.9	15.6						24	F
NC 13	33.6	29.4	27.9	28.8	18.5	7.39						25	F
NC 14	39.9	53.7	36.4	28.2	12.3	19.3						28	F
NC 15	38.5	37.4	33.6	23.2	15.4	17		1.34723				41	F
NC 16	38.6	32.2	28	28.1	20.9	8.63		0.30355				36	F
NC 17	38.6	34.6	31.3	17.1	17.1	14.8		1.6245				30	F
NC 18	40.8	35.8	22.6	32.8	22.9	15.8	3.7					43	F
NC 19	36.7	33.9	21.4	31.2	26.8	14.6	4.69					42	F
NC 20	42.8	32.4	37.2	19.1	13.5	25	6.75					42	F
NC 21	54.1	34.3	27	22.2	21.2	10.8	3.29					25	F
NC 22	33.7	47.2	24.8	22.1	20.1	12.7	4.16					40	F
NC 23	52.7	34.6	29.8	26.9	16.7	19.8	6.04					41	F
NC 24	27.9	39.1	33.6	22.9	16.3	12.3	4.07					37	F
NC 25	47.6	28.1	29.3	26.3	18.5	14.1	4.45					40	F
NC 26	40.2	21.7	29	18.9	15.8	14.3	5.11					46	F
NC 27	38.4	18.6	30.6	13.9	21.6	12.7	7.25	1.42405				26	F
NC 28	29	34.3	25.2	37.4	19.3	13.6	5.79					25	F
NC 29	50.5	25.4	43.3	30.1	10.5	9.64	3.71					30	F
NC 30	40.1	24.6	17.9	31.7	33.4	11.3	3.57					30	F
NC 31	43.4	17.3	19.3	35.5	26.9	13.3	4.7					20	M
NC 32	40.8	22	28.6	28.7	24.3	11.7	7.15	8.05564				30	F
NC 33	46.8	20.2	30.9	24.7	22.7	11.5	4.37	0.95926				32	F
NC 34	32.3	25.7	14.7	38.9	30.8	13.3	8.26	0.73713				27	F
NC 35	39	22.3	26	19.3	19	12.3	7.73	0.52123				36	F
NC 36	35.6	43.8	27.6	42.1	14.9	17.3	4.81	0.30145				35	F
NC 37	46.8	18.2	27.6	25.6	19.3	8.01	4.99	0.18175				26	F
NC 38	34.8	41.8	16.7	43.6	25.3	12.6	2.85	0.34628				25	F

SLE 1	31	35.1	42.7	15.3	28.5	12.6			18			37	F
SLE 2	11.1	47.2	20.7	25.5	36.5	8.11			20			39	F
SLE 3	16.7	61.3	70.5	5.89	12.8	5.31			16			28	F
SLE 4	34.1	76	54.9	13.3	11.9	12.4			16			44	F
SLE 5	32.5	46.1	52.4	28.2	11.6	7.07			4			42	F
SLE 6	19.1	49.6	43.3	25.3	15.8	14.9			4			36	F
SLE 7	22.2	46.1	24.7	39.9	21.5	9.28			16			29	F
SLE 8	48.2	36.5	33.6	42.6	13.9	7.75		0.14161	4	2560	17.2	42	F
SLE 9	17.2	62.7	19.8	49.9	17.5	21			4			40	F
SLE 10	40.7	37.2	34.7	25.7	13.3	11.1			6			45	F
SLE 11	44.2	36	30.8	53.8	7.2	10.4			6			35	F
SLE 12	17.5	50.7	23	44.4	21.4	11.2		0.71203	8	80	50	35	F
SLE 13	23.9	29.8	31.2	12.1	19.9	16.9		1.07923	3	1280	3	41	F
SLE 14	34.9	18.1	44.8	20.4	20.6	8.38		1.65864	2	320	3	22	F
SLE 15	37.7	25.1	27.3	42.4	16.5	5.06	4.73	0.20877	8	2560	50.8	41	F
SLE 16	21.9	36	38.2	15.6	12.6	12.2	5.19	0.31208	1	2560	3	44	F
SLE 17	27.2	40.9	48.2	37.3	7.03	13.2	7.62	0.79554	6	2560	14	48	F
SLE 18	30.4	26.7	40	23.6	12.6	18.1	4.18	1.23114	0	160	4.4	36	F
SLE 19	38.6	38.6	30.7	27	19.4	13.3	3.87	1.27456	2	640	3	37	F
SLE 20	43.3	26.9	20.2	41.5	19.9	10.2	4.1	1.42405	4	80	18.4	41	F
SLE 21	35.4	45.3	46.7	19.4	12.4	15.5	3.83	1.56917	2	640	3.7	38	F
SLE 22	21.7	43.1	34.9	33.8	17.6	12.8	4.82	0.62417	4	320	3	36	F
SLE 23	35.9	32	12.5	73.1	11.6	5.18	8.61	0.37371	4	640	74.9	54	F
SLE 24	50.4	44.7	42.9	22.3	12.7	14.3	8.23	0.62851	2	2560	9.4	45	F
SLE 25	50.8	31.5	44.9	14.4	11.4	13.3	3.31	0.57435	0	80	3	57	F
SLE 26	42.3	51.4	51.8	30.9	7.72	12.6	7.2	0.78458	0	80	3	67	F
SLE 27	25.5	56.1	15.9	56.5	18.3	8.07	12.1	0.37631	12	320	98	38	F
SLE 28	28.4	42.3	25.1	19.1	22.3	14.6	15.7	0.10295	4	2560	3.5	49	F
SLE 29	32.1	45	13.3	36.3	38.9	13.4	11.5	0.39502	10	40	13.7	26	F
SLE 30	20.2	47.7	11	66.8	18.4	9.28	12.4	0.0819	8	640	177	43	F
SLE 31	29.1	61.8	1.7	58.6	39.1	10.8	17.9	0.07179	8	1280	59.7	36	F
SLE 32	43.3	40.3	10.1	73	15.3	5.91	25.6	0.2059	6	1280	3	24	F
SLE 33	42.9	28.1	29.1	37.3	17.7	13	3.05	0.44751	2	40	3	40	F
SLE 34	43.3	30	24.2	35.6	26.9	12.2	5.99	0.25703	4	1280	7	46	F
SLE 35	44	34.1	18.3	48.4	21.7	16.1	6.85	0.46009	6	2560	81	37	F
SLE 36	10.8	74.2	7.53	79.6	11.5	4.04	26.7	0.16724	22	1280	94	44	M
SLE 37	23.1	36.9	28.1	42.4	17.9	11.9	7.15	0.23005	2	2560	6	45	F
SLE 38	23.5	41.7	26.1	46.1	14.8	19.1	4.37	0.26794	3	2560	9	27	F
SLE 39	33.7	36.7	16.5	28.6	25.2	13	8.26	0.30779	2	2560	7	24	M
SLE 40	25.4	47	58.7	15.7	8.87	17.8	19	0.22846					
SLE 41	28.3	48.8	41.3	23.7	15.9	16.7	20.9	0.22376	7	2560	94	31	F
SLE 42	44.4	25.3	27.7	29	17.8	13.7	5.95	0.25703	8	2560	3	47	F
SLE 43	30.2	31.1	48.8	20.7	9.43	15.6	8.76	0.33681	0	640	3	53	F

b. Cohort #2: qPCR to measure *MEF2D* mRNA levels in CD45RA^{+} naïve CD4 T cells.

	SLEDAI	Age	Sex
NC 1		26	F
NC 2		41	F
NC 3		41	F
NC 4		29	F
NC 5		30	F
NC 6		41	F
NC 7		37	F
NC 8		35	F
NC 9		44	F
NC 10		29	F
NC 11		41	F
SLE 1	16	47	F
SLE 2	2	31	F
SLE 3	18	30	F
SLE 4	0	58	F
SLE 5	6	50	F
SLE 6	4	51	F
SLE 7	0	55	F
SLE 8	4	40	F
SLE 9	2	51	F
SLE 10	13	28	F
SLE 11	5	42	F
SLE 12	4	34	F
SLE 13	2	45	F
SLE 14	2	31	F
SLE 15	0	44	F
SLE 16	4	49	F
SLE 17	1	44	F
SLE 18	16	47	F
SLE 19	2	31	F
SLE 20	6	39	F
SLE 21	8	40	F
SLE 22	10	26	F

Table 4. Demographic information from SLE patients and healthy individuals.

a. Cohort #1

	SLE Patients (n=43)	Healthy Individuals (n=38)
Age (years, mean ± SD)	39.74 ± 9.17	33.26 ± 7.20
Female / Male	40 / 2 (1 unknown)	37 / 1
SLEDAI (mean, (range))	6.29 (0 - 22)	-
Active SLE (SLEDAI, n=13)	13.08 (8 - 22)	-
Inactive SLE (SLEDAI, n=29)	3.24 (0 - 7)	-

b. Cohort #2

	SLE Patients (n=22)	Healthy Individuals (n=11)
Age (years, mean ± SD)	41.5 ± 9.26	35.82 ± 6.32
Female / Male	22 / 0	11 / 0
SLEDAI (mean, (range))	5.68 (0 - 18)	-
Active SLE (SLEDAI, n=13)	12.6 (8 - 18)	-
Inactive SLE (SLEDAI, n=29)	2.75 (0 - 7)	-

Table 5. Sequences of sgRNAs and crRNAs used for CRISPR/Cas9-mediated editing and sequences of primers used in qPCR and ChIP assays.

Primers	Sequences	Sources
qPCR	Human *BCL6* F: ACTCTGAAGAGCCACCTGCG	Primer3
	Human *BCL6* R: TTTGTGACGGAAATGCAGGTTA	
	Human *PRDM1* F: TGGAAGATCTGACCCGAATC	Primer3
	Human *PRDM1* R: ATGTCATCCTCCACGTCCTC	
	Human *MEF2A* F: GGCATGGAGCATATGGACTT	Primer3
	Human *MEF2A* R: TTAGCGTCGTCCCCTCTCTA	
	Human *MEF2B* F: CCCCAGTCAGCATCAAGTCT	Primer3
	Human *MEF2B* R: CAAGGGATAGGGGAAGGTCT	
	Human *MEF2C* F: CCATCAGCCATTTCAACAAC	Primer3
	Human *MEF2C* R: CTAGTGCAAGCTCCCAACTG	
	Human *MEF2D* F: GACAAGGCCCAGTTTTGTGT	Primer3
	Human *MEF2D* R: GTAGAGGCCCCTCTGCTTCT	
	Human *GAPDH* F: GGATTTGGTCGTATTGGG	PrimerBank
	Human *GAPDH* R: GGAAGATGGTGATGGGATT	
	Mouse *Mef2d* F: AACCGTCCAGGAAACTGTTG	Primer3
	Mouse *Mef2d* R: GAGGAAGGCAAGAACACAGC	
	Mouse *Bcl6* F: CCTGAGGGAAGGCAATATCA	Primer3
	Mouse *Bcl6* R: TTCACGGGGAGGTTTAAGTG	
	Mouse *Gapdh* F: AAGGTCATCCCAGAGCTGAA	Primer3
	Mouse *Gapdh* R: CTGCTTCACCACCTTCTTGA	
ChIP	*Sh2d1a* F: GTGATTAACAAAGGCACAGCA	Primer3
	Sh2d1a R: GCACAGAAAGACAAATAGTACAAGA	

sgRNAs	Sequences	Sources
sgCd8	GCAGGTTCAGCGACAGAAAGCGG	CHOPCHOP
sgMef2d #1	AGGGCTGCGTTCACGACTTGGGG	CHOPCHOP
sgMef2d #2	TCCGTTCATCAGTGATTCGCTGG	CHOPCHOP

crRNAs	Sequences	Sources
crCd8	GCAGGTTCAGCGACAGAAAGCGG	CHOPCHOP
crMef2d #1	AGGGCTGCGTTCACGACTTGGGG	CHOPCHOP
crMef2d #2	CACTGATGAACGGAACCGCCAGG	CHOPCHOP
crMef2d #3	CGTAAGGGATGATGTCACCAGGG	CHOPCHOP
crMef2a #1	TTAGTGTACGACAAAGCATTAGG	CHOPCHOP
crMef2a #2	GCTTTGTCGTACACTAACCCAGG	CHOPCHOP
crMef2a #3	GATGGGGTCATTCTATCACGGGG	CHOPCHOP

RESULTS

The differentiation of GC-Tfh cells is suppressed by Mef2d

The MEF2D (Mef2d) transcription factor is known to play a crucial role in regulating the transcription of genes involved in the formation of neuronal synapses (*59, 74*). Given that Tfh cells use nervous system molecules to regulate synapse formation with B cells (*1, 75*), MEF2D (Mef2d) transcription factors might also play a role in Tfh differentiation of CD4 T cells. To investigate this hypothesis, I first analyzed the expression of *MEF2D* transcription factor in tonsillar GC-Tfh (PD-1^{hi}CXCR5^{+}) and non-Tfh (PD-1^{-}CXCR5^{-}) cells (**Figure 1A**), which express high levels of *BCL6* and *PRDM1* mRNA, respectively (**Figure 1B**), as previously reported (*76*). I found that *MEF2D* expression was significantly lower in GC-Tfh cells compared to non-Tfh effectors and naïve CD4 T cells at both mRNA (**Figure 1C**) and protein (**Figure 1D**) levels. Similarly, in murine CD4 T cells, Tfh cells showed a significant reduction in *Mef2d* transcripts (**Figure 1E**).

Based on the similarity in expression patterns between MEF2D (Mef2d) and BLIMP-1, a well-known transcription factor that opposes Tfh differentiation, MEF2D (Mef2d) might have an inhibitory role in the Tfh (GC-Tfh) differentiation of CD4 T cells. To test this possibility, I adoptively transferred Mef2d overexpressed OTII T cell receptor transgenic (TCRtg) CD4 T cells, that react with the ovalbumin (OVA) 323-339 peptide, into C57BL/6J recipients and analyzed the GC-Tfh differentiation in these cells following 4-hydroxy-3-nitrophenylacetyl (NP)-OVA immunization (**Figure 2A-B**). The frequency of OTII CD4 T cells in the popliteal lymph nodes (popLNs) after NP-OVA immunization was not altered by the ectopic expression of Mef2d in OTII CD4 T cells (**Figure 2C**). However, GC-Tfh cells were significantly reduced, and non-Tfh cells were expanded in Mef2d-RV OTII CD4 T cells compared to the controls (**Figure 2D**). In addition, the

surface expression of PD-1 and CXCR5 on the Mef2d-RV OTII CD4 T cells was significantly decreased compared to the controls (**Figure 2E-F**).

Significant defects in GC-Tfh differentiation caused by ectopic Mef2d expression were also observed in Sm TCRtg CD4 T cells that recognize the glycoprotein (gp) 66-77 peptide of the lymphocytic choriomeningitis virus (LCMV). Eight days after gp61-keyhole limpet hemocyanin (KLH) immunization (**Figure 3A**), Mef2d-RV Sm CD4 T cells developed significantly lower PD-1^{+}CXCR5^{+} GC-Tfh cells compared to the controls (**Figure 3B**), with reduced surface expression of PD-1 and CXCR5 (**Figure 3C-D**). Thus, these findings indicate that Mef2d negatively regulates GC-Tfh differentiation of CD4 T cells in the context of acute protein immunization.

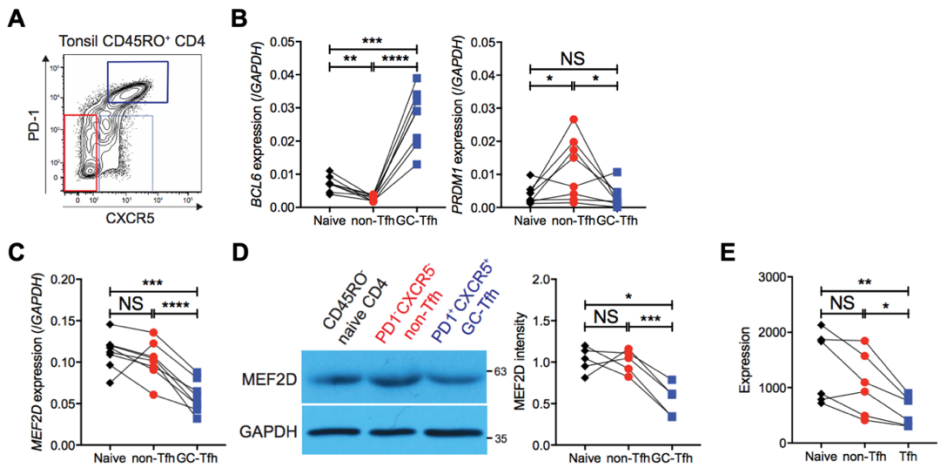

Figure 1. *MEF2D* (*Mef2d*) expression in human and murine effector CD4 T cells.

(A) A gating strategy was used to isolate PD-1^{+}CXCR5^{+} GC-Tfh cells and PD-1^{-} CXCR5^{-} non-Tfh cells from tonsillar CD45RO^{+} CD4 T cells.

(B) The mRNA expression levels of *BCL6* and *PRDM1* were measured by qPCR. The expression levels were normalized to *GAPDH* mRNA.

(C) *MEF2D* mRNA expression by human tonsillar naïve, non-Tfh, and GC-Tfh cells.

(D) Representative immunoblots of MEF2D and GAPDH protein. The band intensity of MEF2D was normalized by GAPDH band intensity.

(E) *Mef2d* expression in murine naïve, non-Tfh, and Tfh cells.

Statistical significance values were determined using two-tailed Student's *t*-test. NS, statistically non-significant; * p <0.05; ** p <0.01; *** p <0.001; **** p <0.0001.

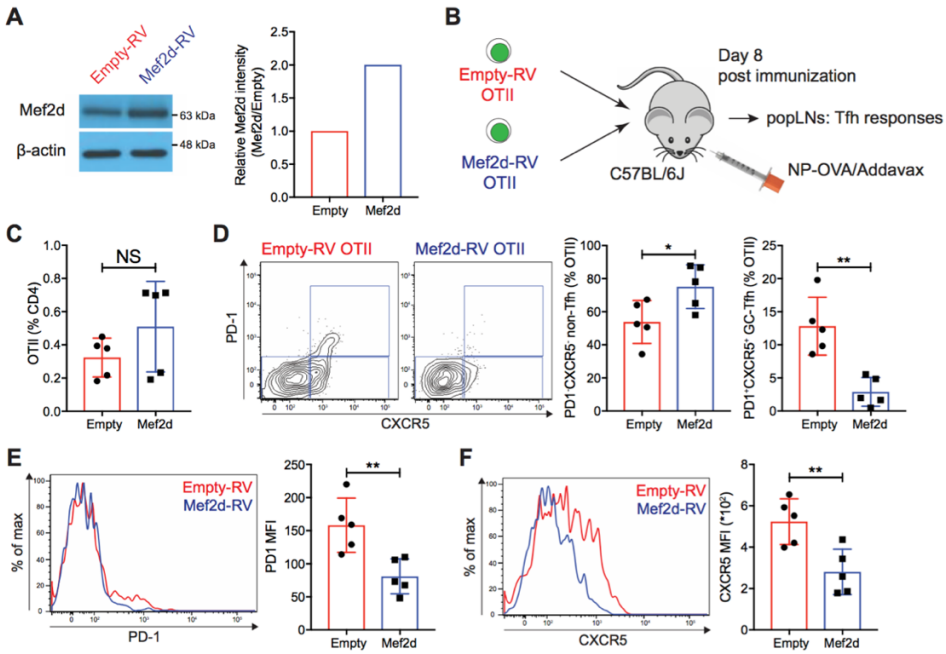

Figure 2. Inhibition of GC-Tfh formation of OTII CD4 T cells by Mef2d.

(A) Immunoblots of β-actin and Mef2d protein. Relative Mef2d band intensity of Mef2d-RV cells compared to those of empty-RV cells.

(B) The experimental scheme: Equal numbers of empty-RV or Mef2d-RV OTII CD4 T cells were adoptively transferred into recipients. Eight days after NP-OVA immunization, popLNs were examined for GC-Tfh differentiation of GFP^+ OTII CD4 T cells.

(C) The frequencies of GFP^+ OTII CD4 T cells in total CD4 T cells.

(D) The flow cytometry plots of GFP^+ OTII CD4 T cells and quantified frequencies of $PD\text{-}1^-CXCR5^-$ non-Tfh and $PD\text{-}1^+CXCR5^+$ GC-Tfh cells among GFP^+ OTII CD4 T cells.

(E and F) Overlaid histograms of PD-1 **(E)** and CXCR5 **(F)** in empty-RV (red) or Mef2d-RV (blue) OTII CD4 T cells. The MFIs were calculated.

Representative of two independent experiments with n=4-5 per group. Error bars indicate mean with SD. Statistical significance values were determined using two-tailed Student's *t*-test. NS, statistically non-significant; * p <0.05; ** p <0.01.

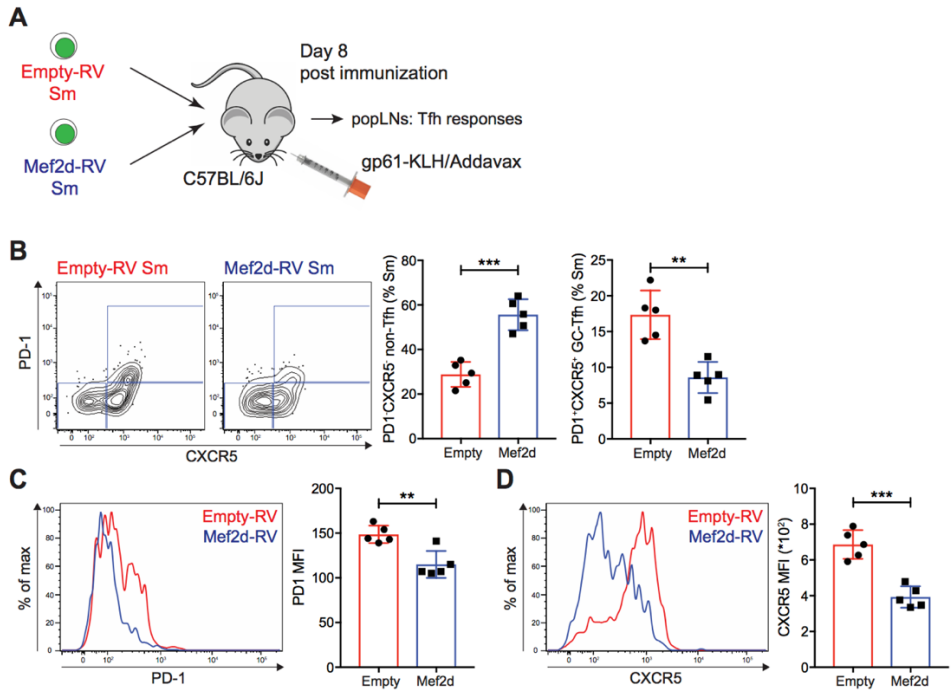

Figure 3. Impaired GC-Tfh differentiation of Sm CD4 T cells by ectopic Mef2d expression.

(A) The experimental scheme: Empty-RV or Mef2d-RV Sm CD4 T cells were transferred to recipients. Eight days after gp61-KLH immunization, popLNs were analyzed for GC-Tfh differentiation of donor GFP^+ Sm CD4 T cells.

(B) The flow cytometry plots of GFP^+ Sm CD4 T cells. The frequencies of $PD\text{-}1^-CXCR5^-$ non-Tfh and $PD\text{-}1^+CXCR5^+$ GC-Tfh cells were quantified.

(C and D) Overlaid histograms of PD-1 **(C)** and CXCR5 **(D)**. The MFIs were calculated.

Representative of two independent experiments with n=5 mice per group. Error bars indicate mean with SD. Statistical significance values were determined using two-tailed Student's *t*-test. ** p <0.01; *** p <0.001.

Mef2d function in CD4 T cells hinders the early Tfh differentiation

As ectopic Mef2d expression resulted in significant defects in GC-Tfh cell formation, I examined whether Mef2d might play inhibitory roles during the early stage of Tfh differentiation of CD4 T cells as well. Three days after NP-OVA immunization (**Figure 4A**), ectopic Mef2d expression did not affect the frequency of OTII CD4 T cells in the popLNs (**Figure 4B**), indicating that it does not induce apoptosis in mature CD4 T cells during the immune response to acute protein immunization. This is in contrast to its known pro-apoptotic functions downstream of TCR-mediated Ca^{2+} influx during T cell development (*77*). Again, Mef2d overexpression resulted in a significant reduction in the frequencies of PD-1^{+}CXCR5^{+} and PSGL-1^{lo}CXCR5^{+} Tfh cells (**Figure 4C-D**), which was accompanied by a decrease in the expression levels of canonical Tfh cell markers (PD-1 and CXCR5) (**Figure 4E-F**) and an increase in the expression levels of PSGL-1 (**Figure 4G**).

The expression of CD25, a high-affinity IL-2 receptor subunit, as well as IL-2 production was comparable between empty-RV and Mef2d-RV OTII CD4 T cells (**Figure 5A-B**). Furthermore, there was no significant difference in IFN-γ and IL-17A production between these groups (**Figure 5C**), indicating that ectopic Mef2d expression did not influence the overall activation and Th1/Th17 differentiation of CD4 T cells.

While cognate B cells are the primary APCs responsible for Tfh differentiation between 72 and 96 hours after acute viral infection (*78*), an earlier dependence of antigen (Ag)-specific CD4 T cells on cognate B cells for Tfh differentiation was observed in the context of protein immunization. 72 hours after NP-OVA immunization (**Figure 6A**), the generation of PD-1^{+}CXCR5^{+} and PSGL-1^{lo}CXCR5^{+} Tfh cells from OTII CD4 T cells was significantly reduced in B cell-

deficient μMT mice compared to C57BL/6J mice (**Figure 6B-C**). These results suggest that Mef2d might function during cognate B cell-dependent Tfh differentiation.

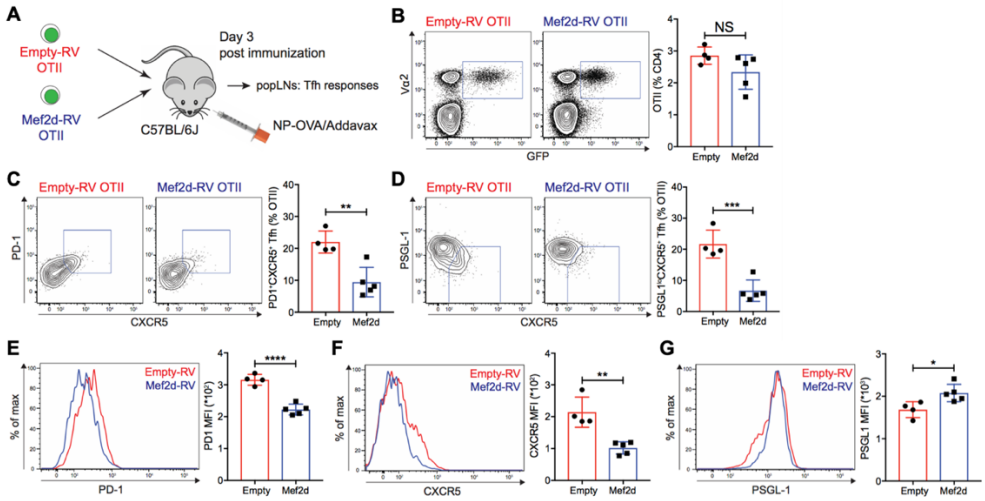

Figure 4. Early Tfh differentiation of OTII CD4 T cells is impeded by Mef2d.

(A) The experimental design: Empty-RV or Mef2d-RV OTII CD4 T cells were transferred to recipients. Three days after NP-OVA immunization, Tfh differentiation of the donor OTII CD4 T cells was examined.

(B) The flow cytometry plots of CD4 T cells. The frequencies of $V\alpha2^{+}GFP^{+}$ OTII CD4 T cells were quantified.

(C and D) The flow cytometry plots of the donor OTII CD4 T cells. The frequencies of PD-$1^{+}CXCR5^{+}$ **(C)** and PSGL-$1^{lo}CXCR5^{+}$ **(D)** Tfh cells were calculated.

(E to G) Overlaid histograms of PD-1 **(E)**, CXCR5 **(F)**, and PSGL-1 **(G)**. The MFIs were quantified.

Error bars indicate mean with SD. Statistical significance values were determined using two-tailed Student's *t*-test. NS, statistically non-significant; * p <0.05; ** p <0.01; *** p <0.001; **** p <0.0001.

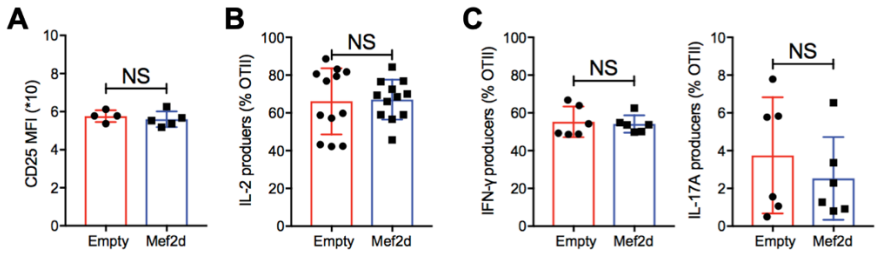

Figure 5. Enhanced Mef2d expression does not perturb the expression of CD25 and production of IL-2, IFN-γ, and IL-17A in CD4 T cells.

(A) Quantification of CD25 MFIs from empty-RV and Mef2d-RV OTII CD4 T cells in **Figure 4**.

(B and C) RV^+ OTII CD4 T cells were adoptively transferred into C57BL/6J recipients, which were subsequently immunized with NP-OVA/Addavax (to analyze IL-2 and IFN-γ producers) and NP-OVA/CFA (to measure IL-2 and IL-17A producers). Three days later, RV^+ OTII CD4 T cells were examined for cytokine production. The frequencies of IL-2 **(B)** and IFN-γ and IL-17A **(C)** producing OTII CD4 T cells among the RV^+ OTII CD4 T cells were quantified. Composite data from two independent experiments using n=6-12 recipient mice per group for NP-OVA/Addavax and NP-OVA/CFA conditions **(B-C)**.

Error bars indicate mean with SD. Statistical significance values were determined using two-tailed Student's *t*-test. NS, statistically non-significant.

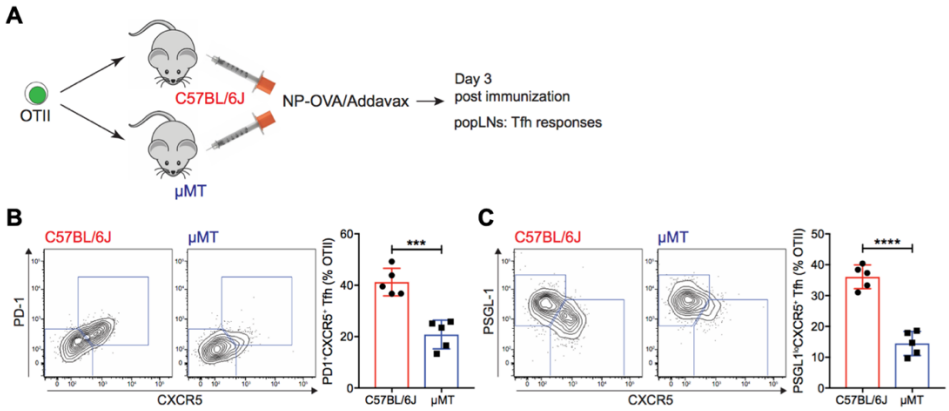

Figure 6. Cognate B cell-dependent Tfh differentiation of CD4 T cells.

(A) Naïve CD45.1 OTII CD4 T cells were adoptively transferred into either CD45.2 C57BL/6J or CD45.2 B cell-deficient μMT mice. Three days after immunization with NP-OVA, the donor OTII CD4 T cells were examined for Tfh differentiation.

(B and C) The flow cytometry plots of the transferred OTII CD4 T cells. The frequencies of PD-1^{+}CXCR5^{+} **(B)** and PSGL-1^{lo}CXCR5^{+} **(C)** Tfh cells were quantified.

Representative of two independent experiments with n=5-6 mice per group. Error bars indicate mean with SD. Statistical significance values were determined using two-tailed Student's *t*-test. *** p <0.001; **** p <0.0001.

Mef2d transcriptionally represses the *Sh2d1a* gene in CD4 T cells

I next aimed to investigate the mechanism by which Mef2d negatively regulates cognate B cell-dependent Tfh and GC-Tfh differentiation. I performed RNA-seq on PSGL-1^{lo}CXCR5^{+} Tfh and PSGL-1^{hi}CXCR5^{-} non-Tfh cells derived from OTII CD4 T cells infected with empty-RV (control Tfh and control non-Tfh) or Mef2d-RV (Mef2d Tfh and Mef2d non-Tfh) three days after NP-OVA immunization (**Figure 7A**). DE-seq analyses showed that genes related to positive regulation (*Cxcr5*, *Bcl6*, *Tox2*, *Sh2d1a*, *Tcf7*, and *Pdcd1*) and negative regulation (*Ccr7*, *Klf2*, *Id2*, *Bach2*, and *Selplg*) of Tfh differentiation were highly expressed in control Tfh and control non-Tfh cells, respectively (**Figure 7B**). The quality of RNA-seq datasets was further validated by the observation that control Tfh cells exhibited a strong enrichment for Tfh gene signatures, which were previously identified from transcriptomic analyses of Tfh and non-Tfh cells that developed in response to various immunological stimuli (*79-81*) (**Figure 7C**).

To identify potential targets of Mef2d, gene expression profiles between control Tfh cells and Mef2d Tfh cells, as well as between control non-Tfh cells and Mef2d non-Tfh cells were compared. The analysis showed that Mef2d-RV OTII CD4 T cells and empty-RV OTII CD4 T cells that developed into Tfh and non-Tfh compartments differentially expressed approximately 320 genes ($p_{adj} < 0.05$; more than 1.5-fold). Specifically, the Tfh compartment had 175 differentially expressed genes and the non-Tfh compartment had 142 differentially expressed genes (**Figure 8A**). Although the possibility of Mef2d directly or indirectly regulating genes involved in Tfh (*Bcl6*, *Tcf7*, and *Cxcr5*) or non-Tfh (*Prdm1*, *Bach2*, *Klf2*, and *Ccr7*) differentiation could not be excluded (**Figure 8B-C**), I focused on identifying genes that showed changes in expression in the same direction (upregulated or downregulated) in both Tfh and non-Tfh compartments as a result

of increased Mef2d function. Among the 317 genes, 21 and 17 genes met this criterion, respectively (**Table 2**). These genes were regarded as potential targets of Mef2d in the regulation of Tfh and GC-Tfh differentiation of CD4 T cells.

One of the 17 genes that exhibited decreased expression in both Tfh and non-Tfh cells upon ectopic Mef2d expression was *Sh2d1a*. In Mef2d Tfh cells, the *Sh2d1a* RPKM was as low as that in control non-Tfh cells, which are effector CD4 T cells that do not require interaction with cognate B cells, and its expression further decreased in Mef2d non-Tfh cells (**Figure 9A**). This gene encodes SAP, an essential adapter molecule required for CD4 T cells to establish a synapse with cognate B cells (*9, 82*), thus is crucial for the cognate B cell-dependent Tfh differentiation and full maturation of GC-Tfh (*1, 75*). Therefore, Mef2d might control Tfh and GC-Tfh differentiation of CD4 T cells by repressing the transcription of the *Sh2d1a* gene. To test this hypothesis, I searched for potential DNA-binding sites ([C/T]TA[T/A]$_4$TA[G/A]) of the Mef2 transcription factor family (*83*) in the genomic DNA region of the murine *Sh2d1a* gene. The putative DNA-binding site for Mef2 (TATTTTTAG) was found in the region around the +6.9 kb from the transcription start site (TSS) of the *Sh2d1a* gene (**Figure 9B**). To investigate whether Mef2d could directly regulate *Sh2d1a* expression, a 1 kb DNA region of the *Sh2d1a* gene including the putative Mef2 binding site was cloned into the pGL4.10 luciferase plasmid (*Sh2d1a* +6.9kb-Luc). The pGL4.10 luciferase plasmid containing three Mef2 binding sites (Mef2 3X-Luc) was used as a positive control. Co-expression of Mef2d with the *Sh2d1a* +6.9kb-Luc plasmid increased luciferase activity in a dose-dependent manner (**Figure 9C**), indicating that Mef2d can bind to this regulatory region of the *Sh2d1a* gene and modulate its expression. To confirm the direct binding of the Mef2d transcription factor to identified site, I conducted ChIP-qPCR using an anti-HA$_{98\text{-}106}$ antibody that specifically pulled down DNA regions bound by the Mef2d transcription factor with its N-terminal domain tagged with an influenza hemagglutinin (HA$_{98\text{-}106}$) molecule. The DNA

region containing the corresponding Mef2 binding site within the +6.9 kb region on the *Sh2d1a* gene was enriched approximately three-fold in the presence of Mef2d-HA co-transfection (**Figure 9D**), providing further evidence of direct binding of Mef2d to the regulatory region of the *Sh2d1a* gene. Then, I investigated whether Mef2d could inhibit the expression of SAP protein in CD4 T cells. Polyclonal CD4 T cells were stained for intracellular SAP protein after transduction with either empty-RV or Mef2d-RV. Ectopic Mef2d expression of CD4 T cells significantly reduced SAP protein expression compared to that of controls (**Figure 9E**), strongly indicating that Mef2d is able to directly modulate SAP expression in murine CD4 T cells.

MEF2D also negatively regulates SAP expression in human effector CD4 T cells. In human tonsils, $BCL6^{+}CXCR5^{+}$ GC-Tfh cells expressed SAP protein at higher levels than $BCL6^{-}CXCR5^{-}$ non-Tfh cells (**Figure 10A-B**). The magnitude of SAP expression was inversely correlated with *MEF2D* mRNA expression in these two compartments (**Figure 10C**). Additionally, the negative correlation between *MEF2D* and *SH2D1A* gene expression observed in tonsillar GC-Tfh cells (**Figure 10D**) suggests that, apart from its ability to bind to the *Sh2d1a* loci and repress its expression in CD4 T cells, MEF2D might control GC-Tfh differentiation through transcriptional regulation of SAP expression.

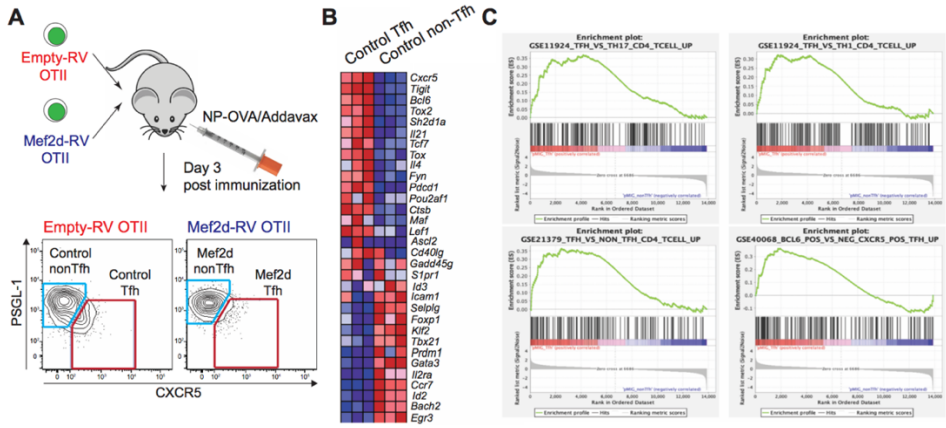

Figure 7. Gene expression analyses for screening potential Mef2d target genes.

(A) Empty-RV or Mef2d-RV CD45.1 OTII CD4 T cells were transferred to recipients and subsequently immunized with NP-OVA. Three days post-immunization, CD45.1 GFP^{+} OTII CD4 T cells were sorted into PSGL-1^{hi}CXCR5^{-} non-Tfh cells and PSGL-1^{lo}CXCR5^{+} Tfh cells.

(B) The heatmap displays the expression of genes of interest in control Tfh and control non-Tfh cells, with high expression (red) and low expression (blue).

(C) GSEA of the Tfh cell gene signatures observed by control Tfh cells compared to control non-Tfh cells.

RNA-seq analysis was performed on three biological replicates of Tfh cells and non-Tfh cells developed from empty-RV or Mef2d-RV OTII CD4 T cells. Each biological sample was obtained by sorting GFP^{+} Tfh and GFP^{+} non-Tfh cells from 8-12 recipient C57BL/6J mice per group.

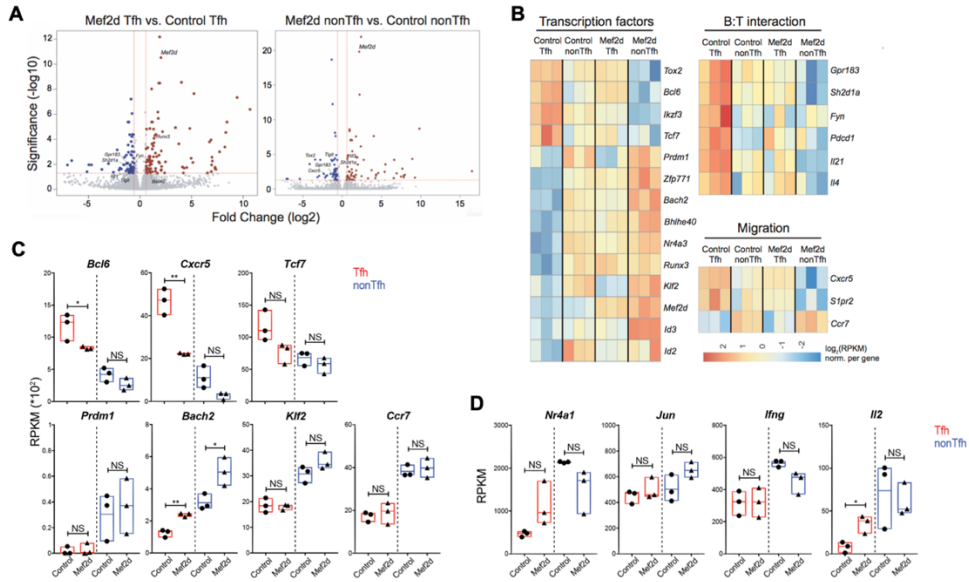

Figure 8. Differentially expressed genes by ectopic Mef2d expression.

(A) Volcano plots, whose gene expression was up-regulated (red) or down-regulated (blue) in Tfh or non-Tfh cells by ectopic Mef2d expression.

(**B**) Genes that were differentially expressed in control Tfh, control non-Tfh, Mef2d Tfh, and Mef2d non-Tfh cells are shown, with high (red) to low (blue) expression levels.

(C) RPKMs of genes that have been shown to play important roles in Tfh differentiation and function were measured in Tfh and non-Tfh cells developed from empty-RV (circles) or Mef2d-RV (triangles) OTII CD4 T cells **(Figure 7)**.

(D) RPKMs of *Nr4a1, Jun, Ifng, and Il2* genes in control Tfh, Mef2d Tfh, control non-Tfh, and control Tfh cells.

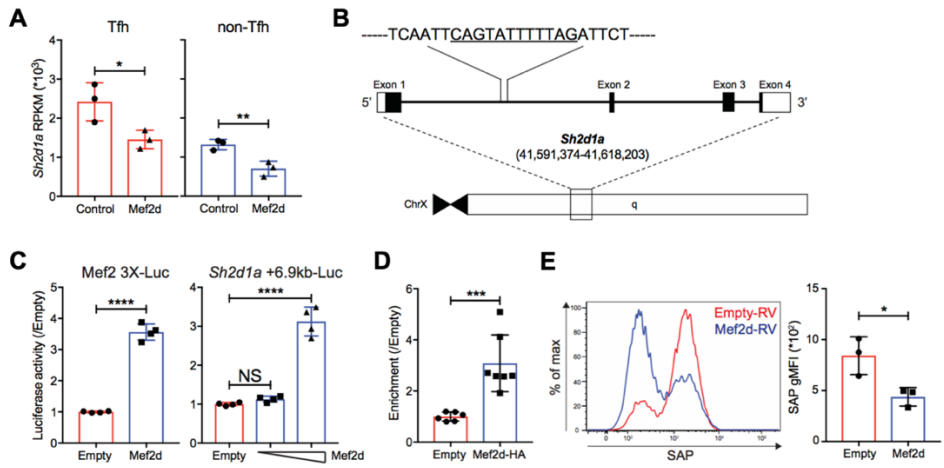

Figure 9. Direct regulation of the *Sh2d1a* gene by Mef2d.

(**A**) RPKMs of the *Sh2d1a* gene were measured in Tfh and non-Tfh cells developed from empty-RV (circles) or Mef2d-RV (triangles) OTII CD4 T cells **(Figure 7)**. **(B)** The genomic region of the murine *Sh2d1a* gene with a putative Mef2d binding site (CAGTATTTTTAG) at +6.9 kb from the transcription start site of the gene. **(C)** The luciferase activities of the Mef2 3X-Luc or the *Sh2d1a* +6.9kb-Luc plasmid were measured in the presence or absence of Mef2d co-expression. Data are from two independent experiments with duplicate wells per each condition. **(D)** The fold enrichment of the DNA region at +6.9kb of the *Sh2d1a* gene bound by HA-tagged Mef2d. Data are from three independent experiments with duplicate samples for each condition. **(E)** Overlaid SAP histograms of *in vitro* stimulated polyclonal CD4 T cells. The geometric MFIs (gMFIs) of SAP in GFP^+ CD4 T cells were calculated from three independent experiments.

Error bars indicate mean with SD. Statistical significance values were determined using two-tailed Student's *t*-test **[A, C (left)-E]** and one-way ANOVA with Tukey's multiple comparisons test **[C (right)]**. * p <0.05; ** p <0.01; *** p <0.001; **** p <0.0001.

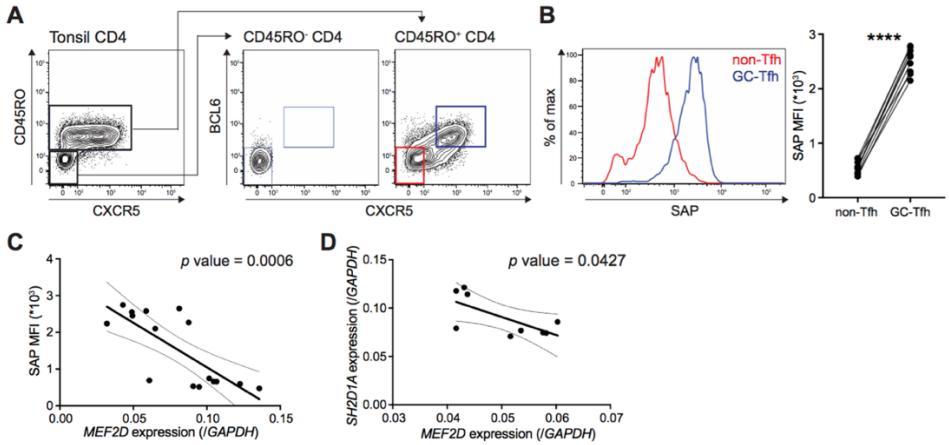

Figure 10. A negative correlation of SAP expression and *MEF2D* mRNA quantity in human tonsillar CD4 T cells.

(A) Gating strategy used to identify $BCL6^{-}CXCR5^{-}$ non-Tfh cells (red box) and $BCL6^{+}CXCR5^{+}$ GC-Tfh cells (blue box).

(B) Overlaid SAP histograms of non-Tfh (red) and GC-Tfh (blue) cells. Paired comparison of SAP MFIs between the respective population.

(C) Pearson's correlation analysis of SAP MFIs with *MEF2D* mRNA expression **(Figure 1C)** in non-Tfh and GC-Tfh cells.

(D) Pearson's correlation analysis of *SH2D1A* mRNA expression with *MEF2D* mRNA levels in human tonsillar $BCL6^{+}CXCR5^{+}$ GC-Tfh cells.

Statistical significance values were determined using two-tailed Student's *t*-test **(B)** and Pearson's correlation analysis **(C-D)**. **** $p < 0.0001$.

Mef2d inhibits SAP-dependent Tfh and GC-Tfh differentiation of CD4 T cells

The negative regulatory effect of Mef2d on SAP-dependent Tfh differentiation in CD4 T cells was explored by disrupting the *Mef2d* gene using RNP-mediated gene editing. The expression of SAP and the cognate B cell-dependent Tfh differentiation of CD4 T cells in the popLNs three days after NP-OVA immunization were examined, which was the same time point as the RNA-seq analysis. Naïve OTII CD4 T cells were transfected with Cas9 protein complexed with a crRNA targeting the murine *Mef2d* gene (**Table 5**), resulting in a significant reduction in Mef2d protein expression (**Figure 11A**). OTII CD4 T cells with *Mef2d* gene editing (crMef2d #2, crMef2d-RNP) expressed higher levels of SAP protein compared to control cells (**Figure 11B**). The difference in SAP expression was not due to differences in their activation status, as indicated by similar levels of CD44 expression regardless of *Mef2d* gene editing (**Figure 11C**). The increased SAP expression in crMef2d-RNP$^+$ OTII CD4 T cells was accompanied by enhanced formation of PD-1$^+$CXCR5$^+$ and PSGL-1^{lo}CXCR5$^+$ Tfh cells compared to controls (**Figure 11D-E**).

To investigate whether Mef2d modulates SAP-dependent GC-Tfh differentiation in CD4 T cells in a DNA binding-dependent manner, a point mutation was introduced at the 24th amino acid position in the MADS-box domain (R to L, R24L hereafter), as this mutation has been shown to compromise the DNA binding ability of Mef2c (*84*) and the N-terminal MADS-box and Mef2 domain are highly conserved among the Mef2 isoforms (*85*). The luciferase activity induced by wild-type Mef2d in the Mef2 3X-Luc plasmid was not observed with the R24L mutant (**Figure 12A**). The impact of the R24L point mutation on GC-Tfh differentiation and SAP expression was then evaluated. OTII CD4 T cells that were transduced with empty-RV, wild-type Mef2d-RV, or R24L Mef2d-RV were examined seven

days after NP-OVA immunization. The ectopic expression of wild-type Mef2d suppressed the differentiation of OTII CD4 T cells into PD-1^{+}CXCR5^{+} and PSGL-1^{lo}CXCR5^{+} GC-Tfh cells (**Figure 12B-C**). However, the R24L point mutation almost completely abolished Mef2d's inhibitory role, as R24L Mef2d-RV OTII CD4 T cells not only formed GC-Tfh cells (**Figure 12B-C**) but also expressed comparable levels of PD-1 and CXCR5 to the controls (**Figure 12D-E**).

The expression of SAP in CD4 T cells was found to be dynamically regulated depending on activation status (**Figure 13A**) and during differentiation into effector cells (**Figure 13B**). Following immunization with NP-OVA, the highest SAP expression was observed in PD-1^{+}CXCR5^{+} GC-Tfh cells, followed by PD-1^{-} CXCR5^{+} Tfh cells, with the lowest levels of SAP expression detected in PD-1^{-} CXCR5^{-} non-Tfh cells in popLNs. Therefore, the SAP^{hi} compartment was primarily observed among CD4 T cells with high expression of CXCR5, which were mostly PD1^{+}CXCR5^{+} GC-Tfh cells (**Figure 13C**). OTII CD4 T cells transduced with Mef2d-RV did not form the SAP^{hi} compartment, which is consistent with their inability to differentiate into GC-Tfh cells. However, when Mef2d R24L was ectopically expressed, the formation of the SAP^{hi} compartment in OTII CD4 T cells was rescued (**Figure 13D**). These data demonstrate that the DNA binding-dependent function of Mef2d controls GC-Tfh differentiation and SAP expression in CD4 T cells.

To further validate whether Mef2d negatively regulates GC-Tfh differentiation through transcriptional control of SAP expression. I performed experiments to determine whether Mef2d-dependent inhibition of GC-Tfh differentiation could be reversed by restoring SAP expression in Mef2d-RV OTII CD4 T cells. OTII CD4 T cells which were transduced with empty-RV, Mef2d-RV, or Mef2d-Sh2d1a-RV (M+S) (**Figure 14A**) were transferred, and their GC-Tfh differentiation was examined in the popLNs seven days after NP-OVA immunization (**Figure 14B**). The overexpression of Mef2d resulted in a significant reduction in PSGL-

$1^{lo}CXCR5^{+}$ GC-Tfh differentiation, while co-expression of SAP in Mef2d-RV OTII CD4 T cells restored their ability to differentiate into PSGL-$1^{lo}CXCR5^{+}$ GC-Tfh cells similar to the control group (**Figure 14C**). Collectively, these findings provide evidence that Mef2d negatively regulates GC-Tfh differentiation in CD4 T cells through transcriptional repression of the *Sh2d1a* gene.

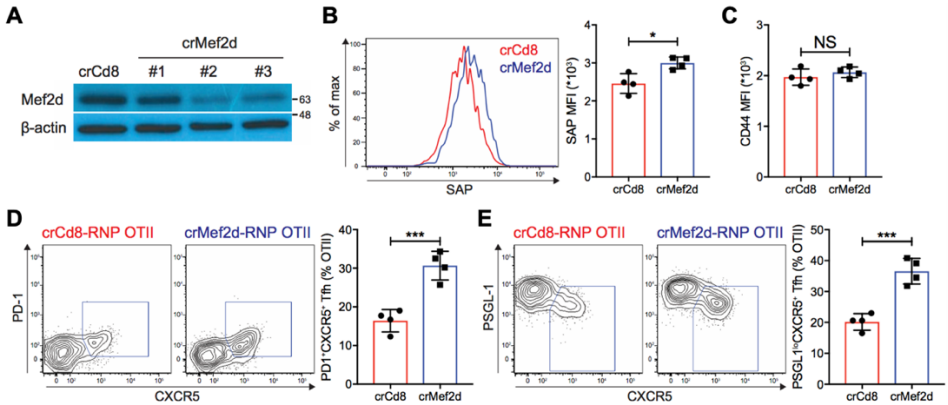

Figure 11. *Mef2d* editing results in increased SAP expression and enhanced Tfh differentiation.

CD45.1 OTII CD4 T cells were transfected with either crCd8-RNP or crMef2d-RNP (#2) and adoptively transferred into recipients. Three days after NP-OVA immunization, Tfh differentiation and SAP expression of the donor cells were examined.

(A) Immunoblots of β-actin and Mef2d protein with cell lysates obtained from crCd8-RNP^{+} or crMef2d-RNP^{+} OTII CD4 T cells.

(B) Overlaid histograms of SAP of the donor cells. SAP MFIs were quantified.

(C) CD44 MFIs of the donor OTII CD4 T cells were calculated.

(D and E) The flow cytometry plots of the donor OTII CD4 T cells. The frequencies of PD-1^{+}CXCR5^{+} and PSGL-1^{lo}CXCR5^{+} Tfh cells among the donor OTII CD4 T cells were calculated.

Representative of two independent experiments with n=4 mice per group. Error bars indicate mean with SD. Statistical significance values were determined using two-tailed Student's *t*-test. NS, statistically non-significant; * p <0.05; *** p <0.001.

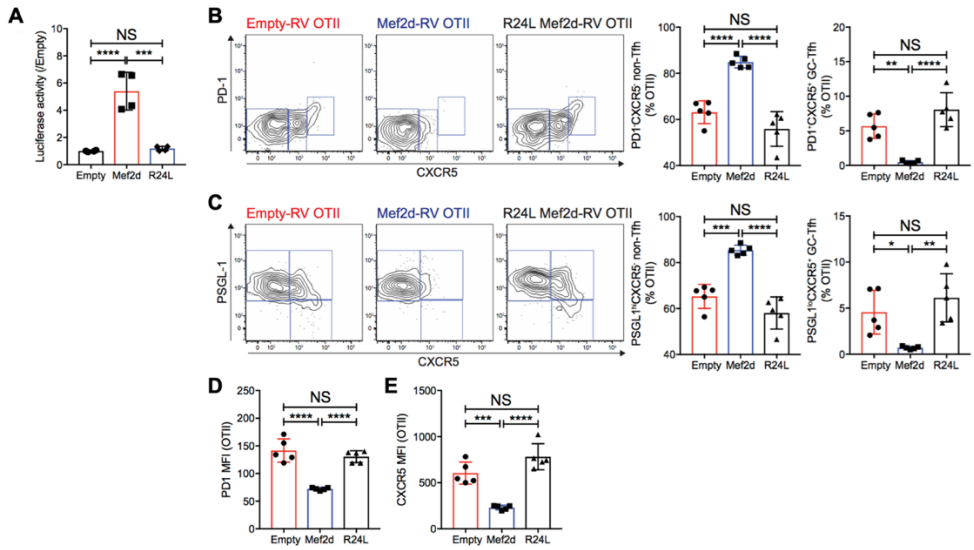

Figure 12. Mef2d controls GC-Tfh differentiation via a DNA-binding-dependent manner.

(A) Luciferase activities of the Mef2 3X-Luc plasmid in the presence of Mef2d or R24L Mef2d co-expression. Data from two independent experiments with duplicate wells per each condition.

(B to E) Empty-RV, Mef2d-RV, or R24L Mef2d-RV CD45.1 OTII CD4 T cells were adoptively transferred into recipients. Seven days after NP-OVA immunization, the donor cells were analyzed for GC-Tfh differentiation.

(B and C) The flow cytometry plots of the donor OTII CD4 T cells. The frequencies of non-Tfh (PD-1^{-}CXCR5^{-} or PSGL-1^{hi}CXCR5^{-}) and GC-Tfh (PD-1^{+}CXCR5^{+} or PSGL-1^{lo}CXCR5^{+}) cells developed from the respective donor cells were calculated.

(D and E) The MFIs of PD-1 **(C)** and CXCR5 **(D)** of the donor cells were quantified.

Representative of three independent experiments with n=5 mice per group **(B-E)**. Error bars indicate mean with SD. Statistical significance values were determined using one-way ANOVA with Tukey's multiple comparisons test. NS, statistically non-significant; * p <0.05; ** p <0.01; *** p <0.001; **** p <0.0001.

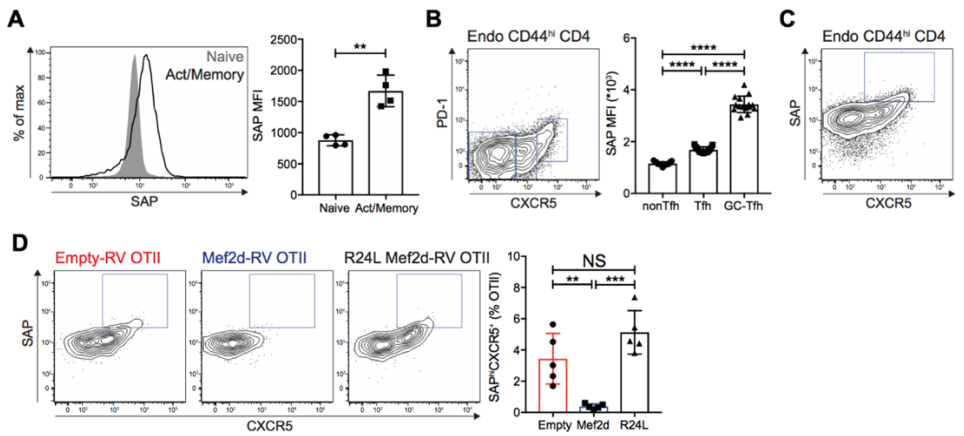

Figure 13. SAP expression in different types of CD4 T cells.

(A) Overlaid SAP histograms of CD44^{lo} naïve and CD44^{hi} activated/memory CD4 T cells in naïve mice. SAP MFIs were calculated.

(B) The flow cytometry plot of CD44^{hi} activated endogenous CD4 T cells in recipient mice seven days after NP-OVA immunization. SAP MFIs of the respective populations were calculated.

(C) The flow cytometry plot of the endogenous CD44^{hi} CD4 T cells. The gate indicates SAP^{hi}CXCR5^{+} cells.

(D) The flow cytometry plots of the donor cells **(Figure 12)**. The SAP^{hi}CXCR5^{+} cell frequencies were calculated.

Error bars indicate mean with SD. Statistical significance values were determined using two-tailed Student's *t*-test **(A)** and one-way ANOVA with Tukey's multiple comparisons test **(B-D)**. NS, statistically non-significant; ** p <0.01; *** p <0.001; **** p <0.0001.

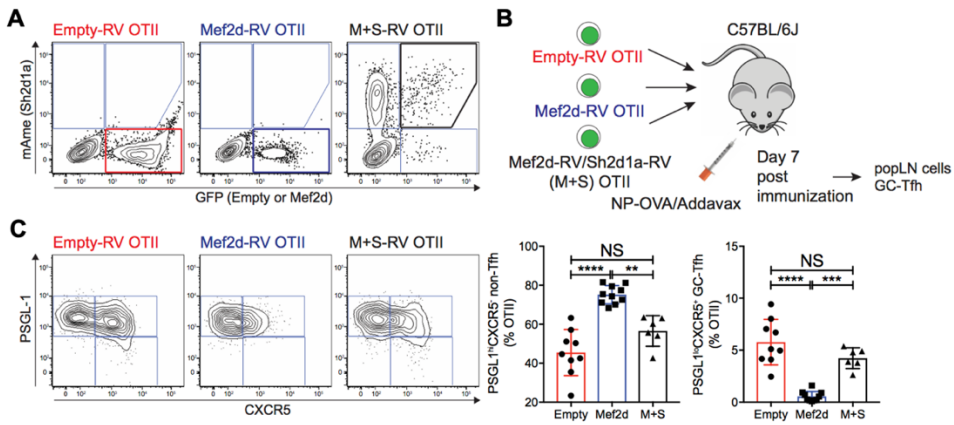

Figure 14. Mef2d restrains GC-Tfh differentiation via inhibition of SAP expression.

(A) The flow cytometry plots of OTII CD4 T cells transduced with empty-RV_{GFP} (Red) or Mef2d-RV_{GFP} with (Blue) or without Sh2d1a-$RV_{mAmetrine}$ (Black).

(B) The respective RV^+ OTII CD4 T cells were transferred to recipients. Seven days after NP-OVA immunization, GC-Tfh differentiation of the donor OTII CD4 T cells was examined.

(C) The flow cytometry plots of the donor OTII CD4 T cells. The frequencies of $PSGL1^{hi}CXCR5^-$ non-Tfh and $PSGL1^{lo}CXCR5^+$ GC-Tfh cells were calculated. Composite data from two independent experiments using n=6-10 recipient mice per group.

Error bars indicate mean with SD. Statistical significance values were determined using one-way ANOVA with Tukey's multiple comparisons test. NS, statistically non-significant; ** p <0.01; *** p <0.001; **** p <0.0001.

The B:T immune synapse is impeded by Mef2d function in CD4 T cells

Given its roles in the transcriptional repression of *Sh2d1a* expression and during SAP-dependent GC-Tfh differentiation, I analyzed whether Mef2d might affect B:T synapse formation. For this, an *in vitro* B:T conjugation assay was performed (*9, 82*). Equal numbers of OTII CD4 T cells transduced with either empty-RV (CD45.11) or Mef2d-RV (CD45.12) were co-cultured with splenic B cells that had been pre-stimulated with LPS and pulsed with $OVA_{323-339}$ peptide at concentrations of 1 or 10 μg/mL. The background B:T conjugate formation was determined by co-culturing OTII CD4 T cells with pre-activated B cells in the absence of $OVA_{323-339}$ peptide. The Δ conjugate, which represents the antigen-specific B:T synapse, was calculated by subtracting $[CD4^+CD19^+$ % among the total $CD4^+]_{-Ag}$ from $[CD4^+CD19^+$ % among the total $CD4^+]_{+Ag}$, and it was found to increase in an $OVA_{323-339}$ peptide dose-dependent manner (**Figure 15A**). The frequency of Mef2d-RV OTII CD4 T cells in the Δ conjugate was significantly lower than that of the control OTII CD4 T cells (**Figure 15B**), indicating that Mef2d inhibits the establishment of Ag-specific B:T synapse by CD4 T cells.

The expression level of Vα2 and CD18, which correspond to the TCR alpha chain of the OTII CD4 T cells and β_2 integrin subunit of LFA-1, respectively, were similar in Mef2d-RV and control OTII CD4 T cells (**Figure 16A**), suggesting that Mef2d regulates B:T synapse formation of CD4 T cells in a TCR- and LFA-1-independent manner. Moreover, the RPKMs of *Slam5*, *Slam6*, *Cd40lg*, and *Icos*, which are known to play roles in CD4 T cell synapse formation with B and other APCs (*27, 86*), were not altered in Tfh and non-Tfh cells by ectopic Mef2d expression (**Figure 16B**). Additionally, I observed that Mef2d-RV OTII CD4 T cells formed immune synapse with Ag-presenting DCs at levels similar to the controls (**Figure 17**). All of these data imply that Mef2d could specifically

modulate synapse formation of CD4 T cells with B cells via SAP.

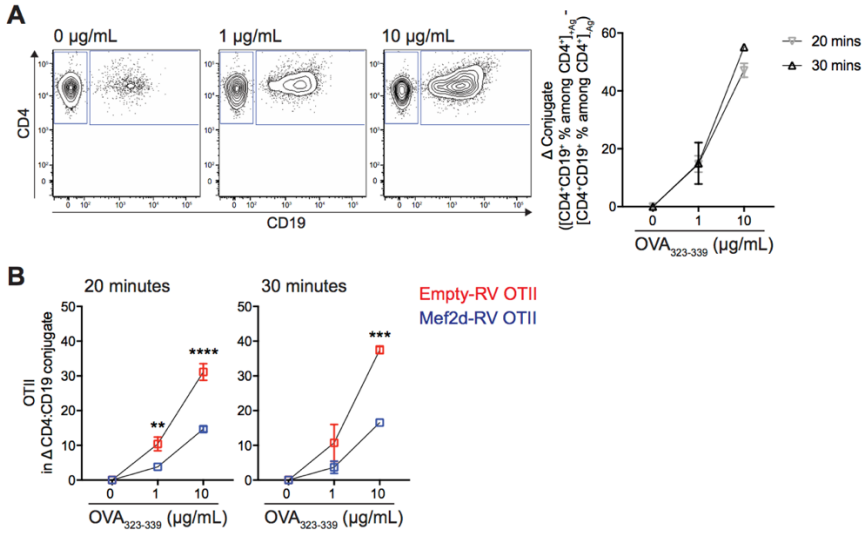

Figure 15. Ag-specific B:T conjugate formation is negatively regulated by Mef2d.

(A) The flow cytometry plots of the $CD4^+$ population. Ag-specific B:T conjugate frequencies were calculated.

(B) The frequencies of CD45.11 empty-RV OTII CD4 T cells (red) and CD45.12 Mef2d-RV OTII CD4 T cells (blue) that were presented in Ag-specific B:T conjugates were quantified.

Composite data from two independent experiments with two replicated samples per group.

Error bars indicate mean with SD. Statistical significance values were determined using two-way ANOVA with Bonferroni's multiple comparisons test. ** p <0.01; *** p <0.001; **** p <0.0001.

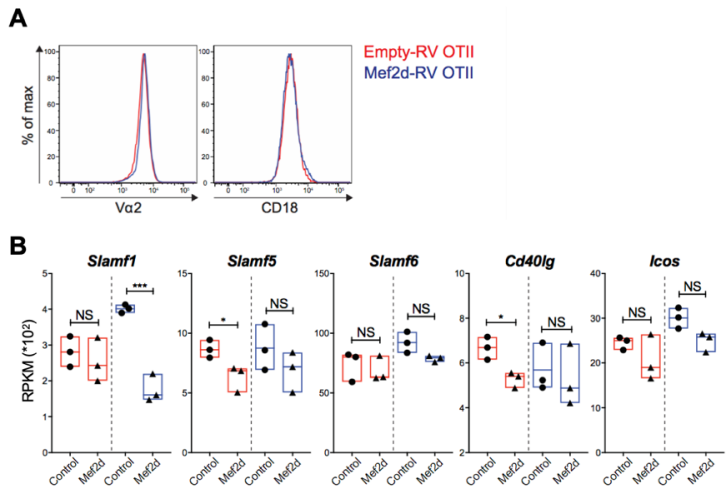

Figure 16. The expression of molecules contributing to the immune synapse in the presence or absence of ectopic Mef2d expression.

(A) Overlaid histograms of Vα2 and CD18 of CD45.11 empty-RV (red) and CD45.12 Mef2d-RV (blue) OTII CD4 T cells.

(B) The RPKMs for genes, known to play important roles in immune synapse formation, of Tfh (red boxes) and non-Tfh (blue boxes) cells developed from empty-RV (circles) or Mef2d-RV (triangles) OTII CD4 T cells **(Figure 7)**. Statistical significance values were determined using two-tailed Student's *t*-test. NS, statistically non-significant; * p <0.05; *** p <0.001.

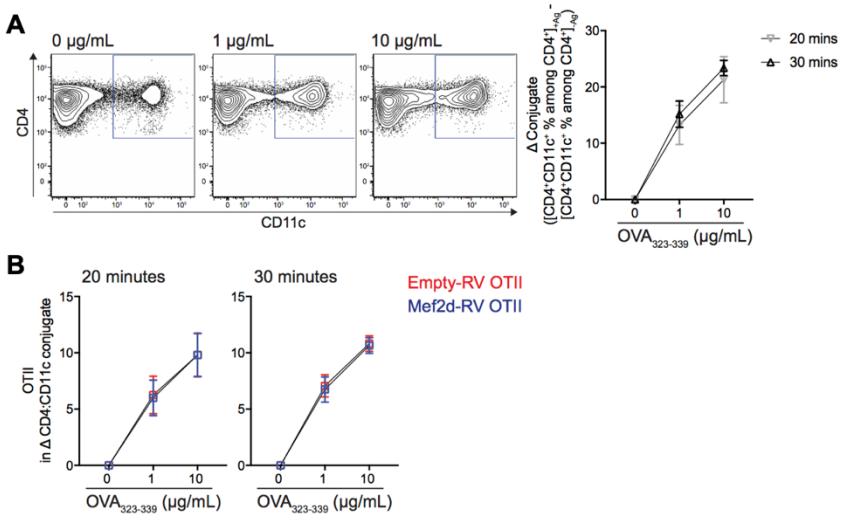

Figure 17. Enhanced Mef2d expression does not affect the formation of Ag-specific DC:T conjugates.

(A) The flow cytometry plots of the $CD4^+$ population. Ag-specific DC:T conjugate frequencies were calculated.

(B) The frequencies of GFP^+ empty-RV OTII CD4 T cells (red) and $mAmetrine^+$ Mef2d-RV OTII CD4 T cells (blue) that were presented in Ag-specific DC:T conjugates were quantified.

Composite data from two independent experiments with two replicated samples per group. Error bars indicate mean with SD.

Mef2d directly regulates IL-21 production of CD4 T cells

In the RNA-seq analysis, the *Il21* gene was also identified as a potential target of Mef2d (**Table 2**). The expression of *Il21* mRNA was markedly decreased in Mef2d Tfh cells, comparable to that in non-Tfh cells, and further reduced in Mef2d non-Tfh cells (**Figure 18A**). Moreover, potential Mef2 binding sites were found at approximately +3.2 kb (TATAAATAG) and +6.6 kb (CTAAAAATAG) regions within the *Il21* locus (**Figure 18B**). Luciferase assays were performed using plasmids containing either +3.2 kb or +6.6 kb region of the *Il21* gene, and the results showed that Mef2d was able to bind to these sites, with stronger binding observed at the +3.2 kb region (**Figure 18C**). These data indicate that Mef2d could also play a role in regulating IL-21 production in CD4 T cells. To test this possibility, I stimulated polyclonal CD4 T cells isolated from naïve mice under a culture condition that induces IL-21 production *in vitro* (*87*). The ectopic expression of Mef2d resulted in a significant decrease in the frequency of CD4 T cells producing IL-21 (**Figure 18D-E**), suggesting that Mef2d might function as a potential transcriptional repressor of the *Il21* gene.

Next, to investigate whether IL-21 production of CD4 T cells could be modulated by Mef2d gene editing (**Figure 11**), intracellular cytokine staining (ICS) for IL-21 was performed with crCd8-RNP$^+$ and crMef2d-RNP$^+$ OTII CD4 T cells from popLNs three days after immunization (**Figure 19A**). The results showed that OTII CD4 T cells with crMef2d-RNP had increased IL-21 production compared to control OTII CD4 T cells, without affecting the production of IL-2 (**Figure 19B**).

To assess whether Mef2d-mediated regulation of IL-21 production occurs in a DNA binding-dependent manner, IL-21 ICS was conducted with empty-RV, wild-type Mef2d-RV or R24L Mef2d-RV OTII CD4 T cells from popLNs. Ectopic expression of wild-type Mef2d resulted in a significant reduction of IL-21 production in OTII CD4 T cells (**Figure 20A**), while their ability to produce IL-2

or IFN-γ was not altered (**Figure 20B-C**). On the other hand, the R24L mutant Mef2d was unable to inhibit IL-21 production (**Figure 20A**), which is consistent with its inability to suppress GC-Tfh differentiation.

Given that IL-21 is a major B cell-help cytokine produced mostly by Tfh and GC-Tfh cells, it is possible that the reduced IL-21 production observed in Mef2d-RV OTII CD4 T cells could be due to the inherent deficiencies of these cells in undergoing SAP-dependent Tfh and GC-Tfh differentiation and might not be a direct result of the transcriptional repression of the *Il21* gene by Mef2d. To test the direct relationship between Mef2d and IL-21, I examined IL-21 production in M+S OTII CD4 T cells. These cells exhibited almost complete restoration of GC-Tfh differentiation defects upon recovery of SAP expression following forced Mef2d expression. However, Defective IL-21 production was not completely rescued by SAP co-expression (**Figure 21A**). The partial restoration of IL-21 production cannot be attributed to potential issues in general CD4 T cell activation, as demonstrated by comparable levels of IL-2 production in OTII CD4 T cells irrespective of ectopic expression of *Mef2d* or *Mef2d* with *Sh2d1a* gene (**Figure 21B**). Overall, these findings confirm that Mef2d is a transcriptional repressor of the *Il21* gene.

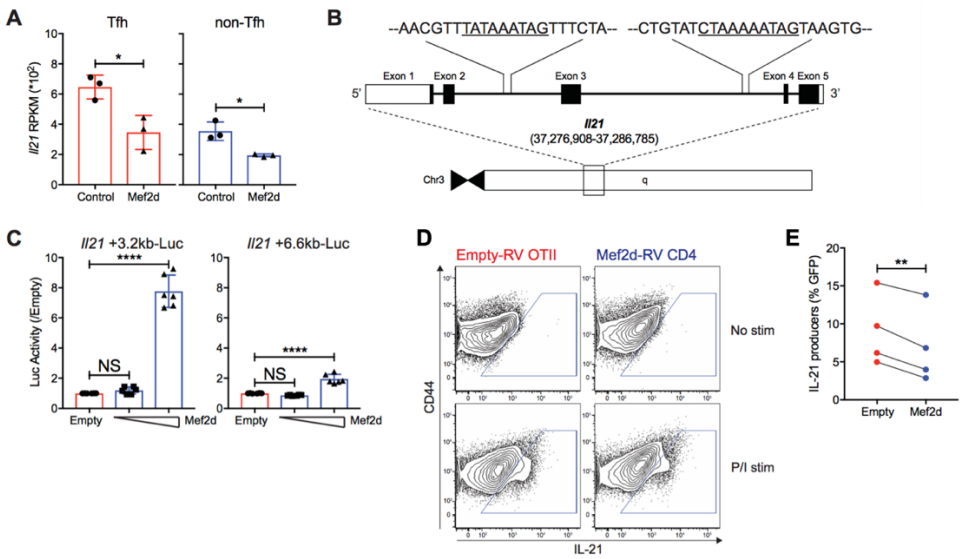

Figure 18. Mef2d directly regulates the *Il21* gene expression.

(A) RPKMs of the *Il21* gene were measured in Tfh and non-Tfh cells developed from empty-RV (circles) or Mef2d-RV (triangles) OTII CD4 T cells **(Figure 7)**.

(B) The genomic region of the murine *Il21* gene with putative Mef2d binding sites at +3.2 kb (TATAAATAG) and +6.6 kb (CTAAAAATAG) from the transcription start site of the gene.

(C) The luciferase activities of the *Il21* +3.2 kb or the *Il21* +6.6 kb-Luc plasmid were measured in the presence or absence of Mef2d co-expression. Data were obtained from three independent experiments with duplicate wells per each condition.

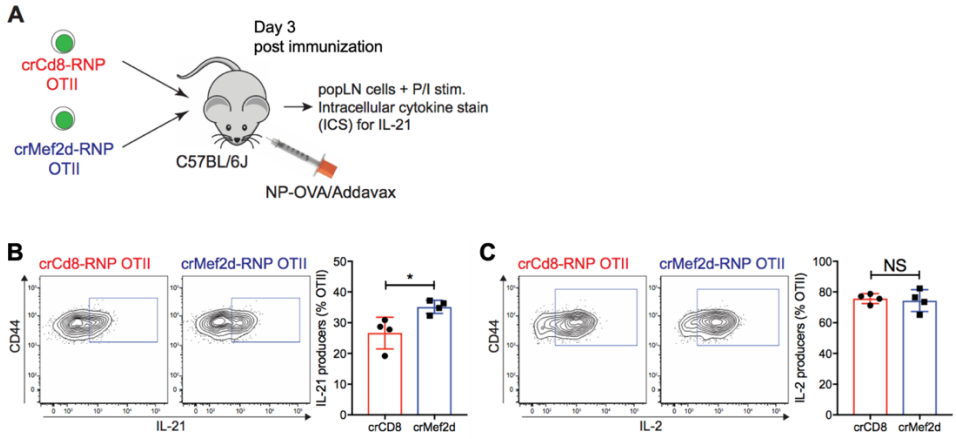

Figure 19. *Mef2d* editing leads to increased IL-21 production by CD4 T cells.

(A) CD45.1 OTII CD4 T cells were transfected with either crCd8-RNP or crMef2d-RNP (#2) and adoptively transferred into recipients. Three days after NP-OVA immunization, IL-21 production of the donor cells was examined.

(B) The flow cytometry plots of the donor OTII CD4 T cells. The frequencies of IL-21 producers were quantified.

(C) The flow cytometry plots of the donor OTII CD4 T cells with the calculated frequencies of IL-2 producers.

Representative of two independent experiments with n=4 mice per group. Error bars indicate mean with SD. Statistical significance values were determined using two-tailed Student's *t*-test. NS, statistically non-significant; * p <0.05.

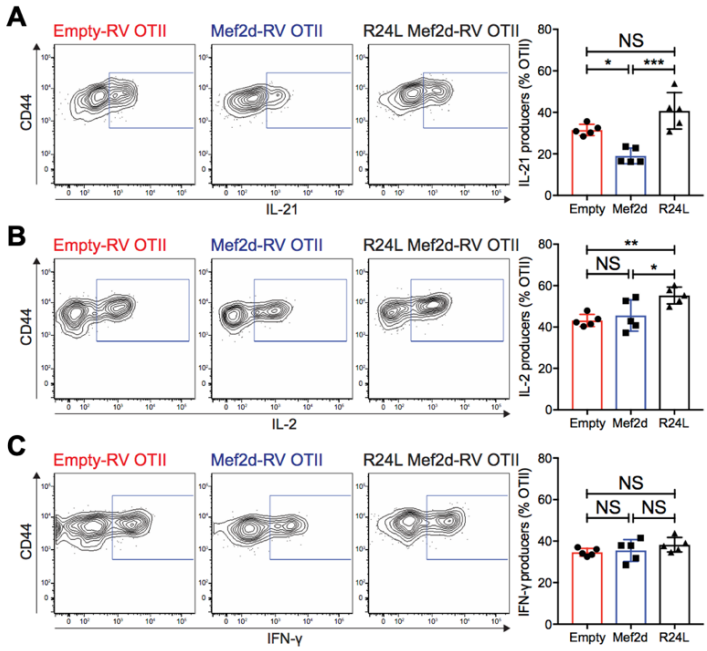

Figure 20. Mef2d hinders IL-21 production in a DNA-binding-dependent manner.

The flow cytometry plots of GFP^+ CD45.1 OTII CD4 T cells **(Figure 12)**. The frequencies of IL-21 **(A)**, IL-2 **(B)**, and IFN-γ **(C)** producers developed from the respective donor OTII CD4 T cells were calculated.

Error bars indicate mean with SD. Statistical significance values were determined using one-way ANOVA with Tukey's multiple comparisons test. NS, statistically non-significant; * p <0.05; ** p <0.01; *** p <0.001.

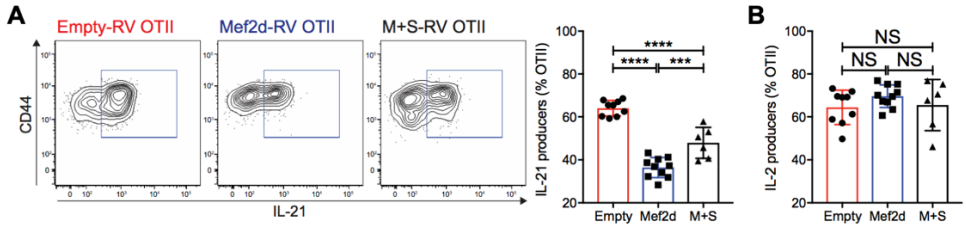

Figure 21. Mef2d regulates SAP expression and IL-21 production independently.

The flow cytometry plots of empty-RV_{GFP}^{+}, Mef2d-RV_{GFP}^{+}, or Mef2d+Sh2d1a-$RV_{GFP+mAmetrine}^{+}$ OTII CD4 T cells **(Figure 14)**. The frequencies of IL-21 **(A)** and IL-2 **(B)** producers among the donor cells were calculated.

Composite data from two independent experiments using n=6-10 recipient mice per group. Error bars indicate mean with SD. Statistical significance values were determined using one-way ANOVA with Tukey's multiple comparisons test. NS, statistically non-significant; *** p <0.001; **** p <0.0001.

Mef2d controls GC formation and antigen-specific antibody production by B cells

The ability of B cells to initiate a CD4 T cell-dependent humoral immune response relies heavily on effective communication with CD4 T cells, and since Mef2d negatively regulates SAP-dependent B:T synapse formation, the impact of Mef2d in CD4 T cells on GC formation and the production of high-affinity antibodies by B cells was investigated. Following NP-OVA immunization, a significant decrease in the number of Mef2d-RV OTII CD4 T cells in the GC and follicle areas of the popLNs was observed (**Figure 22A-B**). To further evaluate the role of Mef2d in the TD humoral immune response, adoptive transfer experiments were performed using *Cd4*^{Cre}*Bcl6*$^{fl/fl}$ mice (*Bcl6* CKO mice hereafter) as recipients, whose endogenous CD4 T cells are unable to differentiate into Tfh cells and provide help to B cells for GC formation (**Figure 22C**). Seven days after immunization, the Mef2d-RV OTII CD4 T cells formed significantly fewer PSGL-1^{lo}CXCR5^{+} GC-Tfh cells compared to the control (**Figure 22D**). The total frequency of CD19 B cells was similar between the groups (**Figure 22E**), however, the Fas^{+}PNA^{+} GC B cells were hardly detectable in the *Bcl6* CKO mice that received Mef2d-RV OTII CD4 T cells (**Figure 22F**).

Additionally, the production of high-affinity (NP_8-bound) IgG antibodies by *Bcl6* CKO mice was significantly reduced when they received Mef2d-RV OTII CD4 T cells compared to control OTII CD4 T cells. Ectopic expression of Mef2d also led to a decrease in B cell production of NP_{49}-bound (low-affinity) IgG antibodies (**Figure 23A**), suggesting that the Mef2d transcription factor might also play a role in the GC-independent antibody response. The ability of B cells to produce Ag-specific IgGs remained diminished in mice receiving Mef2d-RV OTII CD4 T cells up to 28 days after immunization (**Figure 23B**). These results indicate that the intrinsic functions of Mef2d in CD4 T cells control the development of

GCs and CD4 T cell-dependent production of Ag-specific antibodies.

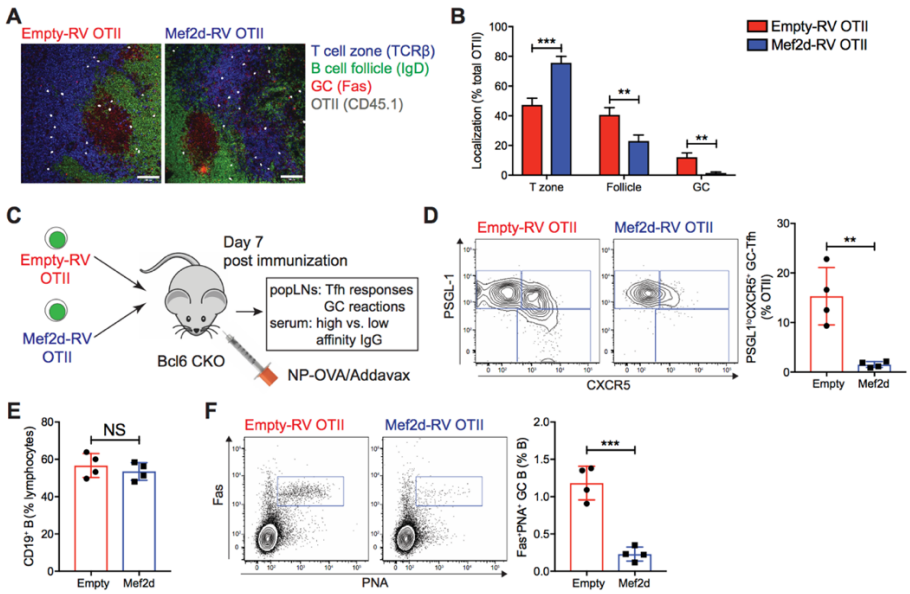

Figure 22. Ectopic Mef2d expression in CD4 T cells controls GC formation.

(**A**) Empty-RV (left) or Mef2d-RV (right) CD45.1 OTII CD4 T cells were transferred to C57BL/6J recipients. Seven days after NP-OVA immunization, popLNs were collected and analyzed by immunofluorescence. CD45.1 OTII CD4 T cells were marked as large dots to clarify. Scale bar = 100μm.

(**B**) The frequencies of CD45.1 OTII CD4 T cells in each location were calculated.

(C to F) Empty-RV or Mef2d-RV OTII CD4 T cells were adoptively transferred into *Bcl6* CKO ($Cd4^{Cre}Bcl6^{fl/fl}$) mice. Seven days after NP-OVA immunization, GC-Tfh differentiation and GC formation by B cells were evaluated **(C)**.

(D) The flow cytometry plots of GFP^+ OTII CD4 T cells. The frequencies of $PSGL\text{-}1^{lo}CXCR5^+$ GC-Tfh cells were quantified.

(E) The frequencies of CD19 B cells present in popLNs of *Bcl6* CKO mice.

(F) The flow cytometry plots of CD19 B cells. The frequencies of Fas^+PNA^+ GC B cells among the total B cells were calculated.

Representative of two independent experiments with n=4-5 per group. Statistical significance values were determined using two-tailed Student's *t*-test. NS, statistically non-significant; ** p <0.01; *** p <0.001.

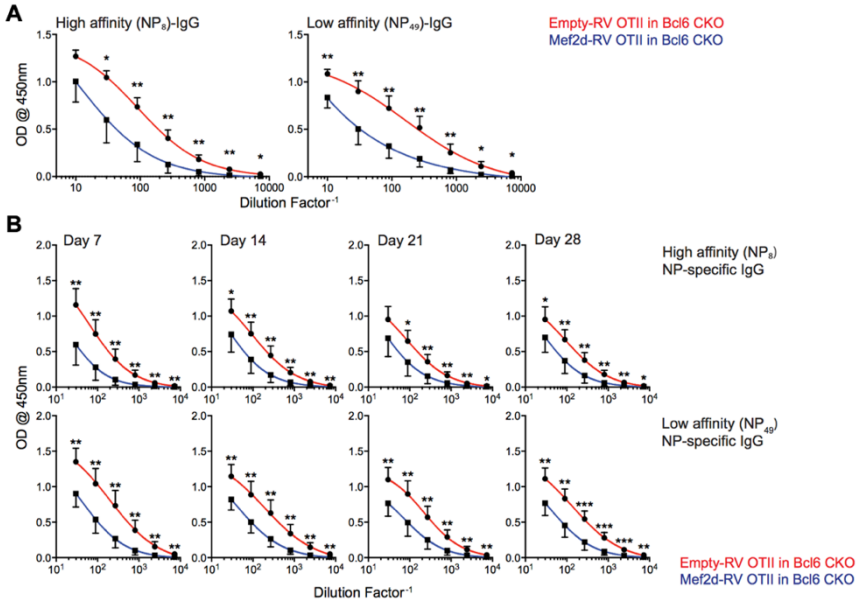

Figure 23. Ag-specific antibody production by B cells is negatively regulated by Mef2d.

(A) The levels of high- (NP_8-BSA) and low- (NP_{49}-BSA) affinity NP-specific IgG antibodies were measured in serum from *Bcl6* CKO mice that received adoptively transferred empty-RV (red) or Mef2d-RV (blue) OTII CD4 T cells **(Figure 22)**. **(B)** Empty-RV (red) or Mef2d-RV (blue) OTII CD4 T cells were transferred to *Bcl6* CKO mice, and serum samples were collected at days 7, 14, 21, and 28 after NP-OVA immunization to measure the production of high- and low-affinity NP-specific IgG antibodies by ELISA.

Representative of two independent experiments with n=4-5 per group **(A)** and composite data from two independent experiments using n=6 recipient mice per group **(B)**.

Error bars indicate mean with SD. Statistical significance values were determined using two-tailed Student's *t*-test. * p <0.05; ** p <0.01; *** p <0.001.

The *Mef2d* gene restrains B:T synapse-dependent GC-Tfh differentiation and TD humoral immune response

I hypothesized that *Mef2d* deficiency could lead to increased GC-Tfh differentiation due to de-repressed SAP expression. To address this hypothesis, I analyzed SAP expression and GC-Tfh differentiation in CD4 T cells where the *Mef2d* gene was disrupted using the CRISPR/Cas9 system (*2*). *Cd4*^{Cre}*ROSA26*$^{CAG\text{-}Cas9\text{-}EGFP/Wt}$ mice were crossed with OTII TCRtg mice to produce Cas9-expressing OTII (Cas9$^+$ OTII, hereafter) CD4 T cells. To confirm the efficacy of *Mef2d* gene disruption, Cas9$^+$ OTII CD4 T cells were transduced with a retrovirus expressing sgCd8, sgMef2d (#1), or sgMef2d (#2), and sgMef2d (#1) resulted in a substantial knockdown of Mef2d protein expression (**Figure 24A**).

sgCd8$^+$Cas9$^+$ and sgMef2d$^+$Cas9$^+$ (#1) OTII CD4 T cells were then transferred into *Cd4*^{Cre}*ROSA26*$^{CAG\text{-}Cas9\text{-}EGFP}$ mice to avoid potential rejection of Cas9$^+$ CD4 T cells in C57BL/6J mice (*88*). The transferred Cas9$^+$ OTII CD4 T cells were evaluated for GC-Tfh differentiation seven days after NP-OVA immunization (**Figure 24B**). Although *Mef2d* gene disruption did not influence OTII CD4 T cell expansion (**Figure 24C**), it significantly induced PSGL-1^{lo}CXCR5$^+$ GC-Tfh differentiation (**Figure 24D**), accompanied by a notable increase in CXCR5 expression (**Figure 24E**). Importantly, sgMef2d$^+$Cas9$^+$ OTII CD4 T cells demonstrated a more robust formation of the SAP^{hi}CXCR5$^+$ compartment than sgCd8$^+$Cas9$^+$ OTII CD4 T cells (**Figure 24F**), possibly due to a lack of transcriptional repression of the *Sh2d1a* gene.

To further explore the function of the *Mef2d* gene, I utilized CD4 T cell-specific *Mef2d* knockout (*Mef2d* CKO, hereafter) mice generated by crossing the *Mef2d*$^{fl/fl}$ mice with *Cd4*^{Cre} mice. Immunoblot analysis confirmed the deficiency of Mef2d protein expression in CD4 T cells of *Mef2d* CKO mice (**Figure 25A**), and these mice did not exhibit any abnormalities in thymic T cell development (**Figure 25B**)

or CD4 and CD8 T cell maturation (**Figure 25C-E**), consistent with previous research (*89*).

CD45.2 OTII CD4 T cells from WT and *Mef2d* CKO mice were adoptively transferred into CD45.1 B6.SJL mice, then, GC-Tfh differentiation, intracellular SAP expression, and IL-21 production were evaluated in the donor cells within the popLNs seven days after NP-OVA immunization. The absence of Mef2d did not alter the activation of Ag-specific CD4 T cells, as shown by comparable CD44 expression between control and *Mef2d* CKO OTII CD4 T cells (**Figure 26A**). However, there was a substantial increase in $PD1^{+}CXCR5^{+}$ and $PSGL1^{lo}CXCR5^{+}$ GC-Tfh differentiation of *Mef2d* CKO OTII CD4 T cells compared to control OTII CD4 T cells (**Figure 26B-C**), which is consistent with the previous findings using CRISPR/Cas9-mediated *Mef2d* gene disruption (**Figure 24**). *Mef2d* CKO OTII CD4 T cells displayed elevated surface expression of canonical Tfh markers, such as PD-1 and CXCR5 (**Figure 26D**), as well as reduced expression of PSGL-1 (**Figure 26E**). Furthermore, *Mef2d* CKO OTII CD4 T cells showed a more robust formation of the $SAP^{hi}CXCR5^{+}$ compartment and higher levels of intracellular SAP protein expression than control OTII CD4 T cells (**Figure 27A-B**). IL-21 production in OTII CD4 T cells was also increased by *Mef2d* gene deficiency (**Figure 27C**).

The impact of *Mef2d* gene deficiency on TD humoral immune response was investigated by transferring *Mef2d* CKO OTII CD4 T cells into *Bcl6* CKO mice, followed by assessing GC-Tfh differentiation and Ag-specific GC formation in the popLNs after NP-OVA immunization. *Mef2d* CKO OTII CD4 T cells exhibited a higher formation of $PD\text{-}1^{+}CXCR5^{+}$ and $PSGL\text{-}1^{lo}CXCR5^{+}$ GC-Tfh cells compared to control OTII CD4 T cells (**Figure 28A-B**). and this resulted in a significant increase in the frequencies of NP-specific GC B cells in the *Bcl6* CKO mice (**Figure 28C**). In addition, the production of high-affinity (NP_9-bound) IgG antibodies was significantly higher in the *Bcl6* CKO mice receiving *Mef2d*-

deficient and *Mef2d*-disrupted OTII CD4 T cells (**Figure 28D**). These findings highlight the critical role of the Mef2d transcription factor in regulating GC-Tfh differentiation and TD humoral immunity.

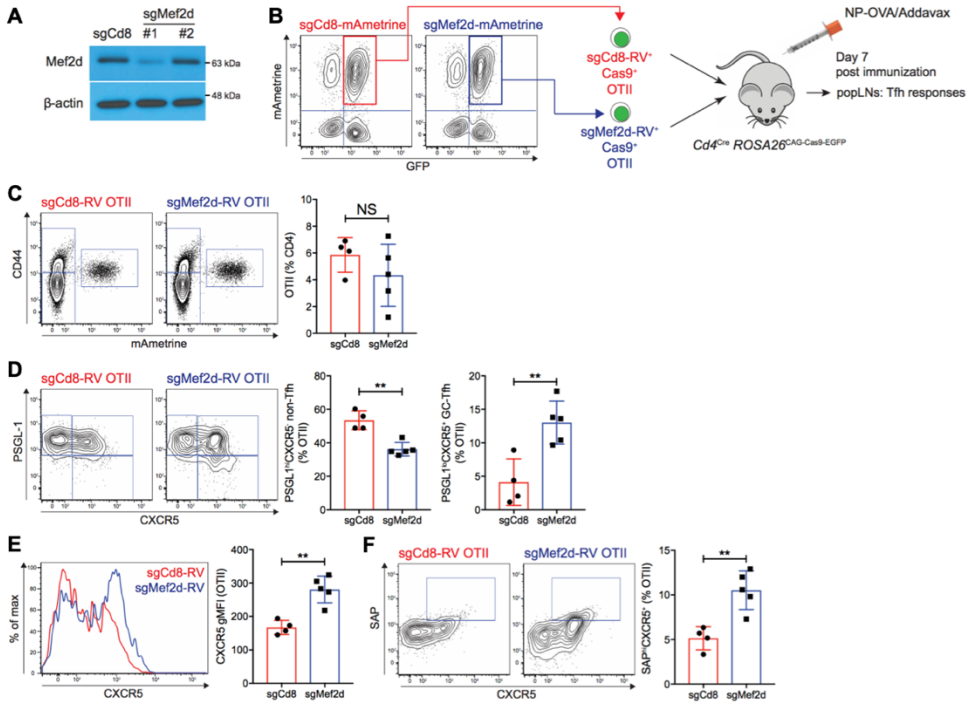

Figure 24. *Mef2d* gene disruption promotes GC-Tfh differentiation of OTII CD4 T cells with de-repressed SAP expression.

(A) Immunoblots of β-actin and Mef2d were performed using lysates obtained from Cas9^{+} CD4 T cells transduced with either sgRNA against the murine *Mef2d* gene or *Cd8* gene (a negative control).

(B to F) Cas9^{+} OTII CD4 T cells were transduced with Lsg-mAmetrine retrovirus expressing sgRNA against the murine *Cd8* or *Mef2d* gene (sgCd8 or sgMef2d #1). The same number of sgCd8-RV Cas9^{+} OTII CD4 T cells (Red) and sgMef2d-RV Cas9^{+} OTII CD4 T cells (Blue) were transferred to *Cd4*^{Cre}*ROSA26*$^{CAG\text{-}Cas9\text{-}EGFP}$ recipients. Seven days after NP-OVA immunization, GC-Tfh differentiation and intracellular SAP expression were analyzed **(B)**.

(C) The flow cytometry plots of the total CD4 T cells in popLNs. The frequencies of mAmetrine^{+}Cas9^{+} OTII CD4 T cells were calculated.

(D) The flow cytometry plots of the donor OTII CD4 T cells. The frequencies of PSGL-1^{hi}CXCR5^{-} non-Tfh and PSGL-1^{lo}CXCR5^{+} GC-Tfh cells were calculated.

(E) Overlaid CXCR5 histograms. MFIs were calculated.

(F) The flow cytometry plots of the donor OTII CD4 T cells. The frequencies of $SAP^{hi}CXCR5^{+}$ cells were calculated.

Representative of two independent experiments with n=5 mice per group. Error bars indicate mean with SD. Statistical significance values were determined using two-tailed Student's *t*-test. NS, statistically non-significant; ** $p < 0.01$.

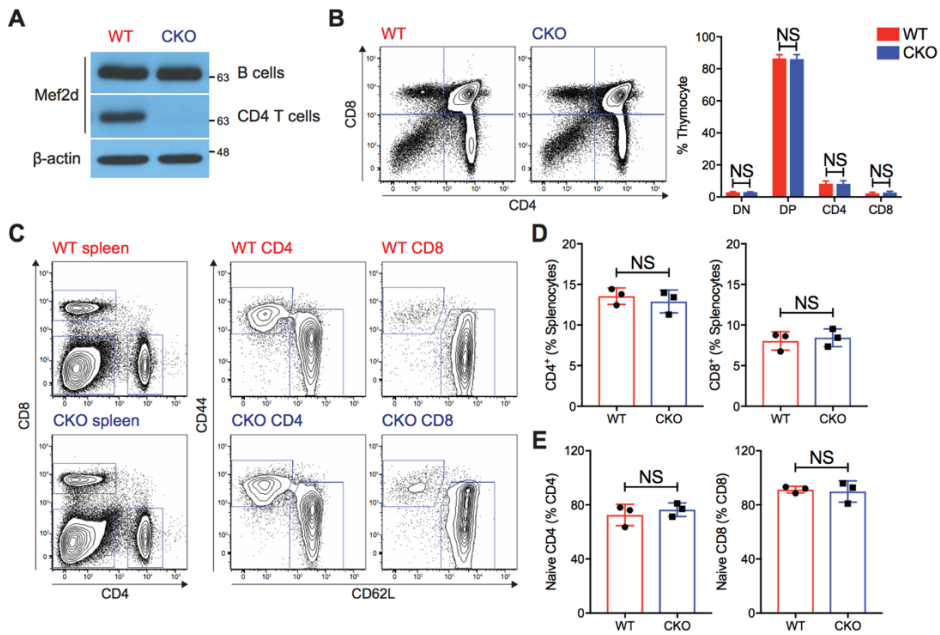

Figure 25. T cell development and maturation normally occur in the *Mef2d* CKO mice.

(A) Immunoblots of β-actin and Mef2d protein with cell lysates obtained from B cells (upper) and CD4 T cells (lower) present in the WT control and the *Mef2d* CKO ($Cd4^{Cre}Mef2d^{fl/fl}$) mice.

(B) The flow cytometry plots of the thymocytes of the WT control and the *Mef2d* CKO mice. The frequencies of $CD4^-CD8^-$ double-negative (DN), $CD4^+CD8^+$ double-positive (DP), $CD4^+$ single-positive (CD4), and $CD8^+$ single-positive (CD8) cells were calculated.

(C) The flow cytometry plots of the total splenocytes and the mature CD4 and CD8 cells of the WT control and the *Mef2d* CKO mice.

(D and E) The frequencies of the mature CD4 and CD8 T cells among the splenocytes **(D)** and the $CD44^{lo}CD62L^{hi}$ naïve compartment of the respective T cells **(E)**.

Composite data from three independent experiments. Statistical significance values were determined using two-tailed Student's *t*-test. NS, statistically non-significant.

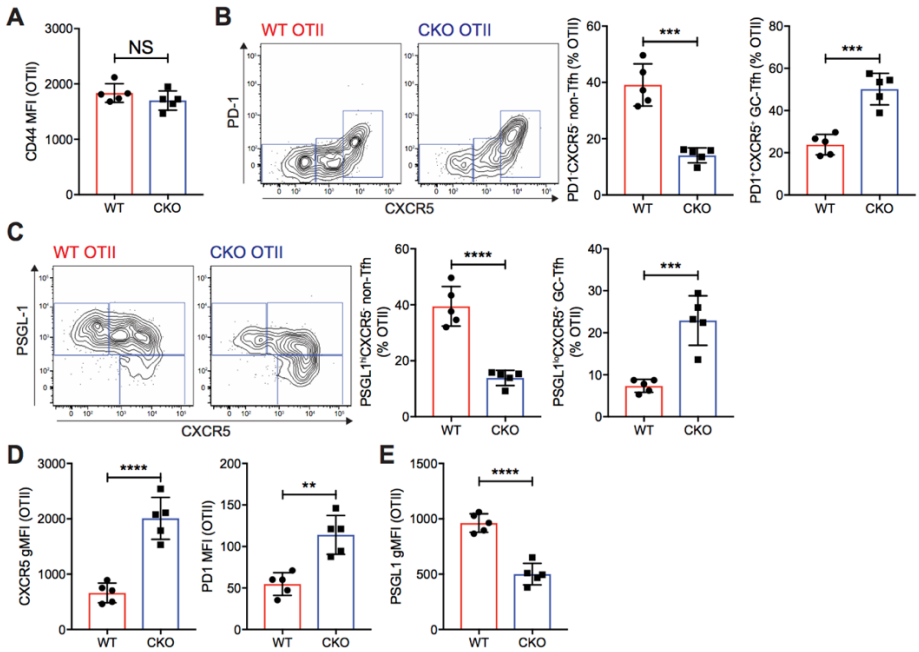

Figure 26. *Mef2d* deficiency in CD4 T cells leads to enhanced GC-Tfh differentiation.

WT control and *Mef2d* CKO (*Cd4*^{Cre}*Mef2d*$^{fl/fl}$) CD45.2 OTII CD4 T cells were transferred to CD45.1 B6.SJL mice. Seven days after NP-OVA immunization, GC-Tfh differentiation of the donor cells was examined.

(A) CD44 MFIs of the donor OTII CD4 T cells were calculated.

(B and C) The flow cytometry plots of the donor OTII CD4 T cells. The frequencies of non-Tfh (PD-1^{-}CXCR5^{-} or PSGL-1^{hi}CXCR5^{-}) and GC-Tfh (PD-1^{+}CXCR5^{+} or PSGL-1^{lo}CXCR5^{+}) cells were quantified.

(D) The gMFIs of CXCR5 and PD-1 were quantified.

(E) PSGL-1 gMFIs of the donor cells were calculated.

Representative of two independent experiments with n=5 mice per group. Error bars indicate mean with SD. Statistical significance values were determined using two-tailed Student's *t*-test. NS, statistically non-significant; ** p <0.01; *** p <0.001; **** p <0.0001.

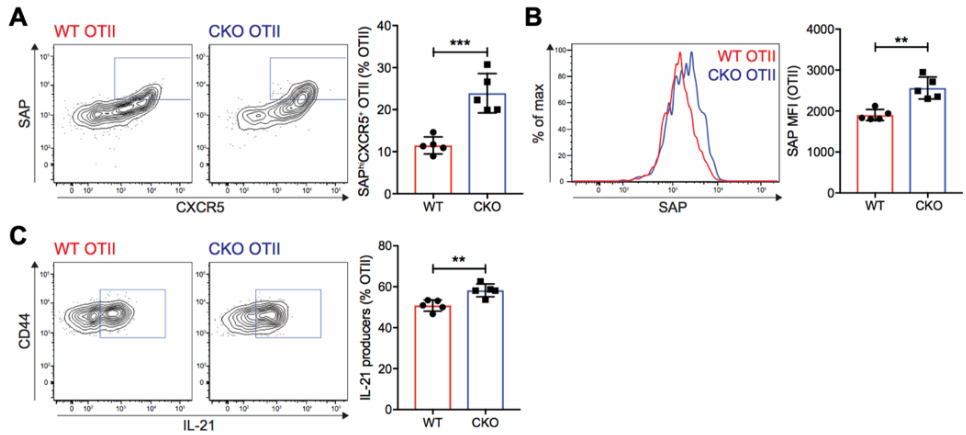

Figure 27. SAP expression and IL-21 production are increased by *Mef2d* deficiency in CD4 T cells.

(A) The flow cytometry plots of the transferred OTII CD4 T cells **(Figure 26)**. The frequencies of $SAP^{hi}CXCR5^{+}$ cells were quantified.

(B) Overlaid SAP histograms. Intracellular SAP MFIs were calculated.

(C) The flow cytometry plots of the transferred OTII CD4 T cells. The frequencies of IL-21 producers were quantified.

Representative of two independent experiments with n=5 mice per group. Error bars indicate mean with SD. Statistical significance values were determined using two-tailed Student's *t*-test. ** p <0.01; *** p <0.001.

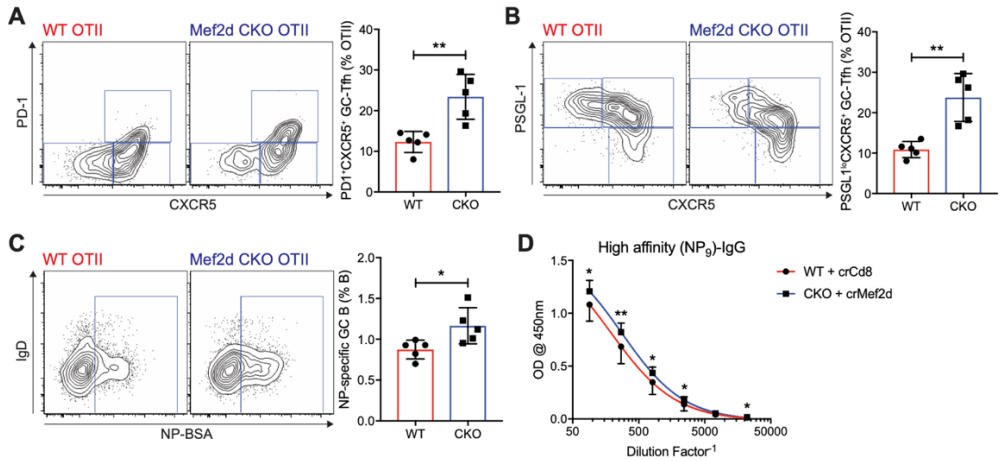

Figure 28. CD4 T cell-specific *Mef2d* CKO mice elicit strong TD humoral immune responses after immunization.

WT control and *Mef2d* CKO (*Cd4*^{Cre}*Mef2d*$^{fl/fl}$) OTII CD4 T cells were adoptively transferred into *Bcl6* CKO (*Cd4*^{Cre}*Bcl6*$^{fl/fl}$) mice. Seven days after NP-OVA immunization, popLNs were examined to assess GC-Tfh differentiation of the donor cells and Ag-specific GC B cells, and serum samples were analyzed for Ag-specific antibody production.

(A and B) The flow cytometry plots of the donor OTII CD4 T cells. The frequencies of PD-1^{+}CXCR5^{+} GC-Tfh **(A)** or PSGL-1^{lo}CXCR5^{+} GC-Tfh **(B)** cells were quantified.

(C) The flow cytometry plots of Fas^{+}PNA^{+} GC B cells. The frequencies of NP-specific GC B cells among the total B cells were calculated.

(D) The amounts of high- (NP_8-BSA) affinity NP-specific IgG antibodies were measured in serum from *Bcl6* CKO mice that received WT and crCd8-RNP^{+} (red) or *Mef2d* CKO and crMef2d-RNP^{+} (blue) OTII CD4 T cells.

Composite data from three independent experiments using n=14-15 recipients per group **(D)**. Error bars indicate mean with SD. Statistical significance values were determined using two-tailed Student's *t*-test. * p <0.05; ** p <0.01.

Autoimmune features in SLE patients are associated with *MEF2D* expression in CD4 T cells

The proper regulation of SAP-dependent GC-Tfh differentiation and IL-21 production by CD4 T cells is critical for controlling CD4 T cell-dependent humoral immunity, which is associated with autoimmune diseases like systemic lupus erythematosus (SLE). Recently, a novel genetic variant (rs200395694: G>T) was identified in the regulatory region of the *MEF2D* gene in a subgroup of Swedish SLE patients that strongly correlates with the magnitude of autoantibodies (*90*). Although its impact on *MEF2D* expression in CD4 T cells was not examined, the variant is located within the transcription factor binding sites, leading to reduced luciferase activity in Jurkat cells (*90*), suggesting that the variant might negatively regulate transcriptional activation of the *MEF2D* gene in CD4 T cells.

To investigate *MEF2D* expression in CD4 T cells and its potential association with autoimmune features of SLE patients, I analyzed peripheral blood mononuclear cells (PBMCs) from healthy individuals and SLE patients (**Table 3a**) for their phenotypic characteristics (**Figure 29A**). The analysis revealed that SLE patients had reduced frequencies of CD4 T cells (**Figure 30A**) and increased frequencies of $CD45RA^-$ (activated/memory) CD4 T cells (**Figure 30B**) compared to healthy individuals. Additionally, the frequency of circulating Tfh (cTfh)-like cells ($ICOS^+PD\text{-}1^+$ cells) in the $CD45RA^-CXCR5^+$ compartment was significantly higher in SLE patients than in controls (**Figure 30C**), with a strong positive correlation with SLEDAI and the amount of serum autoantibodies (anti-dsDNA Ig) (**Figure 30D**).

Then, the mRNA levels of *MEF2D* were measured using qPCR in peripheral blood CD4 T cells from SLE patients and healthy individuals. The CD4 T cells from SLE patients showed a significant three-fold reduction in *MEF2D* mRNA expression compared to that of healthy individuals (**Figure 31A**). This reduction

might be attributed to the increased frequency of cTfh cells in the patients, as GC-Tfh cells in tonsils were found to have lower *MEF2D* expression than non-Tfh effector CD4 T cells (**Figure 1C**). To further assess the pathophysiological significance of reduced *MEF2D* expression in SLE, *MEF2D* mRNA expression was measured in $CD45RA^+$ naïve CD4 T cells from SLE patients and healthy individuals (**Table 3b**). $CD45RA^+$ naïve CD4 T cells from SLE patients had significantly lower *MEF2D* mRNA expression than those from healthy controls (**Figure 31B**), implying reduced *MEF2D* expression in naïve CD4 T cells of SLE patients contributes to the development of cTfh cells. Notably, a significant negative association (p=0.004) was observed between the quantity of *MEF2D* mRNA and the frequency of cTfh in SLE patients (**Figure 31C**). In addition, inverse correlations were observed between *MEF2D* expression and SLEDAI (p=0.04) and serum autoantibody levels [anti-dsDNA (p=0.04) and ANA (p=0.006]) in the patients (**Figure 31D**), suggesting that reduced *MEF2D* expression in CD4 T cells is potentially linked to dysregulated humoral autoimmunity.

While I cannot completely exclude other pathological factors associated with reduced *MEF2D* expression, I did not observe significant inverse correlations between *MEF2D* mRNA level and the magnitude of CD4 T cell activation (**Figure 32A**) or frequencies of other effector CD4 T cells ($CXCR3^+CCR6^-$ Th1, $CXCR3^-CCR6^-$ Th2, and $CXCR3^-CCR6^+$ Th17 cells) (**Figure 32B**). Taken together, this study highlights a possible pathophysiologic role of the Mef2d and *Sh2d1a*/*Il21* gene regulation axis in controlling of T-dependent humoral autoimmunity.

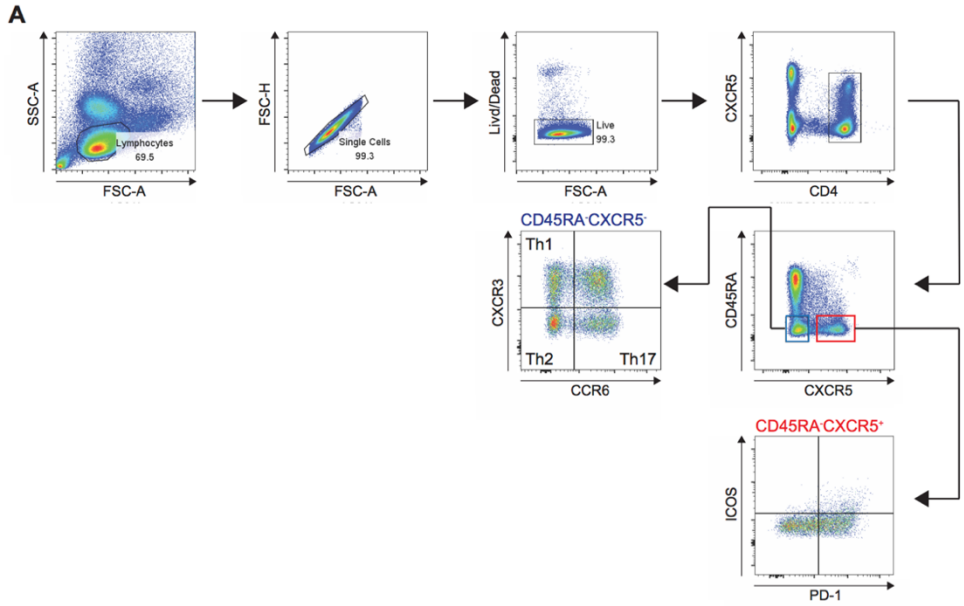

Figure 29. Gating strategies to analyze effector CD4 T cells in human PBMCs.

(A) The gating strategy to identify $CXCR3^{+}CCR6^{-}$ Th1, $CXCR3^{-}CCR6^{-}$ Th2, and $CXCR3^{-}CCR6^{+}$ Th17 cells among $CD45RA^{-}CXCR5^{-}$ CD4 T cells and $ICOS^{+}PD\text{-}1^{+}$ circulating Tfh (cTfh) cells among $CD45RA^{-}CXCR5^{+}$ CD4 T cells.

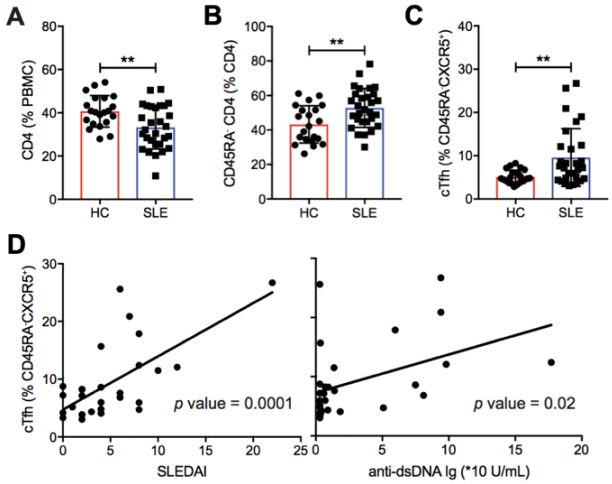

Figure 30. Autoimmune parameters of SLE patients are correlated with increased cTfh cell frequencies.

(A) The frequencies of total CD4 T cells in PBMCs from HC and SLE patients were quantified.

(B) The frequencies of $CD45RA^-$ cells among the total CD4 T cells from HC and SLE patients were calculated.

(C) $ICOS^+PD\text{-}1^+$ cTfh cell frequencies among $CD45RA^-CXCR5^+$ CD4 T cells were analyzed in HC and SLE patients.

(D) Correlations between the frequencies of $ICOS^+PD\text{-}1^+$ cTfh cells and SLEDAI score and anti-dsDNA Ig level were analyzed in SLE patients.

Detailed information is described in **Table S3** and **Table S4**. Error bars indicate mean with SD. Statistical significance values were determined using two-tailed Student's *t*-test **(A-C)** and Pearson's correlation analysis **(D)**. ** $p < 0.01$**.**

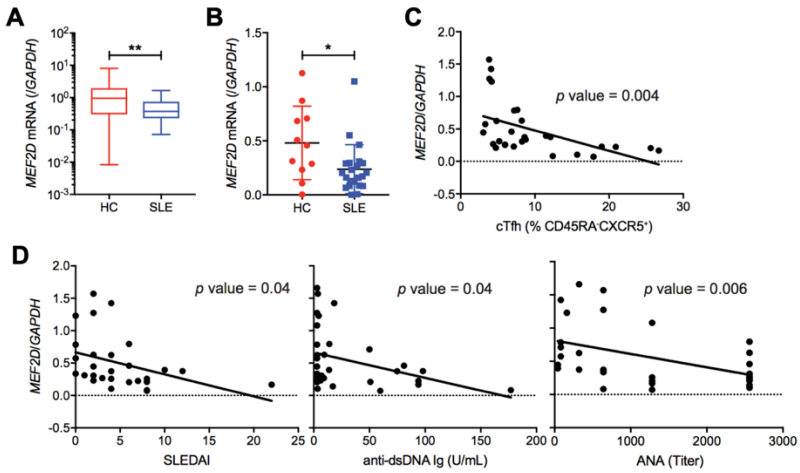

Figure 31. The autoimmune features of SLE patients are inversely associated with *MEF2D* mRNA expression in CD4 T cells.

(A) *MEF2D* mRNA levels were measured by qPCR in CD4 T cells obtained from HC and SLE patients.

(B) *MEF2D* mRNA was quantified in FACS-sorted CD45RA$^+$ naïve CD4 T cells obtained from HC and SLE patients.

(C) The correlation between *MEF2D* expression in CD4 T cells and the frequencies of ICOS$^+$PD-1$^+$ cTfh cells was examined in SLE patients.

(D) The correlations between *MEF2D* expression in CD4 T cells and SLEDAI score, anti-dsDNA Ig, and ANA were analyzed in SLE patients.

Error bars indicate mean with min to max **(A)** and mean with SD **(B)**. Statistical significance values were determined using two-tailed Student's *t*-test **(A-B)** and Pearson's correlation analysis **(C-D)**. * p <0.05; ** p <0.01.

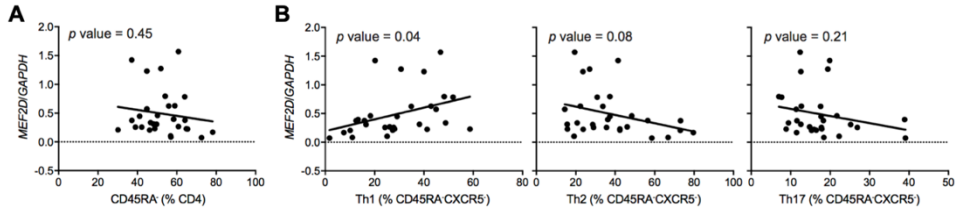

Figure 32. Correlation between *MEF2D* mRNA expression in CD4 T cells and frequencies of non-Tfh effector CD4 T cells.

(A and B) The correlations between *MEF2D* expression in CD4 T cells and the frequencies of $CD45RA^-$ cells **(A)** and Th1, Th2, and Th17 cells **(B)** were examined in SLE patients.

Statistical significance values were determined using Pearson's correlation analysis.

The Mef2 transcription factor isoforms might play distinct roles in GC-Tfh differentiation

Since Mef2 transcription factor isoforms share a conserved DNA binding domain, they could function together. I examined the expression of MEF2 transcription factors in tonsillar GC-Tfh (PD-1^{hi}CXCR5^{+}) and non-Tfh (PD-1^{-}CXCR5^{-}) cells (**Figure 1A**) to identify isoforms with a similar expression pattern to Mef2d. While only *MEF2A* and *MEF2D* are highly expressed in human peripheral blood CD4 T cells (**Figure 33A**), *MEF2B* expression was also highly exhibited in effector CD4 T cells in human tonsils (**Figure 33B**). However, in contrast to the significantly reduced mRNA expression of *MEF2D* in GC-Tfh cells compared to non-Tfh cells, the expression of *MEF2A* and *MEF2B* was comparable between non-Tfh and GC-Tfh cells (**Figure 33B**). In murine CD4 T cells, *Mef2a* mRNA was highly expressed, similar to *Mef2d*, but the expression patterns of *Mef2a* in effector CD4 T cell subsets were different from those of *Mef2d* (**Figure 33C**). Moreover, the overexpression of Mef2d or *Mef2d* gene disruption did not lead to changes in the expression of other Mef2 isoforms (**Figure 33D-E**), suggesting that they are unlikely to compensate for the gain and loss of Mef2d function.

However, despite exhibiting negligible expression in human peripheral blood CD4 T cells and murine CD4 T cells, the ectopic expression of Mef2b resulted in reduced differentiation of PD1^{+}CXCR5^{+} and PSGL1^{lo}CXCR5^{+} GC-Tfh cells (**Figure 34A-B**), similar to what was observed with Mef2d overexpression. Furthermore, a decrease in the expression of Tfh cell markers, including CXCR5, PD-1, and Bcl6 (**Figure 34C**) and an increase in PSGL-1 expression (**Figure 34D**) was observed, indicating that there is a possibility that other Mef2 isoforms could play a redundant role to Mef2d in SAP-dependent GC-Tfh differentiation and IL-21 production of CD4 T cells.

To address this possibility, I assessed the potential role of Mef2a, due to the high

expression of *Mef2a* in both human and murine CD4 T cells. *Mef2a* selectively edited OTII CD4 T cells (crMef2a #2) (**Figure 35A**) and control OTII CD4 T cells were adoptively transferred into recipients, and SAP-dependent GC-Tfh differentiation and IL-21 production were observed seven days after immunization (**Figure 35B**). $PD1^{+}CXCR5^{+}$ and $PSGL1^{lo}CXCR5^{+}$ GC-Tfh differentiation, as well as $SAP^{hi}CXCR5^{+}$ compartment of crMef2d-RNP^{+} OTII CD4 T cells, were comparable with those of control OTII CD4 T cells (**Figure 35C-E**). In addition, there were no differences in SAP protein expression and IL-21 production (**Figure 35F-G**) between these groups, implying that the Mef2a isoform does not play redundant roles to Mef2d in the transcriptional regulation of SAP and IL-21 during GC-Tfh differentiation.

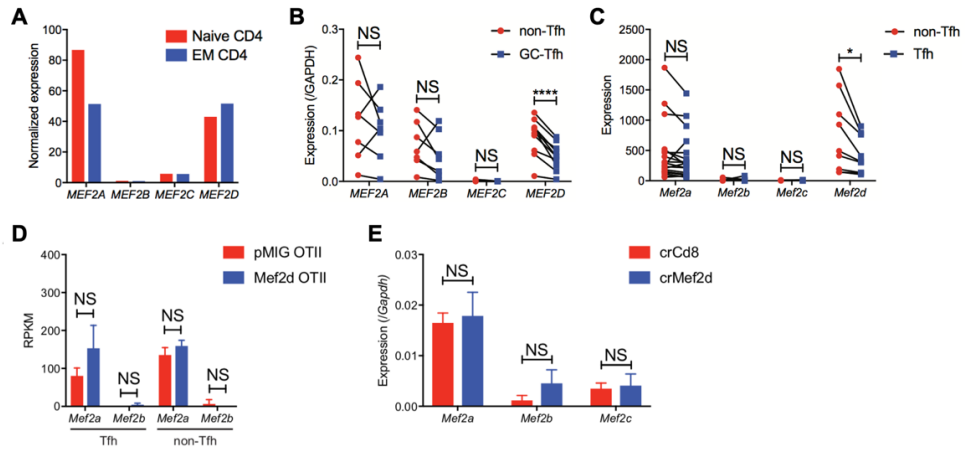

Figure 33. Expression of the MEF2 (Mef2) transcription factor family members in human (murine) CD4 T cell subsets.

(A) The expression of *MEF2* isoforms in human peripheral blood naïve (red) and effector memory (blue) CD4 T cells (Data obtained from the Human Cell Atlas database).

(**B**) Pairwise comparisons of *MEF2A-D* mRNA expression were performed between human tonsillar non-Tfh (red) and GC-Tfh (blue). The expression values were normalized to *GAPDH* mRNA.

(C) The expression of *Mef2a*, *Mef2b*, *Mef2c*, and *Mef2d* in murine non-Tfh (red) and Tfh (blue) cells.

(D) RPKMs of *Mef2a* and *Mef2b* in empty-RV OTII (red) and Mef2d-RV OTII (blue) CD4 T cell subsets were quantified **(Figure 7)**.

(E) The expression of *Mef2a*, *Mef2b*, and *Mef2c* in crCd8-RNP^{+} OTII (red) and crMef2d-RNP^{+} OTII (blue) CD4 T cells were calculated **(Figure 11)**.

Error bars indicate mean with SD. Statistical significance values were determined using two-tailed Student's *t*-test. NS, statistically non-significant.

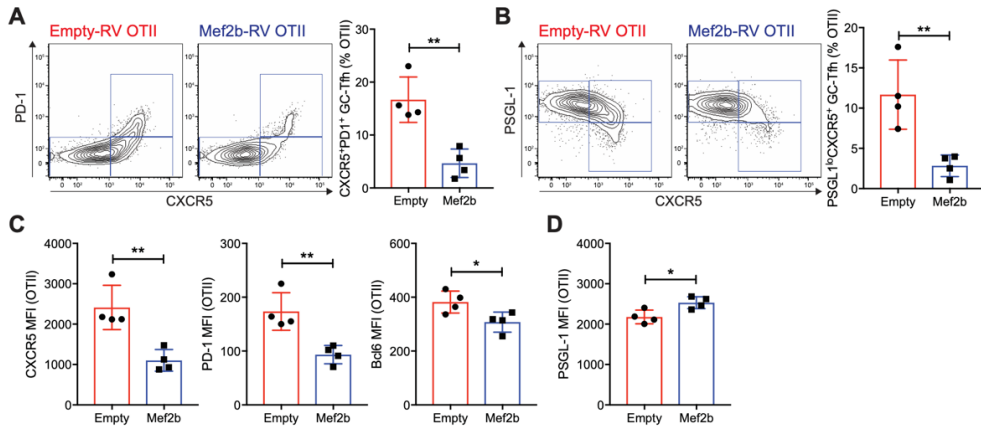

Figure 34. Ectopic Mef2b expression inhibits OTII CD4 T cells from differentiating into GC-Tfh cells.

Empty-RV or Mef2b-RV OTII CD4 T cells were adoptively transferred into C57BL/6J recipients. Seven days after NP-OVA immunization, GC-Tfh cell differentiation of the donor cells was analyzed.

(A and B) The flow cytometry plots of the transferred OTII CD4 T cells. The frequencies of PD-1^{+}CXCR5^{+} **(A)** and PSGL-1^{lo}CXCR5^{+} **(B)** GC-Tfh cells were calculated.

(C and D) The MFIs of CXCR5, PD-1, Bcl6 **(C)**, and PSGL-1 **(D)** were quantified.

Error bars indicate mean with SD. Statistical significance values were determined using two-tailed Student's *t*-test. * p <0.05; ** p <0.01.

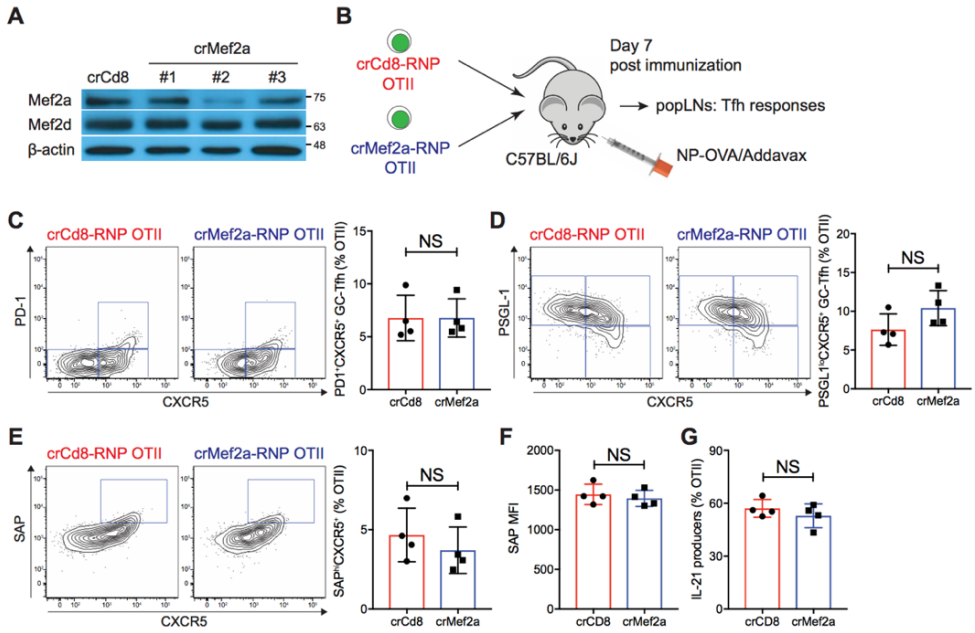

Figure 35. Mef2a does not play redundant roles to Mef2d in the negative regulation of SAP-dependent GC-Tfh differentiation and IL-21 production.

(A) Immunoblots of β-actin, Mef2a, and Mef2d proteins. Cell lysates were obtained from crCd8-RNP^{+} or crMef2a-RNP^{+} OTII CD4 T cells.

(B) Seven days after NP-OVA immunization, GC-Tfh differentiation, SAP expression, and IL-21 production of the donor OTII CD4 T cells were analyzed.

(C and D) The flow cytometry plots of the transferred OTII CD4 T cells. The frequencies of PD-1^{+}CXCR5^{+} GC-Tfh **(C)** and PSGL-1^{lo}CXCR5^{+} **(D)** were calculated.

(E) The flow cytometry plots of the donor OTII CD4 T cells. The frequencies of SAP^{hi}CXCR5^{+} cells were quantified.

(F) The MFIs of SAP were calculated.

(G) The frequencies of IL-21 producers were quantified.

Representative of two independent experiments with n=4-5 mice per group. Error bars indicate mean with SD. Statistical significance values were determined using two-tailed Student's *t*-test. NS, statistically non-significant.

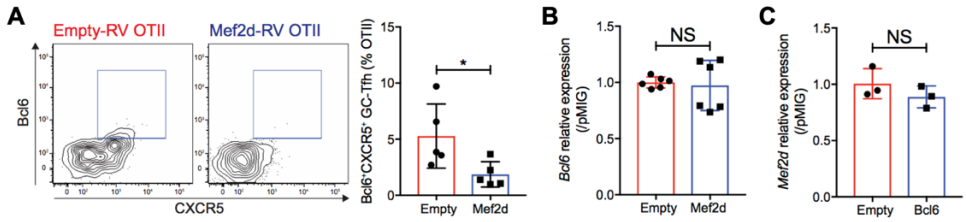

Figure 36. The inhibition of GC-Tfh/Tfh differentiation by Mef2d may occur in a Bcl6-independent manner.

(A) The flow cytometry plots of the transferred RV^+ OTII CD4 T cells **(Figure 2)**. The frequencies of $Bcl6^+CXCR5^+$ GC-Tfh cells were quantified.

(B and C) Polyclonal CD4 T cells were obtained from naïve C57BL/6J mice, activated *in vitro*, and transduced with Mef2d-RV **(B)** or Bcl6-RV **(C)**. Four days after transduction, RV^+ CD4 T cells were sorted, and the respective gene expression was analyzed by qPCR. The relative gene expression of Mef2d-RV^+ or Bcl6-RV^+ CD4 T cells compared to empty-RV^+ CD4 T cells was determined. Samples were prepared from two **(B)** or one **(C)** experiment with triplicate wells per group.

Error bars indicate mean with SD. Statistical significance values were determined using two-tailed Student's *t*-test. NS, statistically non-significant. * $p < 0.05$.

DISCUSSION

1. Transcriptional regulation of Tfh differentiation and TD humoral immunity by Mef2d

The formation of B:T synapse ensure proper interactions of CD4 T cells with cognate B cells, a critical check point for the immune system to initiate TD humoral immunity. Through B:T synapses, signaling molecules can transfer between cognate B cells and Tfh cells that have developed in the T cell zone at the B:T border. This determines whether Tfh cells would further differentiate into GC-Tfh cells and whether cognate B cells would migrate deep into follicles to form GCs. Within GCs, the effective formation of B:T synapses between GC-Tfh cells and cognate GC B cells plays a fundamental role in the selection of affinity-matured GC clones and, therefore, in the evolution of Ag-specific B cell responses during TD humoral immunity.

SAP, an essential signaling molecule for CD4 T cells to stably form immune synapse with cognate B cells, is required during this process and needs to be tightly controlled to ensure that only cognate B cells undergo clonal evolution during GC responses. My doctoral research aimed to reveal signaling pathway(s) or molecule(s) that could control SAP expression in CD4 T cells. Here, I demonstrated that the Mef2d transcription factor functions as a negative regulator of SAP expression and, therefore, is a critical controller of TD humoral immunity. I found that Mef2d prohibits SAP-dependent B:T synapse formation and the differentiation of Ag-specific CD4 T cells into GC-Tfh cells by directly inhibiting the *Sh2d1a* gene in CD4 T cells. Consequently, Mef2d function in CD4 T cells negatively modulated Ag-specific TD humoral immunity against exogenous protein Ags.

GCs are biological machinery contributing to a robust proliferation of Ag-

specific B cells, enabling the immune system to effectively develop sufficient B cell clones for controlling invading pathogens or exogenous Ags. In the light zone, GC B cells are instructed to migrate to the dark zone only when they form stable immune synapses with GC-Tfh cells, where they undergo a round of cell proliferation. IL-21, produced by GC-Tfh cells in the light zone, functions as an important signal for Ag-specific GC B cells to proliferate. Therefore, my finding of Mef2d-mediated IL-21 production in CD4 T cells highlights the Mef2d transcription factor as an essential transcriptional switch that turns on and maintains the GC program with cognate B cells.

Antibody-secreting B cells develop via two different routes after B cell activation in the secondary lymphoid tissues: extrafollicular responses and GCs. The former gives rise to plasmablasts that are responsible for the early production of low-affinity antibodies outside of B cell follicles, whereas the latter engenders long-lived plasma cells that produce high-affinity and isotype-switched antibodies. Interestingly, these spatiotemporally distinct waves of antibody-producing B cell differentiation occur in an IL-21-dependent manner (*91*). In this study, I revealed that IL-21 production of CD4 T cells is transcriptionally inhibited by Mef2d, which compromises the production of high-affinity Ag-specific antibodies along with the negative regulation of SAP-dependent B:T synapse formation and GC-Tfh differentiation, as well as the production of low-affinity Ag-specific antibodies. Collectively, my doctoral work sheds light on the transcriptional mechanisms of CD4 T cells that control not only Ag-specific GC formation but also GC- and extrafollicular response-driven Ag-specific antibody production of cognate B cells (**Figure 37**).

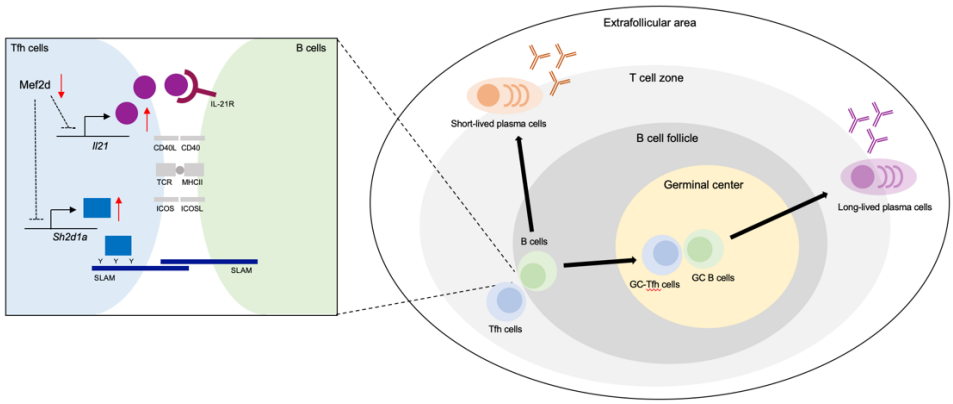

Figure 37. The graphical summary of this study.

2. The physiological roles of the Mef2 transcription factor family in Tfh differentiation

The conserved DNA binding domain at the N-terminus enables the four Mef2 isoforms to share target genes, indicating possible redundant transcriptional regulatory roles of the Mef2 transcription factor family in the muscular, nervous, and immune systems. For example, both Mef2a and Mef2d have been shown to induce the *Glut4* gene in skeletal muscle (*92*) and the *Arc* and *SynGAP* genes in hippocampal neurons (*59*). In the large pre-B cell stage of B cell development, Mef2c and Mef2d collaborate to regulate the expression of *Klf2* and immediate early genes (IEGs) such as *Egr1/2*, *Ier2*, *Jun*, and *Fos*, facilitating the transition to the next stages of B cell development (*53*). The redundant roles of the Mef2 isoforms are also observed during GC formation of mature B cells. In the context of sheep red blood cell (SRBC) immunization, *Mef2b*$^{-/-}$ *Mef2c*$^{-/-}$ B cells scarcely formed GCs, whereas deficiency of a single gene induced only partial reductions in GC formation of B cells (*93*).

Based on these previous findings, I speculated that other Mef2 isoforms, if

expressed as robustly as Mef2d, may play redundant roles with Mef2d in regulating Tfh-related genes in CD4 T cells. In the current study, Mef2a was tested due to its high expression in naive and effector CD4 T cells in both humans and mice. However, I found that RNP-mediated *Mef2a* gene disruption failed to phenocopy the enlarged SAP expression and GC-Tfh differentiation, as well as the increased IL-21 production observed in OTII CD4 T cells whose *Mef2d* gene was disrupted or deleted. This result suggests that Mef2 isoforms might not function harmoniously in regulating the Tfh differentiation of CD4 T cells.

My doctoral research revealed that Mef2d is a critical negative regulator of SAP-dependent GC-Tfh differentiation and IL-21 production in CD4 T cells, which are essential immunological phenomena for eliciting TD humoral immunity. TD humoral immune responses are controlled by transcriptional circuits that program not only CD4 T cells but also Ag-activated B cells to acquire the cellular and molecular characteristics of GC B cells (*94*). Among the two isoforms redundantly required for GC formation in B cells (*93*), MEF2B was shown to transcriptionally activate *BCL6* in B cells (*54*), a transcription factor unconditionally required for B cells to form GCs (*95*). Since Bcl6 is a major fate-determining transcription factor for Tfh differentiation (*96*), it could be speculated that Mef2b might function as a positive regulator of Tfh differentiation. To test this hypothesis, I ectopically induced Mef2b expression in CD4 T cells, considering its almost negligible expression in murine CD4 T cells (**Figure 33C**). Contrary to my expectations, Mef2b exhibited a completely different behavior in B cells and CD4 T cells. Instead of activating *Bcl6* expression and positively regulating Tfh differentiation, ectopically induced Mef2b strongly inhibited Tfh and GC-Tfh differentiation of CD4 T cells.

The Mef2 transcription factors appear to potentially function as antagonizers of Tfh differentiation and TD humoral immunity. Mef2a, even though it does not appear to play redundant roles with Mef2d (**Figure 35**), was found to impede GC-

Tfh differentiation of CD4 T cells, similar to Mef2b and Mef2d, when ectopically expressed (**Data not shown**). Then, it is a conundrum how Mef2a plays similar roles to Mef2d when it is expressed at higher than physiological levels. I contemplate that the elevated Mef2a isoform might enhance the Mef2d-mediated transcriptional repression of the *Sh2d1a* and *Il21* genes via Mef2a-Mef2d heterodimer formation and, therefore, could inhibit Tfh differentiation. This speculation will be examined with *Mef2d*-deficient OTII CD4 T cells, in which Mef2a is ectopically expressed.

3. The possible mechanisms of regulating *Mef2d* expression

3.1 MicroRNA (miRNA)-mediated *Mef2d* expression

From my doctoral research, I discovered that Mef2d functions as a critical rheostat of TD humoral immunity. Given its crucial roles in immune protection against infectious pathogens, as well as in autoantibody-mediated autoimmunity, understanding how *Mef2d* expression is regulated in CD4 T cells becomes an important question to reveal, both for the development of efficacious vaccines and for establishing therapeutic strategies for autoimmune diseases. Recently, miRNAs, small non-coding RNAs approximately 22 nucleotides in length, were revealed to regulate *Mef2* expression in brain and muscle cells. In glioma cells, a type of brain tumor cells, Xue and colleagues found that miR-18a bound to the 3'-UTR of the *Mef2d* mRNA, resulting in the downregulation of its expression. The miR-18a-mediated downregulation of Mef2d translation subsequently affected the expression of tight junction-related proteins, ultimately leading to an increase in the permeability of the blood-tumor barrier (*97*). In muscle myoblast, miR-155 was discovered to function as an antagonistic factor of Mef2a translation (*98*). In this study, miR-155 overexpression resulted in the suppression of endogenous Mef2a

levels by binding to the 3'-UTR of the *Mef2a* mRNA, thereby inhibiting Mef2a-dependent myotube formation during myoblast differentiation (*98*). Collectively, these findings underscore the critical roles of miRNAs in regulating *Mef2* expression and their potential to modulate immunological functions downstream of Mef2 transcription factors.

Interestingly, various miRNAs, such as miR-18a, miR-19b1, miR-21, miR-61, miR-78, miR-142-3p, miR-189, miR-198, miR-298, miR-299-3p, and miR-342, were found to be upregulated in patients with SLE and, thus, have been proposed as potential diagnostic markers for SLE (*99, 100*). Given that dysregulated Tfh differentiation and functions are associated with SLE autoimmunity (*101*), one possible pathological role of the upregulated miRNA expressions might be associated with abnormal Tfh biology. Indeed, the miRNA cluster miR-17~92, which includes miR-18a, was found to play a critical role in the differentiation and function of Tfh cells. Jeker and colleagues discovered that miR-17~92 promotes Tfh differentiation of CD4 T cells during viral infection by restricting the expression of genes inappropriate to the Tfh differentiation program, including *Ccr6*, *Il1r2*, *Il1r1*, *Rora*, and *Il22* (*102*). It will be important to determine miRNA expression profiles associated with the Tfh/GC-Tfh differentiation program, to screen potential miRNAs that can bind to the UTR regions of the *Mef2d* mRNA, and to examine whether these miRNAs, including miR-18a, could function upstream of the Mef2d-mediated transcriptional repression of SAP expression and IL-21 production of CD4 T cells.

3.2 BCL6-mediated *MEF2D* expression

In 2009, BCL6 (Bcl6 in mice) was revealed as a key transcription factor for Tfh/GC-Tfh differentiation of CD4 T cells (*96, 103*). Since then, myriad research groups have made tremendous efforts to reveal how BCL6 functions in Tfh/GC-

Tfh differentiation, and it is now understood that this transcription factor programs Tfh/GC-Tfh differentiation in two ways: by positively regulating genes that favor Tfh differentiation and by negatively controlling genes that antagonize this pathway (*3*). One of the major inhibitory functions is to transcriptionally repress the *PRDM1* (*Prdm1* in mice) gene encoding BLIMP1 (Blimp1 in mice), which suppresses *BCL6* expression and blocks the BCL6-dependent Tfh differentiation (*103*). Expression of *BCL6* and *PRDM1* genes is thus reciprocally regulated in non-Tfh and Tfh/GC-Tfh cells (*103*).

During my doctoral research, I observed a parallel expression pattern between the *MEF2D* and *PRDM1* genes in PD-1^{-}CXCR5^{-} non-Tfh and PD-1^{hi}CXCR5^{+} GC-Tfh cells in human lymphoid tissues (**Figure 1**). This finding indicates that *MEF2D* expression might be associated with the transcriptional activity of BCL6 in effector CD4 T cell differentiation. Interestingly, I found BCL6 binding motifs in the *MEF2D* gene locus from a previous study, in which BCL6-bound regions were examined genome-wide in human effector CD4 T cells (*104*). This led me to speculate that *MEF2D* expression might be under the control of BCL6 during Tfh/GC-Tfh differentiation. If this hypothesis is confirmed, it could provide a potential explanation for how BCL6 positively regulates SAP expression in CD4 T cells (*6*) and would add additional support for the recently proposed repressor-of-repressor functions of Bcl6 (*2*). Preliminary studies, however, suggest that Bcl6 does not seem to regulate the Mef2d - *Sh2d1a* axis. I found that ectopic Bcl6 expression failed to reduce *Mef2d* mRNA expression in *in vitro* stimulated murine CD4 T cells (**Figure 36C**). Further investigations are required to test this regulatory axis using physiologically relevant samples, as ectopic Bcl6 expression alone is insufficient to induce Tfh differentiation in human and murine CD4 T cells in the context of *in vitro* stimulation (*6, 103*).

3.3 Post-translational modification-mediated Mef2d protein expression

Post-translational modifications (PTMs), such as phosphorylation, acetylation, and sumoylation, play important roles in supporting delicate cellular controls of protein expression and function (*105*). Phosphorylation of transcription factors or coactivators can significantly impact effector CD4 T cell differentiation and its effector function. For example, when the C-terminal of Foxp3 is phosphorylated, it results in reduced DNA binding of target genes, ultimately decreasing its suppressive activity (*106*). Additionally, the Ser21 phosphorylation of Ezh2, a histone methyltransferase that functions as a transcriptional coactivator in Tfh cells, is critical for the optimal induction of *Bcl6* transcription, leading to the activation of the Tfh program (*107*). Thus, PTMs could play regulatory roles in Mef2d-mediated Tfh/GC-Tfh differentiation and IL-21 production of CD4 T cells. This speculation is supported by the presence of multiple phosphorylation sites within the MADS, Mef2, and TAD domains of the Mef2 transcription factors (*44*), and by previous findings of the regulation of Mef2 isoforms in the context of phosphorylation (ERK, GSKβ, and Cdk5) and dephosphorylation (PP2B and calcineurin) enzyme activities (*44*). Regarding the Mef2d protein stability, Cdk5 was defined as a key kinase. Giguère and colleagues reported that Cdk5 phosphorylates a serine residue (Ser-444 in human and Ser-437 in murine) of the MEF2D (Mef2d) isoform, which subsequently leads to sumoylation of a lysine residue (Lys-439 in human and Lys-432 in murine) (*108*). Sumoylated MEF2D (Mef2d) becomes loss of its transcriptional activity (*108*), as well as undergoes proteasomal degradation via the unconventional 20s proteasomal pathway (*109*). This degradation pathway was shown to play an important role in controlling the neurotoxin-induced apoptosis of cerebellar granule neurons (*110*). Given these reported functions, it will be interesting to study potential roles of PTMs in the

regulation of Mef2d in CD4 T cells and its impact on SAP-dependent Tfh/GC-Tfh differentiation and IL-21 production in CD4 T cells.

4. Clinical implications of Mef2d function in CD4 T cells

Emerging evidence suggests that precise control of synapse formation is essential for proper intercellular communication in the nervous system. Synaptic dysfunction in the nervous system leads to neurodegenerative diseases such as Parkinson's disease (PD), Alzheimer's disease (AD), and Huntington's disease (HD), resulting in the gradual loss of neural tissue and a decline in cognitive and behavioral functions (*111*). Transcription factors such as GATA-1, GATA-2, TFEB, STAT1, and CTCF play crucial roles in preventing synaptic dysfunction by controlling the accumulation of specific disease-associated proteins, such as α-synuclein, Tau, and Huntingtin, which can lead to proteostasis imbalance and disturb synaptic organization, in pre- and post-synaptic neurons. These transcription factors achieve this by regulating the gene expressions of these proteins or facilitating their clearance (*112-114*).

My doctoral research focused on the role of the Mef2d transcription factor in regulating synapse formation within the immune system. By directly repressing SAP, Mef2d plays a crucial role in B:T synapse formation, leading to the control of Tfh differentiation, the dysregulation of which can lead to the development of autoimmune diseases. An important finding in this study was the reduced expression of *MEF2D* in CD4 T cells from patients with SLE compared to healthy individuals. This decrease in *MEF2D* expression was associated with an increased frequency of cTfh-like cells and the presence of autoimmune conditions, such as elevated levels of autoantibodies and disease severity, in SLE patients. Therefore, these findings underscore the critical importance of precise transcriptional regulation, particularly in the context of B:T synapse formation. This

transcriptional mechanism ensures that Tfh cells could exclusively interact with cognate Ag-specific B cells through immune synapse formation, thereby promoting their quantitative expansion and qualitative maturation to generate specific antibodies against Ags, while inhibiting the formation of immune synapses with non-specific B cells, thus preventing their activation and differentiation. This phenomenon is expected to be confirmed through research utilizing CD4 T cell-specific *Mef2d* deletion mice.

Furthermore, IL-21 signaling contributes to autoimmune diseases by promoting the production of pathogenic autoantibodies through both GC and extrafollicular reactions. Dunussi-Joannopoulos and colleagues reported that in MRL^{lpr} mice, which develop lupus-like autoimmune disease manifestations, deletion of IL-21R reduces GC formation, as well as plasmablast accumulation in the extrafollicular region, ultimately resulting in decreased autoantibody production (*115*). Thus, my doctoral study further contributes to the understanding of the mechanisms underlying autoimmune diseases by revealing the involvement of Mef2d in regulating IL-21 production in CD4 T cells. Interestingly, recent studies suggest that age-associated B cells (ABCs), predominantly arising from the extrafollicular region, exhibit elevation in the context of autoimmune diseases (*116*). Since these cells require T cell-derived IL-21 signals for their differentiation (*117*), my work suggests the possibility of Mef2d transcription factor regulating autoimmune conditions by controlling the differentiation of age-associated B cells.

Concluding Remarks

Considering that Mef2d contributes to TD humoral (auto)immunity by regulating the expression of SAP and the production of IL-21 in CD4 T cells, investigating the mechanisms that regulate Mef2d expression or function has the potential to become a pivotal strategy for enhancing vaccine efficacy and developing new therapeutic approaches for patients with autoimmune diseases characterized by reduced *MEF2D* expression.

REFERENCES

1. S. Crotty, T follicular helper cell biology: a decade of discovery and diseases. *Immunity* **50**, 1132-1148 (2019).
2. J. Choi *et al.*, Bcl-6 is the nexus transcription factor of T follicular helper cells via repressor-of-repressor circuits. *Nature immunology* **21**, 777-789 (2020).
3. J. Choi, S. Crotty, Bcl6-mediated transcriptional regulation of follicular helper T cells (TFH). *Trends in immunology* **42**, 336-349 (2021).
4. Y. S. Choi *et al.*, LEF-1 and TCF-1 orchestrate TFH differentiation by regulating differentiation circuits upstream of the transcriptional repressor Bcl6. *Nature immunology* **16**, 980-990 (2015).
5. W. Ise *et al.*, The transcription factor BATF controls the global regulators of class-switch recombination in both B cells and T cells. *Nature immunology* **12**, 536-543 (2011).
6. M. A. Kroenke *et al.*, Bcl6 and Maf cooperate to instruct human follicular helper CD4 T cell differentiation. *The Journal of Immunology* **188**, 3734-3744 (2012).
7. D. Suan *et al.*, T follicular helper cells have distinct modes of migration and molecular signatures in naive and memory immune responses. *Immunity* **42**, 704-718 (2015).
8. J. Shi *et al.*, PD-1 controls follicular T helper cell positioning and function. *Immunity* **49**, 264-274. e264 (2018).
9. H. Qi, J. L. Cannons, F. Klauschen, P. L. Schwartzberg, R. N. Germain, SAP-controlled T–B cell interactions underlie germinal centre formation. *Nature* **455**, 764-769 (2008).
10. G. D. Victora, M. C. Nussenzweig, Germinal centers. *Annual review of immunology* **30**, 429-457 (2012).
11. D. Liu *et al.*, T–B-cell entanglement and ICOSL-driven feed-forward regulation of germinal centre reaction. *Nature* **517**, 214-218 (2015).
12. G. D. Victora, M. C. Nussenzweig, Germinal centers. *Annual review of immunology* **40**, 413-442 (2022).
13. M. A. Linterman *et al.*, IL-21 acts directly on B cells to regulate Bcl-6 expression and germinal center responses. *Journal of Experimental Medicine* **207**, 353-363 (2010).

14. A. Vogelzang *et al.*, A fundamental role for interleukin-21 in the generation of T follicular helper cells. *Immunity* **29**, 127-137 (2008).
15. R. Ettinger *et al.*, IL-21 induces differentiation of human naive and memory B cells into antibody-secreting plasma cells. *J Immunol* **175**, 7867-7879 (2005).
16. L. Moens, S. G. Tangye, Cytokine-Mediated Regulation of Plasma Cell Generation: IL-21 Takes Center Stage. *Front Immunol* **5**, 65 (2014).
17. J. S. Weinstein *et al.*, TFH cells progressively differentiate to regulate the germinal center response. *Nature immunology* **17**, 1197-1205 (2016).
18. W. Ise *et al.*, T follicular helper cell-germinal center B cell interaction strength regulates entry into plasma cell or recycling germinal center cell fate. *Immunity* **48**, 702-715. e704 (2018).
19. N. J. Kräutler *et al.*, Differentiation of germinal center B cells into plasma cells is initiated by high-affinity antigen and completed by Tfh cells. *Journal of Experimental Medicine* **214**, 1259-1267 (2017).
20. R. Shinnakasu *et al.*, Regulated selection of germinal-center cells into the memory B cell compartment. *Nat Immunol* **17**, 861-869 (2016).
21. R. Shinnakasu *et al.*, Regulated selection of germinal-center cells into the memory B cell compartment. *Nature immunology* **17**, 861-869 (2016).
22. D. Suan, C. Sundling, R. Brink, Plasma cell and memory B cell differentiation from the germinal center. *Current opinion in immunology* **45**, 97-102 (2017).
23. M. L. Dustin, The immunological synapse. *Cancer Immunol Res* **2**, 1023-1033 (2014).
24. Y. Gartshteyn, A. D. Askanase, A. Mor, SLAM associated protein signaling in T cells: Tilting the balance toward autoimmunity. *Frontiers in Immunology* **12**, 654839 (2021).
25. R. Proust, J. Bertoglio, F. Gesbert, The adaptor protein SAP directly associates with CD3ζ chain and regulates T cell receptor signaling. (2012).
26. R. Kageyama *et al.*, The receptor Ly108 functions as a SAP adaptor-dependent on-off switch for T cell help to B cells and NKT cell development. *Immunity* **36**, 986-1002 (2012).
27. J. L. Cannons, S. G. Tangye, P. L. Schwartzberg, SLAM family receptors

and SAP adaptors in immunity. *Annual review of immunology* **29**, 665-705 (2011).

28. S. Crotty, E. N. Kersh, J. Cannons, P. L. Schwartzberg, R. Ahmed, SAP is required for generating long-term humoral immunity. *Nature* **421**, 282-287 (2003).
29. M. Morra *et al.*, X-linked lymphoproliferative disease: a progressive immunodeficiency. *Annual review of immunology* **19**, 657-682 (2001).
30. B. Hügle *et al.*, Persistent hypogammaglobulinemia following mononucleosis in boys is highly suggestive of X-linked lymphoproliferative disease—report of three cases. *Journal of Clinical Immunology* **24**, 515-522 (2004).
31. K. Morimoto, K. Nakajima, Role of the immune system in the development of the central nervous system. *Frontiers in Neuroscience* **13**, 916 (2019).
32. M. Simonetti *et al.*, The impact of Semaphorin 4C/Plexin-B2 signaling on fear memory via remodeling of neuronal and synaptic morphology. *Mol Psychiatry* **26**, 1376-1398 (2021).
33. K. Yukawa *et al.*, Semaphorin 4A induces growth cone collapse of hippocampal neurons in a Rho/Rho-kinase-dependent manner. *Int J Mol Med* **16**, 115-118 (2005).
34. A. Kumanogoh *et al.*, Nonredundant roles of Sema4A in the immune system: defective T cell priming and Th1/Th2 regulation in Sema4A-deficient mice. *Immunity* **22**, 305-316 (2005).
35. H. Yan *et al.*, Plexin B2 and Semaphorin 4C Guide T Cell Recruitment and Function in the Germinal Center. *Cell Rep* **19**, 995-1007 (2017).
36. R. Klein, Bidirectional modulation of synaptic functions by Eph/ephrin signaling. *Nature neuroscience* **12**, 15-20 (2009).
37. P. Lu, C. Shih, H. Qi, Ephrin B1–mediated repulsion and signaling control germinal center T cell territoriality and function. *Science* **356**, eaai9264 (2017).
38. C.-Y. Zheng, G. K. Seabold, M. Horak, R. S. Petralia, MAGUKs, synaptic development, and synaptic plasticity. *The Neuroscientist* **17**, 493-512 (2011).
39. J. L. Round *et al.*, Dlgh1 coordinates actin polymerization, synaptic T cell receptor and lipid raft aggregation, and effector function in T cells. *The*

Journal of experimental medicine **201**, 419-430 (2005).

40. G. Rizzi, K. R. Tan, Dopamine and Acetylcholine, a Circuit Point of View in Parkinson's Disease. *Front Neural Circuits* **11**, 110 (2017).
41. X. Zhang *et al.*, Brain control of humoral immune responses amenable to behavioural modulation. *Nature* **581**, 204-208 (2020).
42. C. Sarkar, B. Basu, D. Chakroborty, P. S. Dasgupta, S. Basu, The immunoregulatory role of dopamine: an update. *Brain, behavior, and immunity* **24**, 525-528 (2010).
43. I. Papa *et al.*, TFH-derived dopamine accelerates productive synapses in germinal centres. *Nature* **547**, 318-323 (2017).
44. A. Rashid, C. Cole, S. Josselyn, Emerging roles for MEF2 transcription factors in memory. *Genes, Brain and Behavior* **13**, 118-125 (2014).
45. M. Lisek, O. Przybyszewski, L. Zylinska, F. Guo, T. Boczek, The Role of MEF2 Transcription Factor Family in Neuronal Survival and Degeneration. *International Journal of Molecular Sciences* **24**, 3120 (2023).
46. O. I. Ornatsky, J. C. McDermott, MEF2 protein expression, DNA binding specificity and complex composition, and transcriptional activity in muscle and non-muscle cells. *Journal of Biological Chemistry* **271**, 24927-24933 (1996).
47. Y. Yin *et al.*, Modulation of neuronal survival factor MEF2 by kinases in Parkinson's disease. *Frontiers in physiology* **3**, 171 (2012).
48. D. G. Edmondson, G. E. Lyons, J. F. Martin, E. N. Olson, Mef2 gene expression marks the cardiac and skeletal muscle lineages during mouse embryogenesis. *Development* **120**, 1251-1263 (1994).
49. M. V. Taylor, S. M. Hughes, Mef2 and the skeletal muscle differentiation program. *Semin Cell Dev Biol* **72**, 33-44 (2017).
50. C. M. Anderson *et al.*, Myocyte enhancer factor 2C function in skeletal muscle is required for normal growth and glucose metabolism in mice. *Skelet Muscle* **5**, 7 (2015).
51. A. J. Harrington *et al.*, MEF2C regulates cortical inhibitory and excitatory synapses and behaviors relevant to neurodevelopmental disorders. *Elife* **5**, (2016).
52. B. J. Swanson, H. M. Jäck, G. E. Lyons, Characterization of myocyte enhancer factor 2 (MEF2) expression in B and T cells: MEF2C is a B cell-restricted transcription factor in lymphocytes. *Mol Immunol* **35**, 445-458

(1998).
53. J. Herglotz *et al.*, Essential control of early B-cell development by Mef2 transcription factors. *Blood, The Journal of the American Society of Hematology* **127**, 572-581 (2016).
54. C. Y. Ying *et al.*, MEF2B mutations lead to deregulated expression of the oncogene BCL6 in diffuse large B cell lymphoma. *Nature immunology* **14**, 1084-1092 (2013).
55. E. Di Giorgio *et al.*, MEF2D sustains activation of effector Foxp3+ Tregs during transplant survival and anticancer immunity. *The Journal of Clinical Investigation* **130**, 6242-6260 (2020).
56. E. Di Giorgio *et al.*, A Biological Circuit Involving Mef2c, Mef2d, and Hdac9 Controls the Immunosuppressive Functions of CD4+ Foxp3+ T-Regulatory Cells. *Frontiers in Immunology* **12**, 703632 (2021).
57. M. V. Taylor, S. M. Hughes, in *Seminars in cell & developmental biology*. (Elsevier, 2017), vol. 72, pp. 33-44.
58. K. Canté-Barrett *et al.*, MEF2C opposes Notch in lymphoid lineage decision and drives leukemia in the thymus. *JCI insight* **7**, (2022).
59. S. W. Flavell *et al.*, Activity-Dependent Regulation of MEF2 Transcription Factors Suppresses Excitatory Synapse Number. *Science* **311**, 1008-1012 (2006).
60. S. Chowdhury *et al.*, Arc/Arg3. 1 interacts with the endocytic machinery to regulate AMPA receptor trafficking. *Neuron* **52**, 445-459 (2006).
61. A. C. Barbosa *et al.*, MEF2C, a transcription factor that facilitates learning and memory by negative regulation of synapse numbers and function. *Proceedings of the National Academy of Sciences* **105**, 9391-9396 (2008).
62. Y. Omori *et al.*, Mef2d is essential for the maturation and integrity of retinal photoreceptor and bipolar cells. *Genes to Cells* **20**, 408-426 (2015).
63. Y. S. Choi, S. Crotty, Retroviral vector expression in TCR transgenic CD4+ T cells. *T follicular Helper Cells: Methods and Protocols*, 49-61 (2015).
64. Y. Chen *et al.*, SHIP-1 deficiency in AID+ B cells leads to the impaired function of B10 cells with spontaneous autoimmunity. *The Journal of Immunology* **199**, 3063-3073 (2017).
65. C. Chu *et al.*, SAP-regulated T cell–APC adhesion and ligation-

dependent and-independent Ly108–CD3ζ interactions. *The Journal of Immunology* **193**, 3860-3871 (2014).

66. S. L. Rosales *et al.*, A sensitive and integrated approach to profile messenger RNA from samples with low cell numbers. *Type 2 Immunity: Methods and Protocols*, 275-302 (2018).
67. G. Seumois *et al.*, Epigenomic analysis of primary human T cells reveals enhancers associated with TH2 memory cell differentiation and asthma susceptibility. *Nature immunology* **15**, 777-788 (2014).
68. A. Dobin *et al.*, STAR: ultrafast universal RNA-seq aligner. *Bioinformatics* **29**, 15-21 (2013).
69. R. Schmieder, R. Edwards, Quality control and preprocessing of metagenomic datasets. *Bioinformatics* **27**, 863-864 (2011).
70. H. Li *et al.*, The sequence alignment/map format and SAMtools. *bioinformatics* **25**, 2078-2079 (2009).
71. Y. Liao, G. K. Smyth, W. Shi, featureCounts: an efficient general purpose program for assigning sequence reads to genomic features. *Bioinformatics* **30**, 923-930 (2014).
72. M. I. Love, W. Huber, S. Anders, Moderated estimation of fold change and dispersion for RNA-seq data with DESeq2. *Genome biology* **15**, 1-21 (2014).
73. C. J. Kim *et al.*, The transcription factor Ets1 suppresses T follicular helper type 2 cell differentiation to halt the onset of systemic lupus erythematosus. *Immunity* **49**, 1034-1048. e1038 (2018).
74. C. J. Cole *et al.*, MEF2 negatively regulates learning-induced structural plasticity and memory formation. *Nature neuroscience* **15**, 1255-1264 (2012).
75. C. G. Vinuesa, M. A. Linterman, D. Yu, I. C. MacLennan, Follicular helper T cells. *Annual review of immunology* **34**, 335-368 (2016).
76. J. S. Weinstein *et al.*, Global transcriptome analysis and enhancer landscape of human primary T follicular helper and T effector lymphocytes. *Blood, The Journal of the American Society of Hematology* **124**, 3719-3729 (2014).
77. H.-D. Youn, L. Sun, R. Prywes, J. O. Liu, Apoptosis of T cells mediated by Ca2+-induced release of the transcription factor MEF2. *Science* **286**, 790-793 (1999).

78. Y. S. Choi *et al.*, ICOS receptor instructs T follicular helper cell versus effector cell differentiation via induction of the transcriptional repressor Bcl6. *Immunity* **34**, 932-946 (2011).
79. X. Liu *et al.*, Bcl6 expression specifies the T follicular helper cell program in vivo. *Journal of Experimental Medicine* **209**, 1841-1852 (2012).
80. R. I. Nurieva *et al.*, Generation of T follicular helper cells is mediated by interleukin-21 but independent of T helper 1, 2, or 17 cell lineages. *Immunity* **29**, 138-149 (2008).
81. I. Yusuf *et al.*, Germinal center T follicular helper cell IL-4 production is dependent on signaling lymphocytic activation molecule receptor (CD150). *The Journal of Immunology* **185**, 190-202 (2010).
82. J. L. Cannons *et al.*, Optimal germinal center responses require a multistage T cell: B cell adhesion process involving integrins, SLAM-associated protein, and CD84. *Immunity* **32**, 253-265 (2010).
83. T. A. McKinsey, C. L. Zhang, E. N. Olson, MEF2: a calcium-dependent regulator of cell division, differentiation and death. *Trends in biochemical sciences* **27**, 40-47 (2002).
84. J. D. Molkentin, B. L. Black, J. F. Martin, E. N. Olson, Mutational analysis of the DNA binding, dimerization, and transcriptional activation domains of MEF2C. *Molecular and cellular biology* **16**, 2627-2636 (1996).
85. M. J. Potthoff, E. N. Olson, MEF2: a central regulator of diverse developmental programs. (2007).
86. S. Han *et al.*, Cellular interaction in germinal centers. Roles of CD40 ligand and B7-2 in established germinal centers. *Journal of immunology (Baltimore, Md.: 1950)* **155**, 556-567 (1995).
87. A. Suto *et al.*, Development and characterization of IL-21–producing CD4+ T cells. *The Journal of experimental medicine* **205**, 1369-1379 (2008).
88. W. L. Chew *et al.*, A multifunctional AAV–CRISPR–Cas9 and its host response. *Nature methods* **13**, 868-874 (2016).
89. M. J. Pattison, R. J. Naik, K. M. Reyskens, J. S. C. Arthur, Loss of Mef2D function enhances TLR induced IL-10 production in macrophages. *Bioscience Reports* **40**, (2020).
90. F. H. Farias *et al.*, A rare regulatory variant in the MEF2D gene affects gene regulation and splicing and is associated with a SLE sub-

phenotype in Swedish cohorts. *European Journal of Human Genetics* **27**, 432-441 (2019).

91. S. K. Lee *et al.*, B cell priming for extrafollicular antibody responses requires Bcl-6 expression by T cells. *J Exp Med* **208**, 1377-1388 (2011).
92. S. Mora, J. E. Pessin, The MEF2A isoform is required for striated muscle-specific expression of the insulin-responsive GLUT4 glucose transporter. *J Biol Chem* **275**, 16323-16328 (2000).
93. P. Brescia *et al.*, MEF2B Instructs Germinal Center Development and Acts as an Oncogene in B Cell Lymphomagenesis. *Cancer Cell* **34**, 453-465.e459 (2018).
94. S. Song, P. D. Matthias, The Transcriptional Regulation of Germinal Center Formation. *Front Immunol* **9**, 2026 (2018).
95. K. Basso, R. Dalla-Favera, BCL6: master regulator of the germinal center reaction and key oncogene in B cell lymphomagenesis. *Advances in immunology* **105**, 193-210 (2010).
96. R. I. Nurieva *et al.*, Bcl6 mediates the development of T follicular helper cells. *Science* **325**, 1001-1005 (2009).
97. Y. Y. Zhao *et al.*, Overexpression of miR-18a negatively regulates myocyte enhancer factor 2D to increase the permeability of the blood-tumor barrier via Krüppel-like factor 4-mediated downregulation of zonula occluden-1, claudin-5, and occludin. *J Neurosci Res* **93**, 1891-1902 (2015).
98. H. Y. Seok *et al.*, miR-155 inhibits expression of the MEF2A protein to repress skeletal muscle differentiation. *J Biol Chem* **286**, 35339-35346 (2011).
99. M. Chi *et al.*, Immunological Involvement of MicroRNAs in the Key Events of Systemic Lupus Erythematosus. *Front Immunol* **12**, 699684 (2021).
100. P. Coit *et al.*, Hypomethylation of miR-17-92 cluster in lupus T cells and no significant role for genetic factors in the lupus-associated DNA methylation signature. *Ann Rheum Dis* **81**, 1428-1437 (2022).
101. J. Y. Choi *et al.*, Circulating follicular helper-like T cells in systemic lupus erythematosus: association with disease activity. *Arthritis Rheumatol* **67**, 988-999 (2015).
102. D. Baumjohann *et al.*, The microRNA cluster miR-17~92 promotes TFH

cell differentiation and represses subset-inappropriate gene expression. *Nat Immunol* **14**, 840-848 (2013).

103. R. J. Johnston *et al.*, Bcl6 and Blimp-1 are reciprocal and antagonistic regulators of T follicular helper cell differentiation. *Science* **325**, 1006-1010 (2009).
104. K. Hatzi *et al.*, BCL6 orchestrates Tfh cell differentiation via multiple distinct mechanisms. *Journal of Experimental Medicine* **212**, 539-553 (2015).
105. L. Chen, A. Kashina, Post-translational Modifications of the Protein Termini. *Front Cell Dev Biol* **9**, 719590 (2021).
106. Z. Li *et al.*, PIM1 kinase phosphorylates the human transcription factor FOXP3 at serine 422 to negatively regulate its activity under inflammation. *J Biol Chem* **289**, 26872-26881 (2014).
107. F. Li *et al.*, Ezh2 programs T(FH) differentiation by integrating phosphorylation-dependent activation of Bcl6 and polycomb-dependent repression of p19Arf. *Nat Commun* **9**, 5452 (2018).
108. S. Grégoire *et al.*, Control of MEF2 transcriptional activity by coordinated phosphorylation and sumoylation. *J Biol Chem* **281**, 4423-4433 (2006).
109. S. H. Son *et al.*, SUMOylation-mediated PSME3-20S proteasomal degradation of transcription factor CP2c is crucial for cell cycle progression. *Sci Adv* **9**, eadd4969 (2023).
110. X. Tang *et al.*, Cyclin-dependent kinase 5 mediates neurotoxin-induced degradation of the transcription factor myocyte enhancer factor 2. *J Neurosci* **25**, 4823-4834 (2005).
111. E. Taoufik, G. Kouroupi, O. Zygogianni, R. Matsas, Synaptic dysfunction in neurodegenerative and neurodevelopmental diseases: an overview of induced pluripotent stem-cell-based disease models. *Open Biol* **8**, (2018).
112. V. A. Polito *et al.*, Selective clearance of aberrant tau proteins and rescue of neurotoxicity by transcription factor EB. *EMBO Mol Med* **6**, 1142-1160 (2014).
113. C. R. Scherzer *et al.*, GATA transcription factors directly regulate the Parkinson's disease-linked gene alpha-synuclein. *Proc Natl Acad Sci U S A* **105**, 10907-10912 (2008).
114. S. B. Thomson, B. R. Leavitt, Transcriptional Regulation of the Huntingtin

Gene. *J Huntingtons Dis* **7**, 289-296 (2018).
115. A. L. Rankin *et al.*, IL-21 receptor is required for the systemic accumulation of activated B and T lymphocytes in MRL/MpJ-Fas(lpr/lpr)/J mice. *J Immunol* **188**, 1656-1667 (2012).
116. I. C. Mouat, E. Goldberg, M. S. Horwitz, Age-associated B cells in autoimmune diseases. *Cell Mol Life Sci* **79**, 402 (2022).
117. B. Keller *et al.*, The expansion of human T-bet(high)CD21(low) B cells is T cell dependent. *Sci Immunol* **6**, eabh0891 (2021).

국문초록

CD4 T 세포와 동족 B 세포 간의 효과적인 신호 전달은 CD4 T 세포의 종자 중심 여포보조 T 세포로의 적절한 세포 분화를 촉진할 뿐만 아니라, B 세포의 CD4 T 세포 의존적인 체액성 면역반응을 이끌어 내기 위한 필수적인 요소로 작용한다. 이러한 신호 전달은 B:T 면역 시냅스의 형성을 통해 이루어지지만, CD4 T 세포에서 면역 시냅스에 관여하는 분자에 대한 전사 조절 메커니즘은 아직 완전히 알려지지 않았다. 본 연구에서는 Mef2 전사인자 패밀리의 한 동형인 Mef2d 전사 인자가 B:T 면역 시냅스의 형성을 조절하여 종자 중심 여포보조 T 세포의 발달과 CD4 T 세포 의존적인 체액성 면역반응을 규제하는 새로운 메커니즘을 제안한다.

CD4 T 세포에서의 Mef2d 발현은 B:T 시냅스 형성 조절에 중요한 역할을 하는 SLAM-관련 단백질 (SAP)을 인코딩하는 *Sh2d1a* 유전자의 발현을 부정적으로 규제하였다. Mef2d 는 DNA 결합 의존적인 방식으로 *Sh2d1a* 유전자 발현을 직접 억제하여 SAP 의존적인 B:T 시냅스 형성을 제한하고, 항원 특이적인 CD4 T 세포의 종자 중심 여포보조 T 세포로의 분화를 방해하였다. 또한, CD4 세포에서의 Mef2d 는 중요한 B 세포 도움 신호 분자인 IL-21 을 유전자를 수준에서 직접 억제하여 IL-21 생산을 저해하였다. 이 규제는 SAP 의존적인 B:T 시냅스 형성의 억제와 함께 궁극적으로 B 세포의 체액성 면역반응을 제한하였다.

반면, CD4 T 세포 특이적인 Mef2d 결핍은 종자 중심 여포보조 T 세포 분화의 상당한 증가와 함께 SAP 발현 및 IL-21 생산의 의미 있는 상승을 동반하였다. 특히, 루푸스 환자의 CD4 T 세포에서의 *MEF2D* mRNA 발현은 루푸스 환자의 자가면역 매개변수인 순환 여포보조 T 세포의 빈도, 자가 항체 수준 및 SLEDAI 점수와 역 상관 관계를 보였다. 이러한 발견은 Mef2d 가 CD4 T 세포에서 종자 중심의 형성 및 B 세포에 의한 항체 생산을 유지하기 위한 중요한 규제자로 작용한다는 것을 나타낸다.

주요어: 여포보조 T 세포, 종자 중심, 체액성 면역, Mef2d 전사인자, B:T 시냅스, SLAM-연관 단백질, IL-21 사이토카인, 자가면역질환

학번: 2014-22010